Complexes of Technetium(I) and Rhenium(I) – From Radiopharmacy to Photocatalysis

Dissertation

zur

Erlangung der naturwissenschaftlichen Doktorwürde

(Dr. sc. nat.)

vorgelegt der

Mathematisch-naturwissenschaftlichen Fakultät

der

Universität Zürich

von

Philipp Kurz

aus

Deutschland

Promotionskomitee

Prof. Dr. Roger Alberto (Vorsitz)

Prof. Dr. Heinz Berke

Prof. Dr. Jay Siegel

Zürich 2005

TABLE OF CONTENTS

Important Compounds

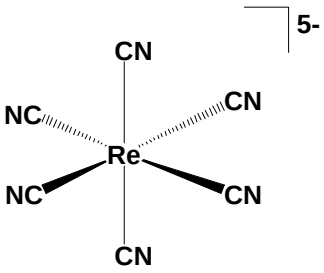

4

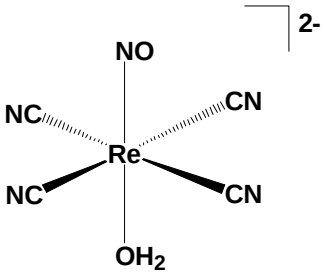

5

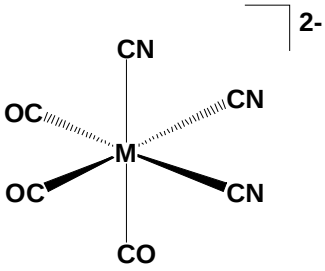

7 (M=^{99}Tc)**, 8** (M=Re)

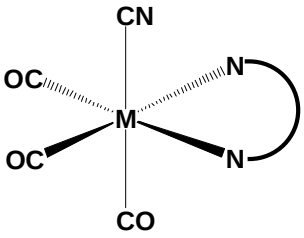

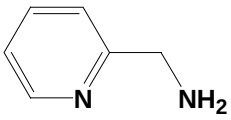

9 (M=^{99m}Tc)**, 11** (M=Re)

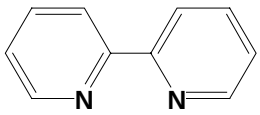

15 (M=Re)

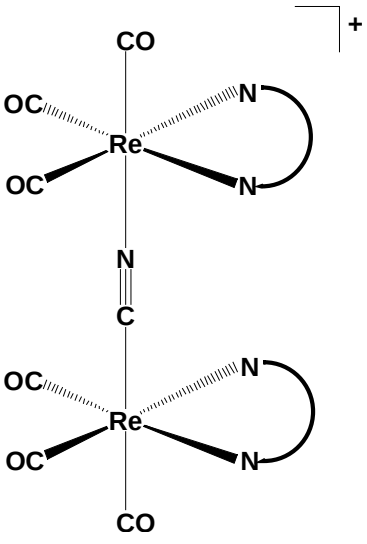

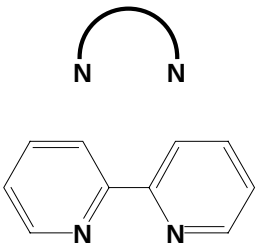

16

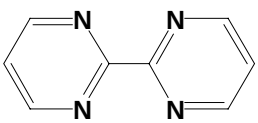

26

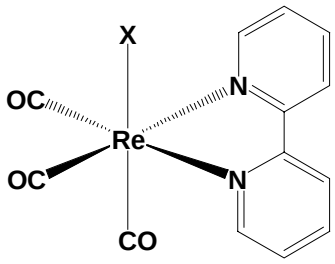

12 (X=Br)**, 14** (X=OH_2)**, 15** (X=CN)**, 17** (X=SCN)

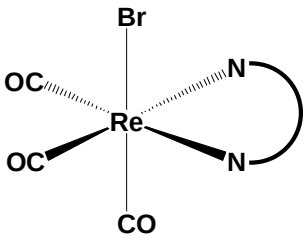

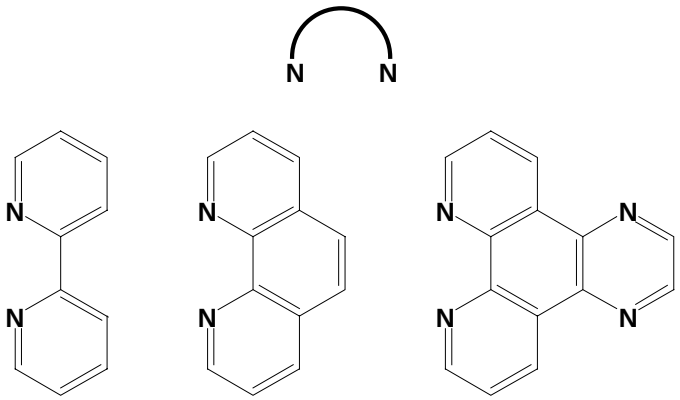

12 **18** **19**

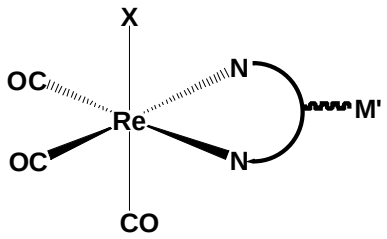

30 (M'= $Cu(PPh_3)_2$; N-N= bpm; X= Br)
31 (M'= $IrCp^*(OH_2)$; N-N= bpm; X= OH_2)
33 (M'= $Pt(PPh_3)_2$; N-N= phd; X= Br)

ABBREVIATIONS

9S3	1,4,7- trithiacyclononane
abpy	2,2'-azobispyridine
ac	acetate
bipy	2,2'-bipyridine
biq	2,2'-biquinoline
BM	any biologically active molecule
bpm	2,2'-bipyrimidine
bptz	3,6-bis(2-pyridyl)-1,2,4,5-tetrazine
D	electron donor molecule
E, $E_{1/2}$	redox potential vs. Ag/AgCl (+221mV vs. NHE)
dien	diethylenetriamine
dpq	dipyrido[3,2-f:2',3'-h] quinoxaline
dppz	dipyrido[3,2-a:2',3'-c] phenazine
EDTA	ethylenediaminetetraacetic acid
en	ethylenediamine
f	vibrational force constant
H2dcbipy	2,2'-bipyridine-4,4'-dicarboxylic acid
hisam	histamine
I	fluorescence intensity
$Kryptofix_{222}$	4,7,13,16,21,24-hexaoxa-1,10-diazabicyclo[8.8.8] hexacosane
K_{SV}	STERN- VOLMER constant
λ_{em}	fluorescence emission maximum
λ_{max}	UV-Vis absorption maximum
L_x	any ligand with denticity x
NHE	normal hydrogen electrode
ν_X	vibrational frequency of moiety X observed by IR spectroscopy [cm^{-1}]
OTf	trifluoromethanesulfonate
phd	1,10-Phenanthroline- 5,6-dione
phen	1,10-phenanthroline
pico	2-picolylamine
PSI, PSII	natural photosystems I and II
ptpy	*p*-(2,6-di-pyridyl-4-pyridyl)phenol
py	pyridine
Q	molecule capable of reductive fluorescence quenching ("quencher")
τ	excited state lifetime
$t_{1/2}$	half-life of radioactive nuclei
thexi-state	thermally equilibrated excited state
TEA	triethylamine
TEOA	triethanolamine
X	any monodentate ligand

1. INTRODUCTION

This thesis is consisting of two parts from two quite different fields of inorganic chemistry: coordination chemistry and photochemistry. As different as these fields are within inorganic chemistry, so were the aims for which research was carried out. In the first part, the goal was to find a new synthon for radiopharmaceuticals with technetium or rhenium at its centre. By coincidence it was found that model compounds synthesized for this first part possess very interesting photochemical properties and might act as photosentisizers in systems designed for solar energy conversion. Thus, research work was conducted in two very different areas but both areas centred around what matters most to the inorganic chemist: the metals - in both cases the homologous centres of rhenium and technetium in the oxidation state +I.

Therefore, the reader will find that this thesis contains all the sections, like this introduction at the beginning, split in two: one part dealing with coordination chemistry, a second with photochemistry.

1.1 ^{99m}Tc radiopharmaceuticals

Among the great pharmaceutical challenges facing people all over the world, especially in industrialized countries, are the large sections of the population suffering from cardiovascular diseases and cancer. For example, about 70% of all deaths in Switzerland, a wealthy country with a high life expectancy of 83 years, are caused by one of these two groups of diseases[1] (Fig 1.1). On the contrary, for a developing country like South Africa (life expectancy 57 years), cardiovascular diseases and cancer are only minor health topics, responsible for about 20% of all deaths; while infectious diseases like tuberculosis, HIV or pneumonia are much larger problems here[2]. Nevertheless, large sections of pharmaceutical research in both academia and industry are dedicated to cancer and cardiovascular diseases. It is therefore no surprise that the development of radioactive agents for diagnosis and treatment of such diseases was a central goal for radiopharmacists right from the beginning.

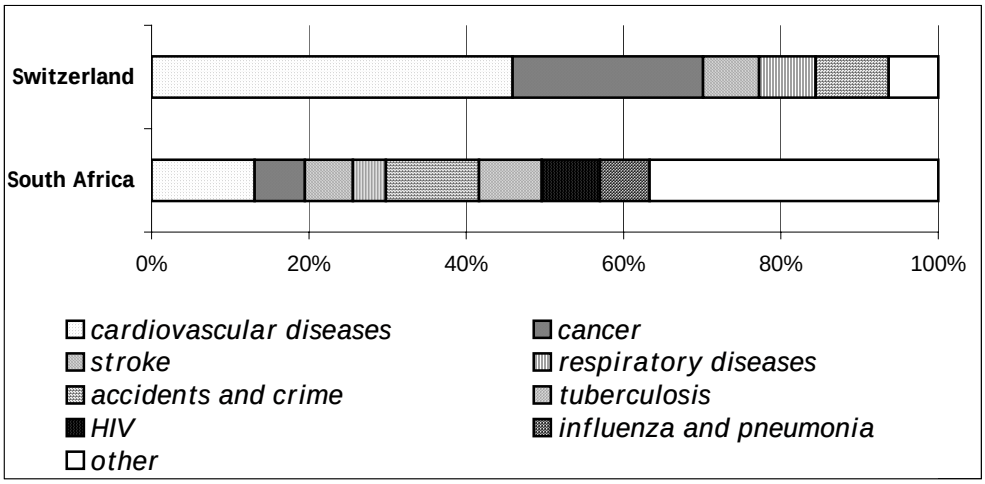

Fig. 1.1 Causes of deaths. Comparison between Switzerland and South Africa.

Before the treatment of many diseases is feasible, the location and function of ill tissue has to be determined, for example the exact position of blocked arteries of a heart attack or the location of metastases of a tumour. One of the radionuclides in wide use for such imaging applications today is the metastable technetium nucleus ^{99m}Tc[3], which decays with a half-life of about $t_{1/2}$= 6h via a 140keV γ-decay to ^{99}Tc. Technetium, as its name suggests, is an element that is found only in traces on earth, but especially the nuclide ^{99}Tc (β-emitter, $t_{1/2}$= 212.000a) is produced in 6% fission yield as a fission product of commercial nuclear reactors using uranium fuel. A schematic picture of a scintigraphic diagnosis using a ^{99m}Tc-radiopharmaceutical is shown in Fig.1.2. After injection into the patient, the ^{99m}Tc- containing compound accumulates in the targeted tissue and the γ-photons emitted are detected by a γ-detector, allowing the calculation of two- and even three- dimensional images of the emitting tissue within the body. After injection of the radiopharmaceutical into the patient, the half-life of the used nuclide should be long enough to allow measurements for multiple hours without exposing the patient to an elevated dose of radiation for extended time. The emitted γ-photons should possess enough energy to be detected by conventional γ-detectors, yet not too high in energy to minimize the effects on healthy tissue. In the case of ^{99m}Tc both the half-life and the energy of the emitted radiation are within the perfect ranges for radiodiagnostic applications of γ-emitters.

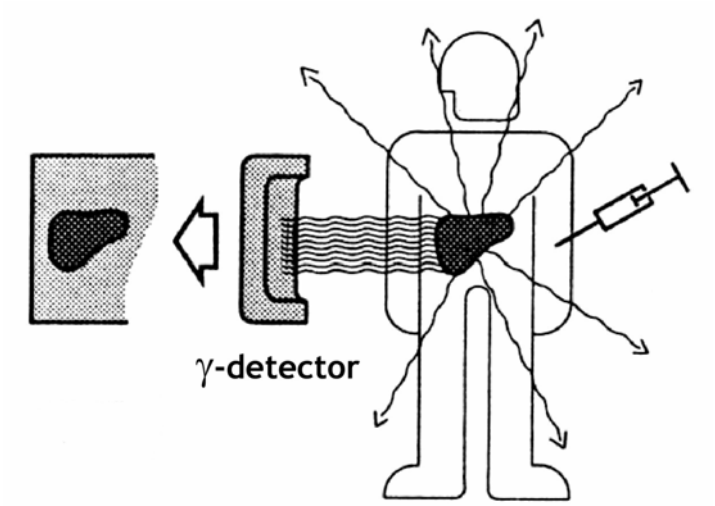

Fig. 1.2 Schematic drawing of the concept of radiodiagnostic imaging using γ-emitters(from ref.[4]).

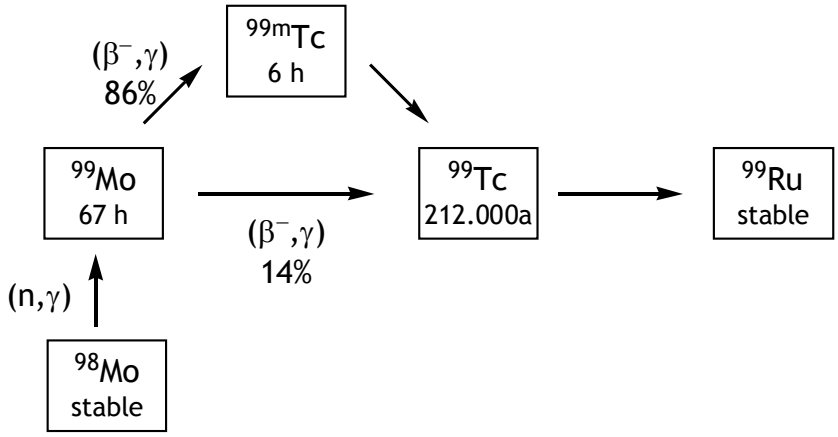

Scheme 1.1 Production and decay route for ^{99m}Tc used in a commercial generator system (modified from ref.[4]).

Additionally it is of key importance that a radionuclide to be used in hospitals and research institutions is relatively cheap and readily available. This prerequisite for the use of ^{99m}Tc was met by the invention of the ^{99m}Tc generator in the 1950's. The generator consists of an alumina column loaded with ^{99}Mo in the form of $[^{99}MoO_4]^{2-}$. ^{99}Mo is available from the nuclear reaction of ^{98}Mo with neutrons at a reactor site (Scheme 1.1). The ^{99}Mo on the column decays relatively slowly ($t_{1/2}$= 67h) by β-emission to $[^{99m}TcO_4]^-$, which can be eluted by 0.9% saline from the column as a ^{99m}pertechnetate solution of a concentration between 10^{-6}M and 10^{-8}M. The biodistribution of $[^{99m}TcO_4]^-$ in the human body was investigated shortly after the invention of the generator system. It was found that $[^{99m}TcO_4]^-$ showed a high affinity for the thyroid[5], probably because $[^{99m}TcO_4]^-$ is similar to iodide, an anion

essential for the thyroid. On the other hand, these studies showed that imaging of any other organ or tissue would require the synthesis of technetium complexes different from $[^{99m}TcO_4]^-$.

The challenges of the task to develop ^{99m}Tc- radiopharmaceuticals directly stem from the nature the generator eluate:

- the pharmaceutical has to be prepared in aqueous solution with a high concentration of chloride present
- the chemical reactions required should be completed within a maximum time of about 1 hour (due to the half-life of ^{99m}Tc) at a maximum temperature of 90°C
- the set of reactants should ideally be provided in a kit form, so that the operations needed prior to use are simply the injection of generator eluate into a vial containing the kit and some heating

A discussion of the large number of ways tried to develop ^{99m}Tc- imaging agents fulfilling all these requirements is beyond the scope of this thesis, but the topic has recently been reviewed in detail[6]. The biodistribution of the agents is known to be greatly influenced by size, charge and type of the metal centre in a way that has not been fully understood in most cases. Therefore, the development of new agents is to a large extend still a trial-and-error procedure. For this it is an advantage to have many possible ^{99m}Tc- fragments available to increase the chances of finding suitable compounds. Despite the difficulties, a series of ^{99m}Tc- complexes have been prepared that meet all the mentioned requirements and are in clinical use (Scheme 1.2). As ^{99m}Tc combines availability and well-established chemistry with reasonably low cost, it is the most widely used radionuclide for diagnostic applications. Additionally, it has been argued that ^{99m}Tc might also be used for therapeutic applications like its higher homologue rhenium[7], for which the use of the strong β-emitters ^{186,188}Re as therapeutic agents has been proposed[8, 9] and is currently in the phase of clinical trials[10].

Concerning their coordination chemistry most of the technetium compounds developed so far for diagnostic applications contain the metal in the oxidation state $+V$[6], accessible by the reduction of $[^{99m}TcO_4]^-$ by $SnCl_2$ in the presence of appropriate multidentate ligands, with typical examples given in Scheme 1.2. Until the middle of the 1990's only one, albeit very successful, commercial product containing technetium in the oxidation state +I had been developed, the myocardial imaging agent Cardiolite®.

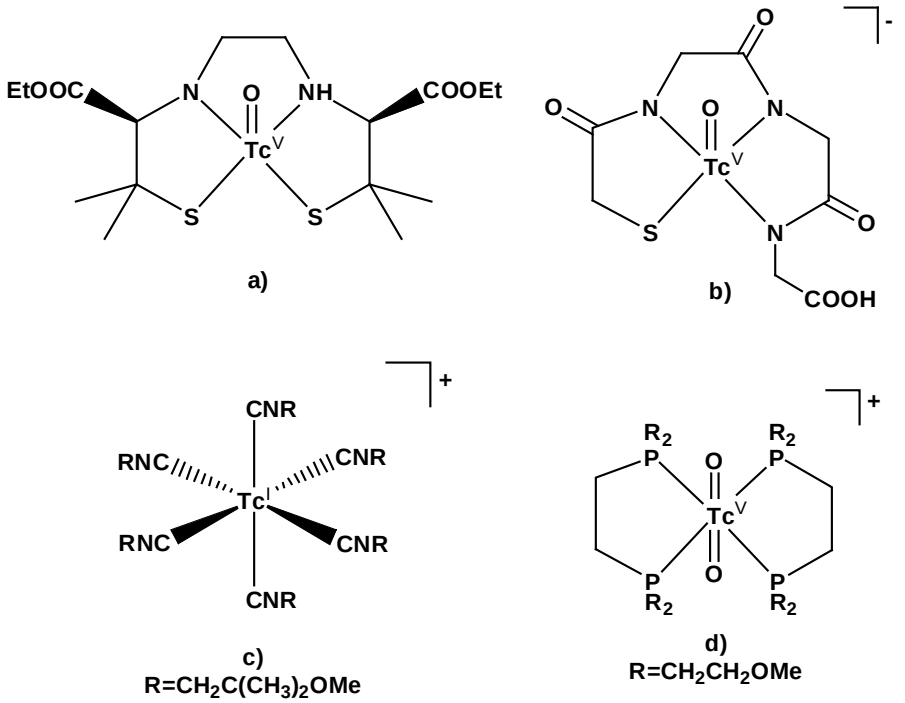

Scheme 1.2 Examples of commercially available ^{99m}Tc radioimaging agents: a) Neurolite® (cerebral imaging); b) Technescan® (renal imaging); c) Cardiolite® and d) Myoview® (both for the imaging of myocardial perfusion).

In 1998, the direct reduction of $[^{99m}TcO_4]^-$ to the organometallic Tc^I-moiety $[^{99m}Tc(OH_2)_3(CO)_3]^+$ was reported by Alberto et al.[11] and within the next years the IsoLink™ kit was developed[12], which has made this new ^{99m}Tc- core accessible for a variety of investigations. Besides its convenient access and great stability in aqueous solution, the main characteristics of this moiety are its very small size and the fact that it consist of two halves: a very small, inert tricarbonyl part that stabilizes the technetium's low oxidation state and a labile half of three aquo ligands that are easily replaced by a variety of ligands.

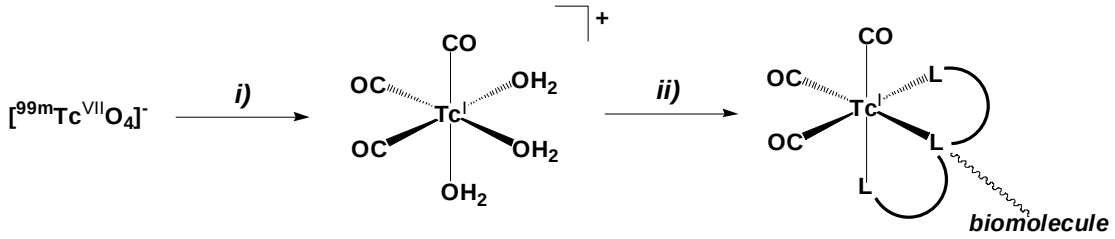

Scheme 1.3 Strategy for the labelling of various biomolecules using the IsoLink™ kit. i) K(H_3BCOOH), H^+, 15min, 90°C, H_2O (IsoLink™-kit); ii) L_3-biomolecule, ≤30min, ≤90°C

As a result, a very versatile labelling strategy for this fragment, depicted in Scheme 1.3, has been developed. A variety of tridentate ligand systems as well as various biomolecules linked to them have since been successfully linked to ^{99m}Tc and very promising biodistributions were observed for some of the Tc^I- tricarbonyl- compounds obtained in this way[13]. As the introduced technetium fragment is very small, it is hoped, that the natural biodistribution of the biomolecule is only changed to a minimal degree.

1.2 Tc^I- and Re^I- complexes containing combinations of NO^+, CO and CN^-

Inspired by the success of the $[^{99m}Tc(OH_2)_3(CO)_3]^+$ fragment, the search for more Tc^I- fragments was started. The starting points of such investigations are usually experiments with rhenium, the non- radioactive homologue of technetium. Due to the low concentration of ^{99m}Tc in the generator eluate, only very few techniques allow the analysis of the products of reactions carried out with generator eluate, the only widely used method being γ-detected HPLC. As the long-lived nuclide ^{99}Tc can be extracted in significant quantities from spent reactor fuels, it can be used for chemical studies[3], but the need to handle a β-emitter and the production of radioactive waste as a result limit such experiments as well. A comparison of the reactivities of the metals of group 7 shows that technetium is much more similar to rhenium than manganese, which can be explained as an effects of lanthanide- contraction. As a result, synthetic studies start usually by the synthesis of the non- radioactive rhenium homologues of the technetium- compounds of interest before the technetium compounds are prepared using similar procedures as developed for rhenium.

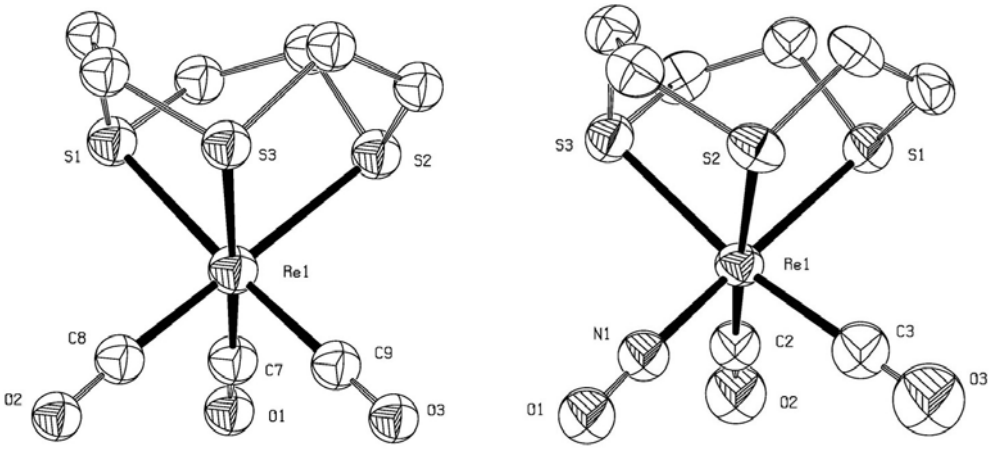

Fig 1.3. Molecular structures of $[Re(CO)_3(9S3)]^+$ (left, from ref.[17]) and $[Re(CO)_2(9S3)(NO)]^{2+}$ (right, from ref. [16]).

In one approach to develop a new technetium(I) core, reactions of the nitrosyl ligand NO^+ with rhenium(I) tricarbonyl compounds were studied. It was found that the isoelectronic nitrosyl ligand was able to replace one carbonyl and by this route complexes containing the $[Re(CO)_2(NO)]^{2+}$- unit could be synthesized and characterized[14]. In aqueous solution, the fragment $[Re(OH_2)_3(CO)_2(NO)]^{2+}$ could be obtained, which is structurally very similar to the versatile $[(Tc/Re)(OH_2)_3(CO)_3]^+$- unit. For example, complexes of the two fragments with the tridentate ligand trithiacyclononane (9S3) have nearly identical geometries, but of course different charges (Fig. 1.3). As the overall charge of the labelled species is known to influence its biodistribution greatly, a molecule containing the dicationic $[^{99m}Tc(CO)_2(NO)]^{2+}$- fragment could have very different, and probably better, biodistribution characteristics compared a the similar one with the $[^{99m}Tc(CO)_3]^+$ -moiety. To develop this promising fragment further towards a potential radiopharmaceutical application, routes to obtain $[^{99m}Tc(OH_2)_3(CO)_2(NO)]^{2+}$ from generator eluate were investigated[15] and the properties of the rhenium fragment $[Re(OH_2)_3(CO)_2(NO)]^{2+}$ were studied in detail in aqueous solution[16]. The fragment showed a high stability in water and reasonably fast exchange of the coordinated water for a variety of ligands. The challenge remaining so far is the development of a kit to synthesize $[^{99m}Tc(OH_2)_3(CO)_2(NO)]^{2+}$ directly from the eluate, which proves to be difficult.

With these experiences of investigations dealing with the starting materials $[(Tc/Re)(OH_2)_3(CO)_3]^+$ and $[(Tc/Re)(OH_2)_3(CO)_2(NO)]^{2+}$ in mind, it seemed attractive to consider a third small diatomic ligand for Tc^I/Re^I, the cyanide ligand CN^-.

The ligands NO^+, CO and CN^- form an isoelectronic series of diatomic ligands containing 14 electrons each. The electronic structure is $(\sigma 1s)^2(\sigma^* 1s)^2(\sigma 2s)^2(\sigma^* 2s)^2(\pi 2p_x)^2(\pi 2p_y)^2(\sigma 2p_z)^2$, corresponding to a triple bond between the two atoms of the ligand[18]. The interaction of these ligands when coordinating to a metal is twofold[19]. Firstly, there is a σ-donating bond between the highest occupied molecular orbital (HOMO) $\sigma 2p_z$ of the ligand and vacant metal orbitals. The $\sigma 2p_z$ is weakly antibonding and there is higher electron density close to the less electronegative atom for all three ligands. Consequently, NO^+ coordinates via the nitrogen, whereas CO and CN^- have their carbon atoms bound to the metal. Secondly, there is back- donation from filled d- orbitals of the metal into vacant, antibonding π- orbitals of the ligand. Therefore, both σ- bonding and π- back- bonding result in a decrease of the strength of the ligand's triple bond in complexes when compared to the free ligands. As the force constant influences the vibration frequency of a bond, vibrational spectroscopy (both infrared and Raman), is an important tool to analyse binding in nitrosyl-, carbonyl and cyano- complexes, which all show characteristic spectroscopic bands[20].

	NO^+	CO	CN^-
free ligand	2200	2155	2080
complexes	1900-1500	2100-1800	2200-1900

Table 1.1 Infrared stretching frequencies in wavenumbers [cm^{-1}] for the ligands NO^+, CO and CN^-.

As is already visible from the very different vibration frequencies in Table 1.1, the electronic properties of the three ligands differ significantly, despite them forming an isoelectronic series. As the elements that are part of the diatomic ligands become less and less electronegative along the series $NO^+ > CO > CN^-$ combined with a decrease in charge, σ- donor and π-acceptor properties change according to Fig. 1.4. As a result, the strong π-

acceptors nitrosyl and carbonyl bind strongly to electron rich metal centres in low oxidation states and stabilize them against oxidation. For cyanide, its quality as a σ- donor becomes as important as π- back- bonding.

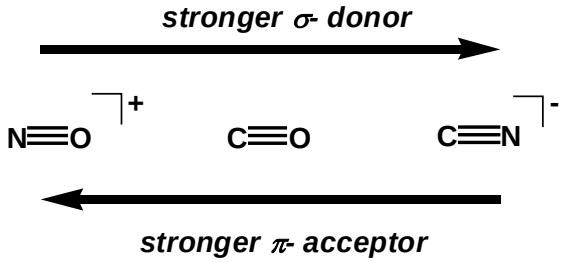

Fig 1.4. Trends in donor and acceptor qualities for NO^+, CO and CN^-.

Ligand 1 ⇒ / Ligand 2 ⇓	NO^+	CO	CN^-
NO^+	$[ReCl_3(MeCN)(NO)_2]$	$[Re(\mu\text{-}Cl)Cl(CO)_2(NO)]_2$	$[Re(CN)_4(OH_2)(NO)]^{2-}$
CO		$[ReBr(CO)_5]$	$[Re(CN)_3(CO)_3]^{2-}$
CN^-			$[Re(CN)_6]^{5-}$

Table 1.2 Important examples of rhenium(I) complexes containing mixtures of two of the three ligands NO^+, CO or CN^-

For rhenium(I), complexes containing only one of the ligands NO^+, CO or CN^- are known, as well as combinations of two of them together. Important examples are given in Table 1.2. A mixed nitrosyl- carbonyl- cyano- rhenium(I) complex, containing all three ligands at the same time, has not been reported so far. For the complexes containing cyanide, only very limited data is available for the rhenium complexes with many of the characterizations rather incomplete[21]. This is even more true for the corresponding technetium complexes, where $[^{99}Tc(CN)_6]^{5-}$ is the only reported Tc(I)- cyanide complex[22].

It therefore seemed worthwhile to investigate the field of Re^I- and Tc^I- cyano- complexes in more detail with the aim of finding a new Tc^I- cyano- fragment suitable for radiopharmaceutical applications. With this goal in mind, a special focus had to be made on synthesis and stability of such a fragment in water and its substitution reactions in aqueous solution. Experiments and results concerning this aim will be discussed in chapter 2.

1.3 Global energy supply, its problems and the vision of a „H_2-economy“

The second part of this thesis (chapters 3 to 6) deals with syntheses and properties of rhenium tricarbonyl diimine complexes – a group of compounds with unusual photochemical properties. The goal here was a to make a contribution to the field of solar energy conversion.

The people of the earth face a paradox situation today[23]: all energy scenarios predict an enormous growth in energy demand for the next coming decades. On the other hand, we have realized the great effects on the world's climate that greenhouse gas emissions have, especially the production of CO_2 by fossil-fuel consumption. So some international meetings try to build a global consensus to reduce CO_2 emissions, while at other meetings the need for economic development of a large number of developing nations is realized. Both targets, less greenhouse gases combined with more industrial development, cannot be realized in parallel if we continue to base our energy supply on fossil fuels. About 80% of our total energy consumption is in the form of fossil fuels, a situation that has not changed significantly over the last three decades[24] (fig 1.5).

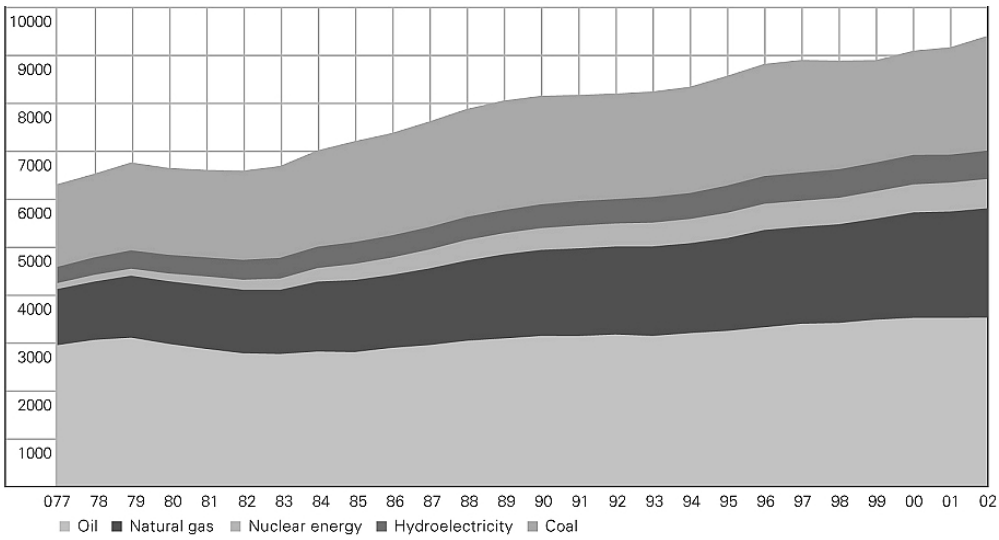

Fig 1.5. World consumption of primary energy, in oil equivalents [million tonnes] (from ref.[24]).

Many researchers and engineers have realized these facts and great efforts are under way to replace fossil fuels with alternative energy sources. The most promising candidate as alternative fuel seems to be molecular

hydrogen H_2[25]. Hydrogen can be stored and transported as compressed gas and used in fuel cells to generate heat or electricity with clean water vapour as single product. Additionally, fuel cells use the energy provided much more efficiently than combustion systems as far less heat is generated as a by-product. After about two decades of very intense research and development, the hydrogen technology is by now very advanced. Hydrogen energy systems to generate both heat and electricity are available for houses, cars (e.g. Fig. 1.6), buses and even ships. To prove that the "hydrogen- economy" could become a reality, projects like the consortium Icelandic New Energy were started, with the aim of making Iceland the first fossil fuel free country by 2030.

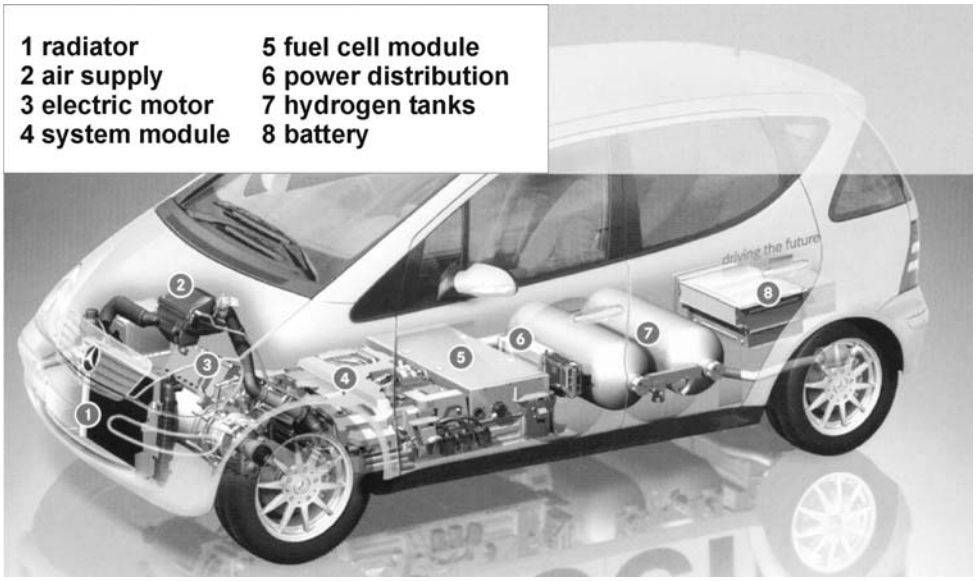

Fig 1.5. View of the fuel cell of the DaimlerChrysler fuel cell car F-Cell (left); The entire fuel-cell system is integrated into the sandwich floor of a long-wheelbase Mercedes-Benz A-Class car (from ref.[26]).

Superb technology is available to transport and use hydrogen very efficiently, but far less efforts seem to be made to develop a feasible, ecologically benign way of producing H_2. In exceptional cases like the Iceland project, using Iceland's abundant alternative energy sources of wind and geothermal power solves this problem. But in most of the world, hydrogen is produced from fossil fuel using the well- established technology of steam reforming, the high temperature reaction of natural gas or oil with water to produce hydrogen and carbon oxides[27] (Scheme 1.4). Both key

reactions of the process are equilibria, so a purification process is needed to separate the product hydrogen from the other gases involved.

An energy system using the combination of steam reforming and hydrogen fuel cells is far more efficient and cleaner than one based on fossil fuel combustion. Nevertheless, it does not avoid the production of CO_2 and still depends on fossil fuel. So other, sustainable ways of producing hydrogen have to be developed to end the world's dependence on fossil fuels.

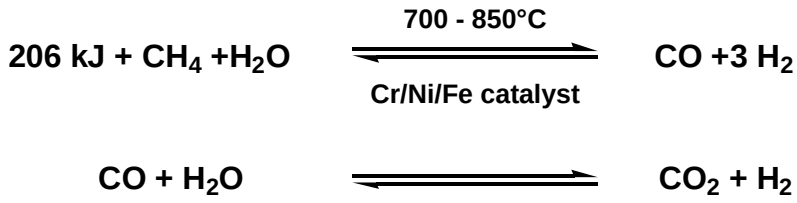

Scheme 1.4 Main reactions of the steam reforming process.

1.4 Systems for photochemical H_2- production

The most abundant alternative energy source available on earth is solar radiation. The amount of energy reaching us from the sun is 10.000 times larger than the total human consumption of energy. This fact is in striking contrast to the situation for wind, hydro, geothermal, tidal or other alternative energy forms, which have, even for the most optimistic scenarios, a potential to supply only a fraction of the global energy need[25] (Table 1.3). This is not to say that the development of techniques to harvest these other alternative energy sources is a bad strategy. On the contrary, their development contributes to the development of a more ecologically benign energy mix. But on the background of ever growing energy demands of a larger world population, many experts agree that only solar energy has the potential of supplying enough energy to mankind in a long-term sustainable fashion.

source	*energy flux*	*% of total flux*
solar	343.000	99.98
geothermal	62	0.018
tidal	6	0.002

Table 1.3 Primary energy sources for the earth (flux in W m^{-2}).

Given the attractiveness of a "hydrogen- economy" discussed above, people have considered the photochemical production of hydrogen for a long time. As a source for hydrogen the most abundant, and therefore best choice seems to be water. Thus, the ultimate challenge is the development of a system that is capable of splitting the nearly limitless substrate water into hydrogen and oxygen using the abundant energy of solar radiation. Chemically, this is a difficult problem, as the energy needed to break the strong hydrogen- oxygen bonds is large[27] (Scheme 1.5). Another intrinsic problem to be solved is the fact that the splitting of water is a multi-electron process involving overall the cleavage and formation of several bonds.

$$\mathbf{286\ kJ + H_2O \rightleftharpoons 1/2\ O_2 + H_2}$$

Scheme 1.5 Reaction of the direct dissociation of water.

Water is among the most fundamental chemical substances and its dissociation is a fundamental process, studied already long ago: it was found found that the (incomplete) thermal dissociation of water is only possible at very high temperatures[27]. For example, only 4% of water vapour is split into H_2 and O_2 at 2500K. As many equilibria are involved, a mixture of products is obtained. Thus, water thermolysis using concentrated solar power is not feasible, because even though such temperatures can be reached by solar furnaces, both reactor materials for the high temperature and separation techniques for the two gases at these temperatures are lacking. The direct photochemical splitting of water by sunlight is equally impossible because water does not absorb visible light: COEHN discovered already in 1910 that the ultraviolet light of a mercury lamp is needed to drive the process[28].

From a thermodynamic point of view, near infrared radiation with a wavelength of about 1000nm should already allow the splitting of water, as the electrolytic cleavage of water is possible at a potential difference of only 1.23V. The spectrum of solar radiation reaching the surface of the earth has its highest energy flux in the much more energy rich visible region between 400 and 700 nm[29]. Therefore, efficient use of the energy provided

by the sun should make it possible to split water using visible light at ambient temperature.

As water does not absorb visible light itself, photosensitisers have to be used for the initial steps of light absorption and charge separation. A simplified scheme for the process of light absorption is shown in Figure 1.6[30, 31]. An electron from an occupied molecular orbital of the light-absorbing molecule is excited to an unoccupied orbital of higher energy by the absorption of a photon. In the simple, but very common case shown in Figure 1.6, both ground and excited state are singlet states, the excited state with two unpaired electrons with opposite spins in two different orbitals.

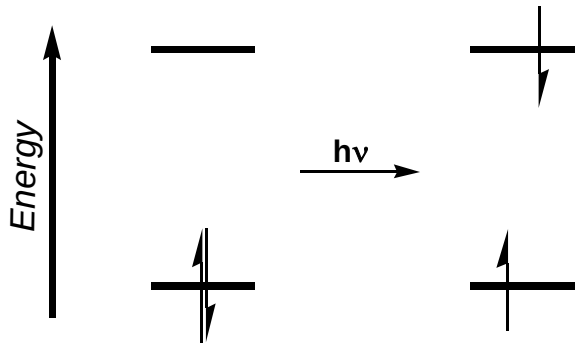

Figure 1.6 Simplified representation of ground and excited states.

As a consequence, in its excited state the molecule is a much stronger reducing agent, as the photoelectron of high energy is now easily accessible. The excitation process also leaves an energetically very low-lying hole at the orbital from where the photoelectron was excited – hence the excited state is also a much stronger oxidising species than the ground state. The REHM- WELLER approximation[32] is usually applied to estimate the difference of the redox potentials E between ground (D/ A) and excited (D*/ A*) states:

oxidation (excited state as electron-donor): $E(D^+/D^*) = E(D^+/D) - E_{00}$

reduction (excited state as electron-acceptor): $E(A^*/A^-) = E(A/A^-) + E_{00}$

Here, the energy difference between the lowest vibrational state of ground and excited states is denoted as E_{00}. Often it is difficult to determine E_{00} with high precision and there is a controversy about methods how to do so[33], but for most processes of visible light absorption E_{00} is within a range

of 1 to 2.5V resulting in a large difference in redox behaviour between ground and excited states.

As a result, photosensitisers used for the photochemical splitting of water have to possess matching redox potentials for the reduction (–0.41V) or oxidation (+ 0.82V, both at pH 7[27]) of water. Additionally, the excited states have to posses a lifetime τ long enough for redox processes to occur with reasonable probability (τ >~25ns). The system should also be able to store the electrons of intermediate redox states. A number of promising strategies have been proposed to meet these requirements and their advantages and disadvantages have been reviewed recently[34, 35]:

- *semiconductor* systems – especially the irradiation of TiO_2
- *electrolysis* of water using photovoltaic electricity
- *photo- biological* systems – photosynthesising cells producing H_2
- *high- temperature* solar chemistry – e.g. splitting of ZnO at >1250K
- *homogeneous* systems using transition metal complexes

Even though extensive research in this field took place for at least the last 40 years, no economically feasible system for the production of hydrogen as a "solar fuel" has been developed so far despite promising results obtained for all the mentioned strategies.

In this work conducted within a research group of coordination chemists, it is hoped to make a contribution to the last approach mentioned above, the use of transition metal photosensitisers in homogeneous solution. With this approach one is basically trying to imitate the only truly working system for the harvesting of solar energy on earth today: the machinery of the natural Photosystem enzymes of the photosynthesising plants and bacteria around us. In the following, this introduction will therefore focus briefly on the natural photosystems and then discuss artificial mimics of it.

The average overall process of natural photosynthesis can roughly be represented by the reaction of Scheme 1.6[29]:

$$106\ CO_2 + 16\ NO_3^- + HPO_4^{2-} + 122\ H_2O + 18\ H^+ + \text{solar energy} \longrightarrow C_{106}H_{263}O_{110}N_{16}P_1 + 138 O_2$$

Scheme 1.6 Reaction of natural photosynthesis, using the average composition of photosynthesising marine plankton for illustration.

Photosynthesis thus involves the reduction of carbon dioxide and the oxidation of water to form organic matter and molecular oxygen, all driven by the energy of visible light. In nature, these processes are taking place in the thylakoid membrane but within different protein assemblies. Photosystem I (PSI) is the site of CO_2 reduction and Photosystem II (PSII) the site of water oxidation. Both are large, very complex assemblies of numerous membrane proteins and cofactors[36, 37] (e.g. Fig. 1.7).

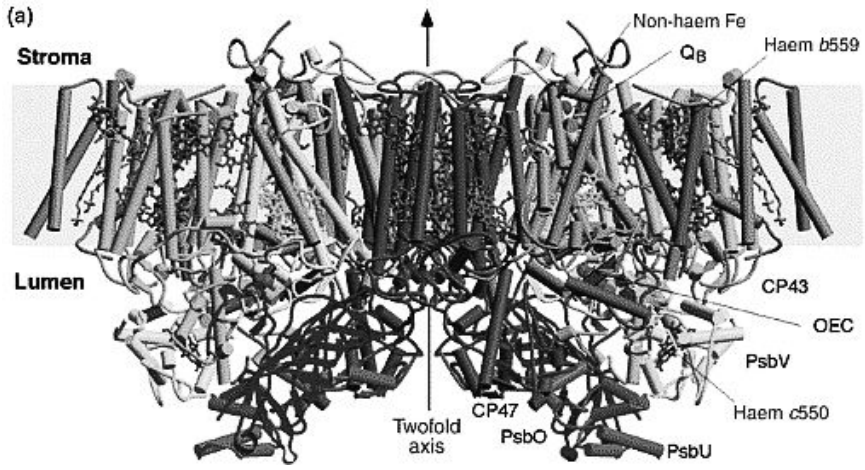

Figure 1.7 Side view of Photosystem II within the thylakoid membrane. The site of water oxidation is the oxygen-evolving complex (OEC) (from ref.[38]).

To understand the amazing complexity of these protein assemblies is a still non- solved puzzle. For the design of artificial mimics of these enzymes, it is apparent that it will only be possible to copy the basic concepts of PSI and PSII, but never their elaborate molecular architecture. One feature that has been very influential for the design of artificial systems has been the overall flow of reducing equivalents from PSII to PSI in the natural system, schematically depicted in Scheme 1.7.

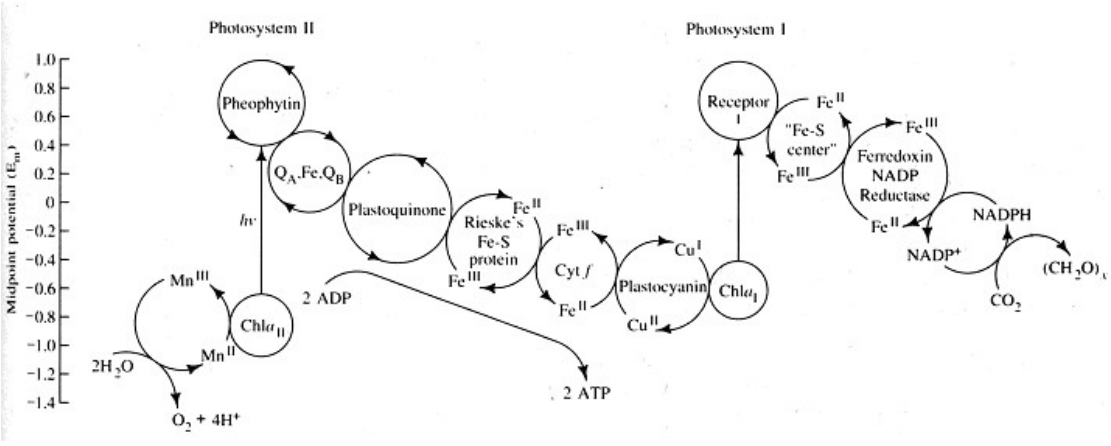

Scheme 1.7 Flow of redox equivalents from PSII to PSI (scale is $-E_0$ vs. NHE) (from ref.[19]).

Upon the absorption of a photon, the chlorophyll assembly $Chla_{II}$ is excited and becomes strongly reducing. It ejects an electron to the acceptor pheophytin from where a cascade of electron transfers takes place terminating in the reduction of plastocyanin, a 10kDa protein, which is mobile in the membrane and acts as electron relay between PSII and PSI. The oxidised primary donor $Chla_{II}^+$ is one of nature's most oxidising species (E_0= +1.2V vs. NHE). This oxidising power is used to oxidise water to oxygen and protons in the mixed calcium- manganese cluster of the OEC, whose exact structure and mechanism is still a topic of intense discussions.

In PSI, the weak redox equivalents arriving from PSII in the form of reduced plastocyanines are transformed into strong reducing agents by the energy of a photon absorbed by the chlorophylls of $Chla_I$. At the end of yet another redox chain these electrons are used for the reduction of $NADP^+$ and finally CO_2.

It was already proposed in 1979 to design artificial systems with the overall goal of splitting water according to Scheme 1.8[39]. The use of a pair of photochemical reactions, that conceptually mimic PSI and PSII, was suggested, coupled via a compound acting as redox relay.

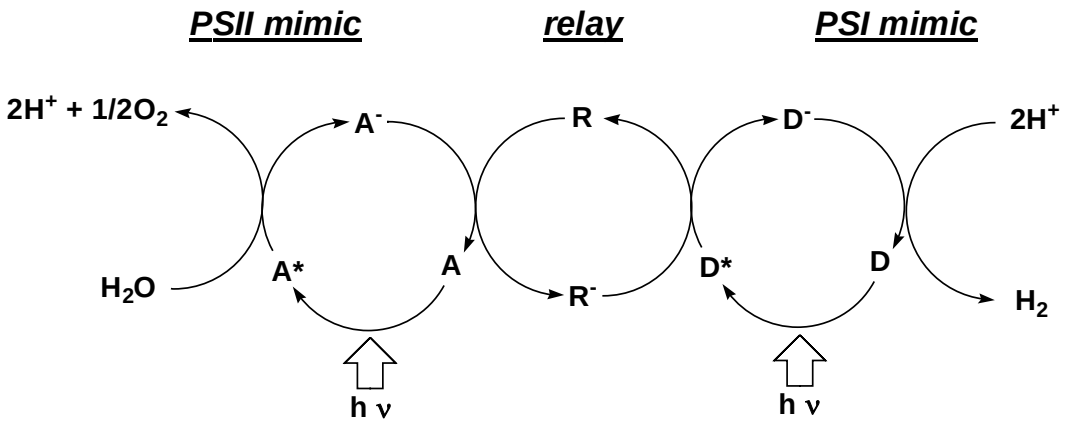

Scheme 1.8 Possible flow of redox equivalents in a bio- inspired artificial water splitting system. **A** is an acceptor system able to oxidise water; **R** represents an electron relay and **D** a strong donor unit able to reduce protons.

The state of the art today is still far away from realizing a working system following the complete outline of Scheme 1.8. The general approach so far has been to study potential systems for one of the two half- reactions, so either the reductive or the oxidative side of the system. So only systems acting either as PSI- or PSII- mimics were prepared so far, leaving the problem of the relay untouched

Among the compounds found as promising candidates to act as photoactive donor molecule D is the rhenium complex $[ReCl(bipy)(CO)_3]$. And it is here where the two different fields of chemistry discussed so far come together, as the compound contains the interesting radiopharmaceutical fragment $[Re(CO)_3]^+$ as well as the diimine ligand bipy, a very common ligand in inorganic photochemistry.

1.5 Photochemistry of [ReX(diimine)(CO)$_3$] complexes

Rhenium(I) carbonyl complexes were first synthesised and characterised in 1941[40]. It was found that the dimeric decacarbonyl $[Re_2(CO)_{10}]$ of rhenium(0) could be formed directly from perrhenate and carbon monoxide. Oxidative addition of molecular halogens to $[Re_2(CO)_{10}]$ resulted in the formation of the rhenium(I) carbonyls $[ReX(CO)_5]$ (X=Cl, Br, I), which can be transformed into water soluble tetraalkylammonium salts of $[ReX_3(CO)_3]^{2-}$ by carbonyl substitution[41] (Scheme 1.9). $[ReX(CO)_5]$ and $[ReX_3(CO)_3]^{2-}$ are the starting points of choice for most syntheses of rhenium(I) carbonyl compounds today.

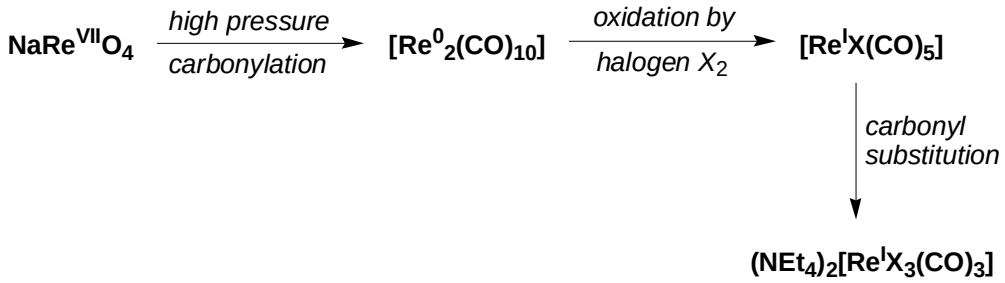

Scheme 1.9 Synthesis of rhenium (I) carbonyl precursors (X = Cl, Br).

One of the first substitution reactions of $[ReCl(CO)_5]$ investigated already in 1941 was the one with the diimine ligand phen[42]. Substitution of two carbonyl ligands occurred and the complex $[ReCl(phen)(CO)_3]$ was isolated. More than 35 years later, a detailed photochemical investigation of $[ReCl(phen)(CO)_3]$ was carried out[43]. It was realised that the compound possesses remarkable photochemical properties, especially a long- living, fluorescing excited state, which can be studied by spectroscopy even at room temperature. This is very peculiar for a metal carbonyl complex, which in most cases are known to undergo rapid excited state decay via carbonyl loss.

The detailed study revealed important information about the excited state of $[ReCl(phen)(CO)_3]$, later found to be equally valid for other $[ReX(diimine)(CO)_3]$ complexes, for example those containing bipy. The complexes absorb visible light up to wavelengths of 450 to 500nm. When exited with light of about 400nm wavelength, a rather strong fluorescence is observed with an emission maximum between 500 and 600nm (Fig. 1.8). The excited state was assigned to be a metal to ligand charge transfer (MLCT) excited state, with the photoelectron ejected from a metal centred π-d orbital into a vacant ligand centred π^* orbital. Therefore a more precise version of the general energy scheme of Fig. 1.6 can be given for the case of $[ReX(diimine)(CO)_3]$ complexes (Fig. 1.9). The photoexcitation process is here a metal-centred oxidation and a ligand-centred reduction. The lifetimes of the excited states are strongly dependent on both diimine and the solvent. Fluorescence decay measurements indicate a range of $4ns < \tau < 500ns$.[44]

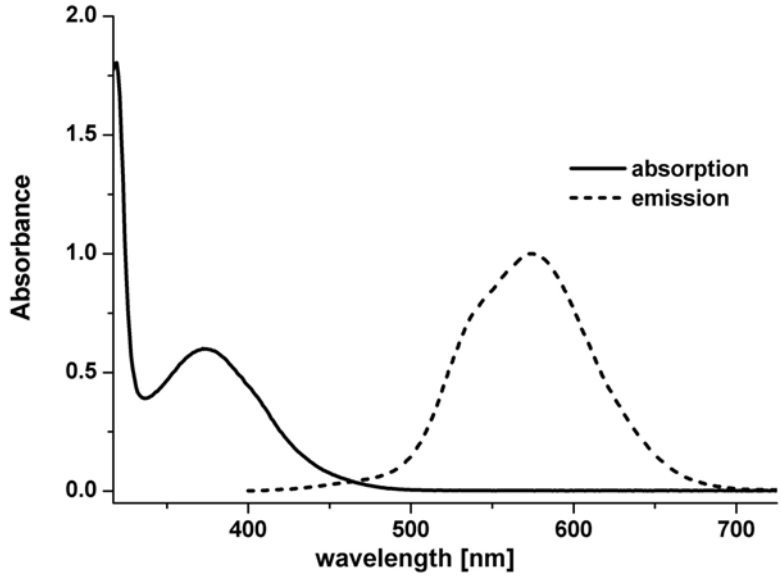

Figure 1.8 Absorption and emission spectra of [ReBr(bipy)$(CO)_3$] at room temperature in DMF (emission in arbitrary units).

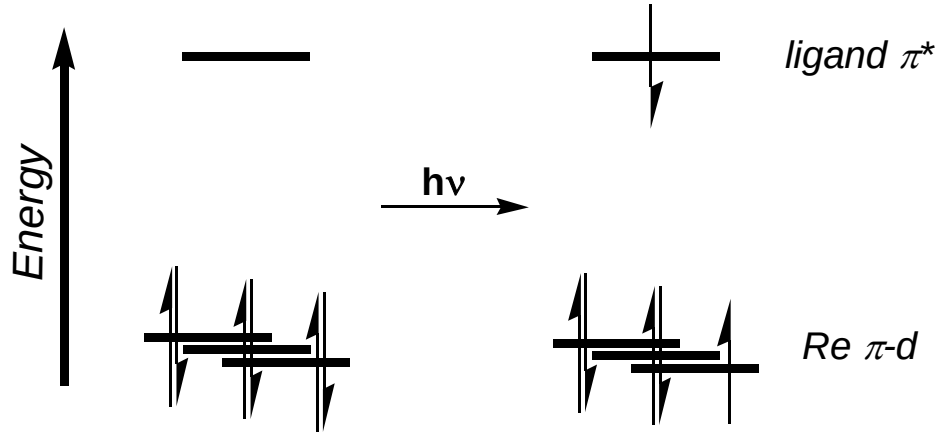

Figure 1.9 Schematic representation of electronic energy levels for the ground and excited states of [Re(Cl,Br)(diimine)$(CO)_3$] complexes (from ref.[43]).

Electrochemical studies of the complexes' ground states showed that an irreversible, oxidation occurs at potentials between +1 and +1.5V. In contrast, the one-electron reduction processes observed at potentials between –0.8 and –1.2V are reversible and the reduced species are stable enough to be studied by spectroscopy. Data from an EPR study of the electrochemically reduced species $[ReCl(bipy)(CO)_3]^-$ suggest that this compound is best described as a rhenium(I) complex bearing a anion radical ligand, $[Re^{I}Cl(bipy^{\bullet-})(CO)_3]$, rather than being a rhenium(0) species. [45]

With the same argumentation as for the discussion of Fig. 1.6, it is obvious that also in this case the excited state is both a more powerful reducing and oxidising agent than the ground state. For [ReCl(phen)(CO)$_3$] as an example, the energy gap E_{00} between ground and excited state was estimated to be 2.3V. The reversible, and therefore potentially useful, reduction process of the excited state of [ReCl(phen)(CO)$_3$] thus takes place at the high potential of +1.3V. From thermodynamics, the excited states of [ReX(diimine)(CO)$_3$] complexes could therefore oxidise very poor electron donors, even water, according to Scheme 1.10.

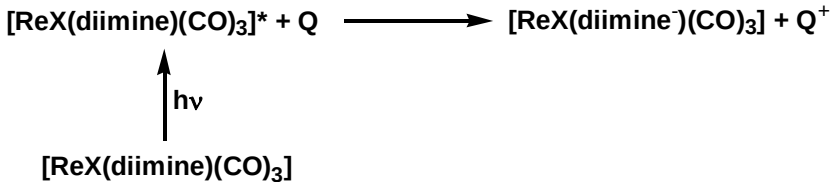

Scheme 1.10 Electron transfer from an electron donor (or quencher) Q to excited states of [ReX(diimine)(CO)$_3$] complexes.

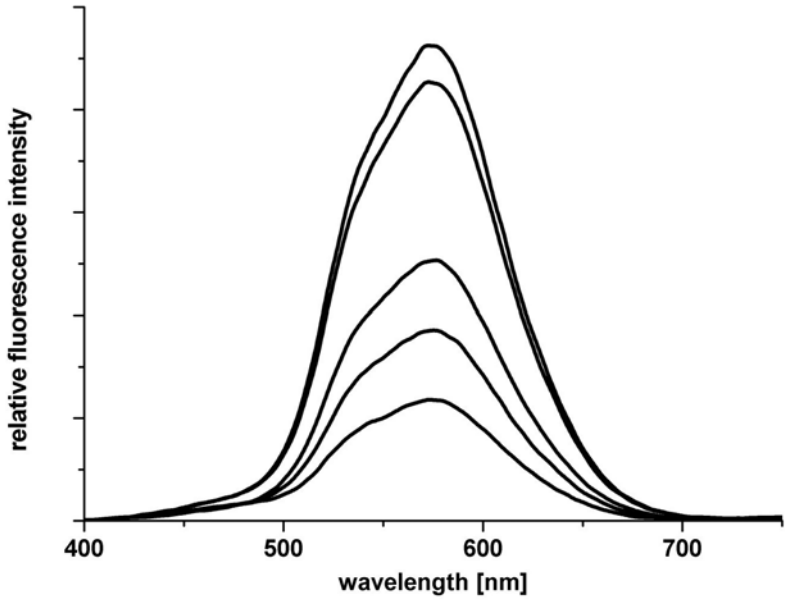

Figure 1.10 Fluorescence spectrum of a [ReBr(bipy)(CO)$_3$] solution (1mM in DMF) containing increasing concentrations of the electron donor triethanolamine (TEOA) (from top: no TEOA; 0.05M; 0.25M; 0.5M; 1M)

As the excited states of many [ReX(diimine)(CO)$_3$] complexes show fluorescence, the reactivity of the excited state with possible electron donors can be tested. If reduction of the excited state by the donor occurs, quenching of the fluorescence is observed (Fig. 1.10). Because of this phenomenon, suitable electron donors are often referred to as quenchers Q.

The reaction between excited state and quencher is a bimolecular process. The rate of this bimolecular reaction depends on the quenching constant k_q, the lifetime of the excited state τ and the concentration of the quencher [Q]. For a bimolecular reductive quenching, the ratio between the fluorescence intensity without (I_0) and with (I) quencher present follows the STERN- VOLMER equation:[31]

$$I_0/I = 1 + k_q \tau [Q] = 1 + K_{SV} [Q]$$

Therefore, a plot of I_0/I vs. [Q] results in a straight line with the gradient corresponding to the STERN- VOLMER constant K_{SV} (Fig. 1.11). If τ is known from time resolved spectroscopy measurements, the bimolecular reaction constant k_q of the quenching reaction can be calculated. As the excited states are radical species, k_q is often found to be in the range of 10^7-10^9 $s^{-1}mol^{-1}l$, so quenching reactions are close to diffusion control.

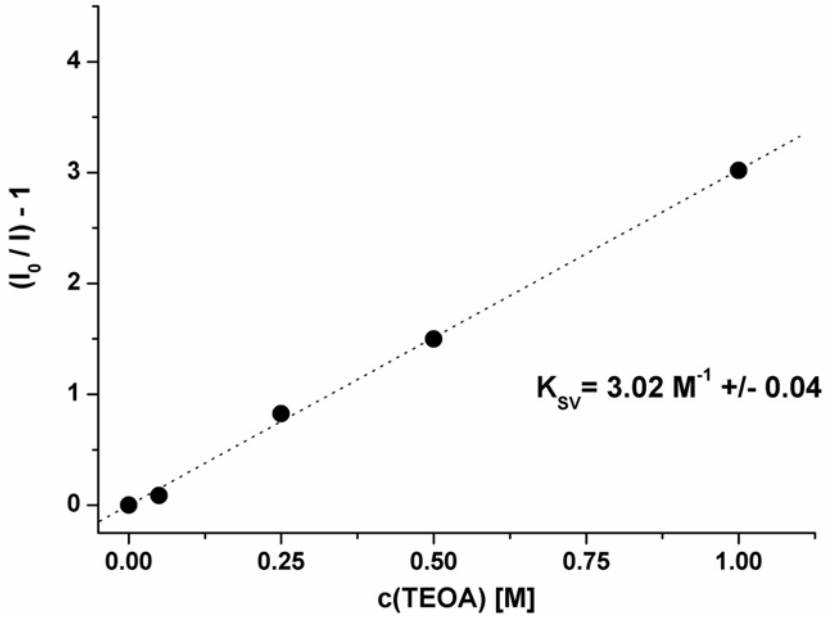

Figure 1.11 STERN-VOLMER plot for the quenching experiment shown in Fig. 1.10.

Unfortunately, only very few compounds with suitable redox potentials react with the excited states to form [ReX(diimine$^{\bullet-}$)(CO)$_3$]. Many substances were tested as possible electron donors for photochemical reactions of [ReX(diimine)(CO)$_3$] complexes, but only very few were found to be useful, among them especially secondary and tertiary amines. In one study on reductive quenching of [ReCl(phen)(CO)$_3$], different quenchers were tested

and their k_q measured.[43] A selection of the electron donors is given in Scheme 1.11. All compounds are amines, whose amine nitrogen gets irreversibly oxidised. The cationic nitrogen radicals produced decompose by a variety of very fast reactions, so the electron transfer process becomes irreversible even on the timescale of photochemical reactions.

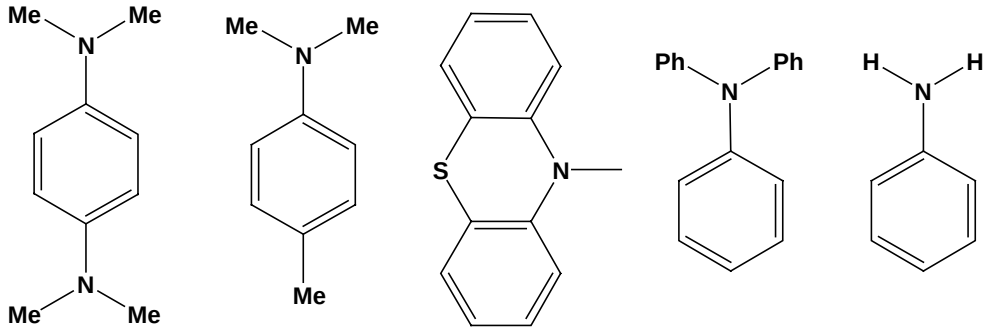

Scheme 1.11 Organic quencher molecules able to reduce the exited state of [ReCl(phen)(CO)$_3$]: tetramethyl-*p*-phenylendiamine (A), dimethyl-*p*-toluidine (B), 10-methylphenothiazine (C), triphenylamine (D), aniline (E).

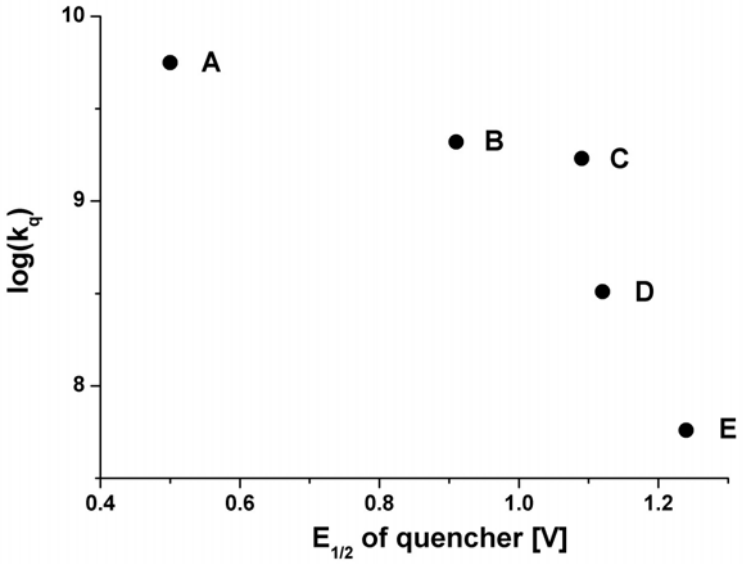

Figure 1.12 Correlation of k_q and ease of oxidation of the quencher (encoded as in Scheme 1.10) (from ref. [43]).

The quenching constant k_q determined for different quenchers showed no correlation with structure, but with the potential needed for quencher oxidation (Fig. 1.12). This indicated that there is no specific interaction between the rhenium complex and the quencher but merely an outer sphere electron transfer governed by redox thermodynamics. As the estimated redox potential of the excited state (+1.3V) is approached, k_q drops sharply

from diffusion control by a factor of 100. For quenchers of even higher $E_{1/2}$, no reaction was observed anymore.

It was known from the 1970's that some [ReX(diimine)$(CO)_3$] complexes were promising candidates with unusual properties for photocatalytic reduction reactions[46] as it was known that they absorb light in the visible region and form very strongly oxidising, long-lived excited states. The excited molecules are able to oxidise poor electron donors resulting in the formation of the stable, strongly reducing complex bearing an anionic radical diimine$^{\bullet-}$ ligand.

Yet it took until 1983 until a reaction was found by HAWAECKER et al. in Strasbourg using a [ReX(diimine)$(CO)_3$] complex for photocatalysis.[47] The unusual reaction discovered was the photocatalytic reduction of carbon dioxide to carbon monoxide by [ReCl(bipy)$(CO)_3$] using triethanolamine (TEOA) as electron donor (Scheme 1.12). This combination of reactants will be called the "Strasbourg system" in this thesis for convenience.

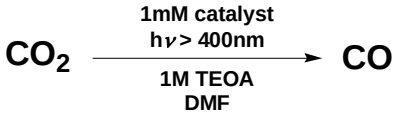

Scheme 1.12 Photochemical reduction of carbon dioxide using [ReCl(bipy)$(CO)_3$] as photocatalyst.

The reaction was the first example of a selective photochemical carbon dioxide reduction to CO (before only some reactions were discovered that simultaneously produced little CO and H_2). Right from the start the reaction mechanism of this unprecedented reaction was of great interest. Two electrons are required for the reduction of CO_2 to CO and a reduction potential of at least –0.5V is needed (Scheme 1.13).

Scheme 1.13 Reduction of carbon dioxide to carbon monoxide and water.

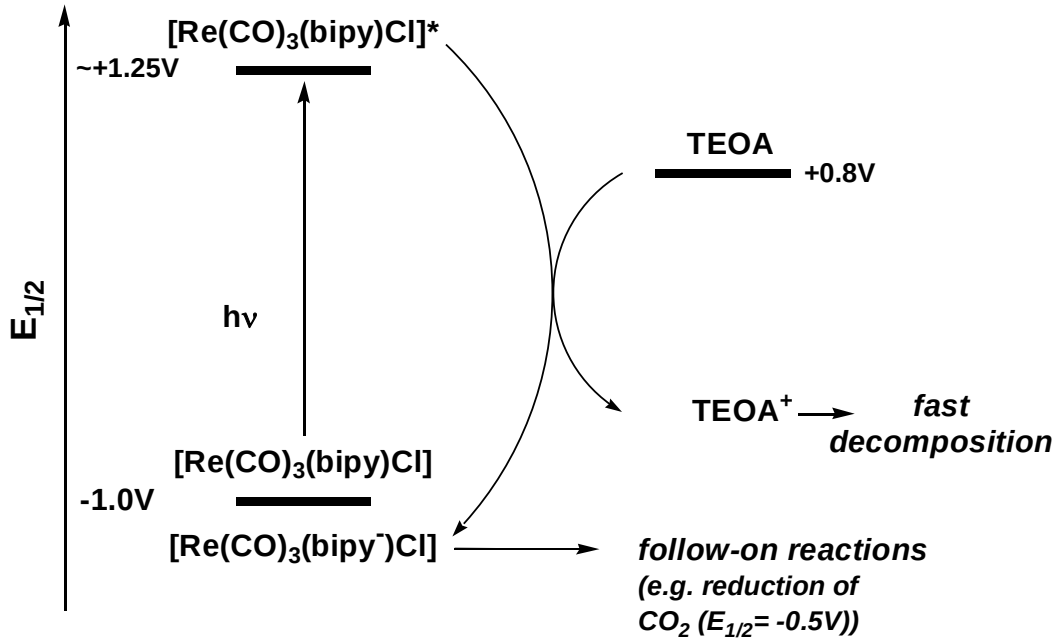

Scheme 1.14 Energy scheme for the photogeneration of $[ReCl(bipy^{\bullet-})(CO)_3]$ representing the first steps of the photocatalytic reduction of CO_2.

Based on the known photoreactions of $[ReX(diimine)(CO)_3]$ complexes, the first steps of the catalysis are well understood (Scheme 1.14): the excited complex $[ReCl(bipy)(CO)_3]^*$ is a strong oxidising agent ($E_{1/2}^*$= +1.25V) able to oxidise the donor TEOA (E= +0.8V). $TEOA^+$ decomposes rapidly and the reduced $[ReCl(bipy^{\bullet-})(CO)_3]$ ($E_{1/2}$= -1V) is able to transfer its electron to CO_2. Consecutively, the reaction was investigated in a number of studies[48-50], especially to learn more about its mechanism. Key results of these experiments were:

- the process exclusively produces CO, no H_2 is detected[47]
- use of $^{13}CO_2$ leads to the formation of ^{13}CO, indicating that CO_2 is indeed the reduction substrate[48]
- in experiments using $^{13}CO_2$, rhenium complexes bearing ^{13}CO ligands are formed, indicating that CO_2 is coordinated to rhenium at some point of the catalytic cycle[48]
- fluorescence measurements show that the excited state $[ReCl(bipy)(CO)_3]^*$ reacts with the donor TEOA following standard STERN-VOLMER kinetics (Fig.1.10 and 1.11)[50]

- no fluorescence quenching is observed for the substrate CO_2, so the formation of $[ReCl(bipy^{\bullet-})(CO)_3]$ seems to be the first step of catalysis[48]
- the activity of the system decreases slowly with time, indicating some decomposition of the catalyst[48]
- excess halide ligand results in faster and more stable catalysis[48]
- the formato complex $[Re(OOCH)(bipy)(CO)_3]$ might be a possible intermediate as it acts as an active catalyst as well[48]
- one group claims that the reaction leads to the formation of H_2 when carried out in a THF/H_2O mixture[51]
- the CO_2- bridged dinuclear species $[Re(bipy)(CO)_3]_2(CO_2)$ leads to the production of CO upon irradiation and is claimed as key intermediate[52]

Many questions remain, especially concerning details of the substrate reduction steps. No detailed explanation has so far been offered for the substrate coordination or the origin of the second electron needed for reduction. Despite the mechanistic uncertainties, the photocatalytic carbon monoxide reduction has raised large interest, as it was immediately realised that it represents a reaction closely related to the one necessary for the reductive side of the solar energy conversion concept of Scheme 1.8.

1.6 Aims of this work

The aim at the beginning of this work was the *development of a new technetium(I) synthon* including the cyanide ligand, based on the background described in chapter 1.1 and 1.2 of this part. As will be described in the initial parts of chapter 2, this goal could not be achieved. Nevertheless, the experiments carried out led to the development of a new labelling method for the $[^{99m}Tc(CO)_3]^+$- moiety. Model complexes synthesised for this method included the mixed cyano- carbonyl compounds $[Re(CN)(bipy)(CO)_3]$ and $[(Re(bipy)(CO)_3)_2(\mu\text{-}CN)]^+$.

The synthesis of the model compounds brought the unusual *photochemistry of the [ReX(diimine)(CO)$_3$] complexes* to our attention. The work was therefore rerouted to focus on the synthesis and investigation of other modifications of the known catalyst [ReCl(bipy)(CO)$_3$]. We expected to gain better insights into the reaction mechanism and additionally hoped to extend the range of application of the catalyst to the use of other solvents than dimethylformamide, other electron sources than triethanolamine or, even more important, other substrates than carbon dioxide - ideally water. The second aim of this thesis was therefore to develop a rhenium based, photoactive donor system for the reductive side of the water splitting system presented in Scheme 1.8.

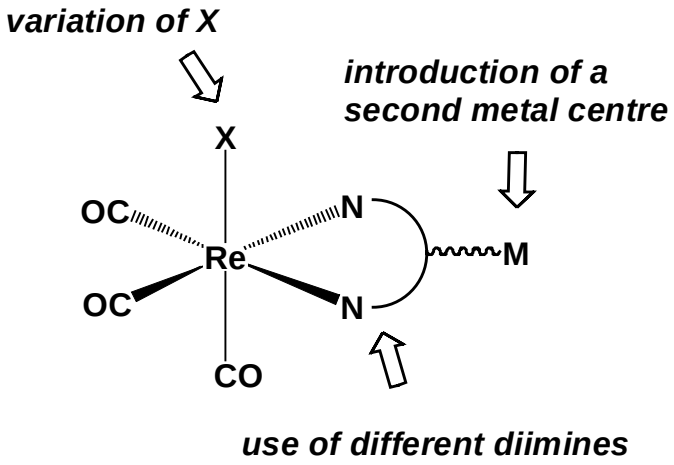

Scheme 1.15 Ideas for the synthesis of modified [ReX(diimine)(CO)$_3$] photocatalysts different from the originally used compound [ReCl(bipy)(CO)$_3$].

To achieve this, three possible sites for modification of the original catalyst [ReCl(bipy)(CO)$_3$] were identified (Scheme 1.15) and it was planned to probe the effects of a) different axial ligands X, b) different diimines and c) the introduction of a second metal centre on the catalyst's reactivity. Surprisingly, it was found that only three modifications of any kind had been probed concerning their effect on photochemical carbon dioxide reduction, in all three cases for single species. Nevertheless, these studies showed that a modification of the system was possible without losing catalytic activity. For variations of X, both cationic complexes [Re(bipy)(CO)$_3${P(OEt)$_3$}]$^{+}$[53] and [Re(bipy)(CO)$_3$(py)]$^{+}$[54] were found to be efficient catalysts. In another study, the complex [ReCl(CO)$_3$ptpy][55] (see chapter 4) was synthesised to

probe the influence of a different diimine than bipy. The complex retained catalytic activity, although it was found to be much less efficient than its bipy analogue.

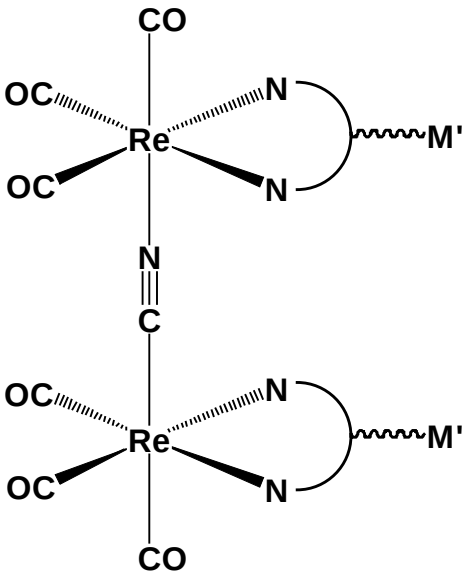

Scheme 1.16 Concept of a "horseshoe" complex, where two catalytically active metal fragments are coordinated to the flexible, photoactive scaffold of $[(Re(diimine)(CO)_3)_2(\mu\text{-}CN)]^+$.

The accidental synthesis of the cyano bridged dimeric complex $[(Re(bipy)(CO)_3)_2(\mu\text{-}CN)]^+$ also sparked the idea of using such complexes as flexible, photoactive scaffolds for the coordination of two additional metal fragments according to Scheme 1.16. The dimeric Rhenium complexes could have enhanced photochemical properties when compared with their mononuclear analogues. Additionally, the use of bridging bridging diimine ligands offers the possibility to coordinate two more catalytically active metals, thus yielding a horseshoe shaped four-metal complexes. The excited states of rhenium diimine complexes could be photoreduced in the presence of electron donors and the combination of these units with catalytically active metal centres such as copper, iridium or platinum could result in very interesting new systems for photoreductions. The syntheses and properties of such modified Strasbourg catalysts will be described in chapters 3 to 5, their photoreactivity in chapter 6.

References

[1] Bundesamt für Statistik Schweiz, Neuchâtel, **2004**.
[2] Statistics South Africa, Pretoria, **2002**.
[3] K. Schwochau, *Technetium: Chemistry and Radiopharmaceutical Applications*, **2000**.
[4] K. Schwochau, *Chem. Ztg.* **1979**, *103*, 41.
[5] P. V. Harper, R. Beck, D. Charleston, K. A. Lathrop, *Nucleonics* **1964**, *22*, 50.
[6] R. Alberto, in *Comprehensive Coordination Chemistry II, Vol. 5* (Ed.: J. A. M. McCleverty, Thomas J.), **2004**.
[7] P. Haefliger, N. Agorastos, B. Spingler, O. Georgiev, G. Viola, R. Alberto, *ChemBioChem* **2005**, *6*, 414.
[8] E. Deutsch, K. Libson, J. L. Vanderheyden, A. R. Ketring, H. R. Maxon, *Nucl. Med. Biol.* **1986**, *13*, 465.
[9] S. Jurisson, D. Berning, W. Jia, D. Ma, *Chem. Rev.* **1993**, *93*, 1137.
[10] F. X. Sundram, S. W. Yu, J. M. Jeong, S. Somanesan, J. Premaraj, M. M. Saw, B. S. Tan, *Ann. Acad. Med., Singapore* **2001**, *30*, 542.
[11] R. Alberto, R. Schibli, A. Egli, A. P. Schubiger, U. Abram, T. A. Kaden, *J. Am. Chem. Soc.* **1998**, *120*, 7987.
[12] R. A. Alberto, in *PCT Int. Appl. 2001025243*, Mallinckrodt Inc., USA, **2001**.
[13] R. Alberto, *Eur. J. Nucl. Med. Mol. Imaging* **2003**, *30*, 1299.
[14] H. U. Hund, U. Ruppli, H. Berke, *Helv. Chim. Acta* **1993**, *76*, 963.
[15] R. Schibli, K. Marti, K. Ortner, V. Gramlich, A. P. Schubiger, in *Technetium, Rhenium and Other Metals in Chemistry and Nuclear Medicine 6* (Eds.: M. Nicolini, U. Mazzi), **2002**.
[16] P. Kurz, D. Rattat, D. Angst, H. Schmalle, B. Spingler, R. Alberto, H. Berke, W. Beck, *Dalton Trans.* **2005**, 804.
[17] C. Pomp, S. Drueeke, H. J. Kueppers, K. Wieghardt, C. Krueger, B. Nuber, J. Weiss, *Z. Naturforsch. B* **1988**, *43*, 299.
[18] A. G. Sharpe, in *Comprehensive Coordination Chemistry, Vol. 2* (Ed.: G. Wilkinson), **1987**.
[19] J. E. Huheey, E. A. Keiter, R. L. Keiter, *Inorganic Chemistry*, 4th ed., **1993**.
[20] K. Nakamoto, *Infrared and Raman Spectra of Inorganic and Coordination Compounds*, 5th ed., **1997**.
[21] A. G. Sharpe, *The chemistry of cyano complexes of the transition metals*, **1976**.
[22] K. Schwochau, W. Herr, *Z. Anorg. Allg. Chem.* **1962**, *319*, 148.
[23] U. Steger, W. Achterberg, K. Blok, H. Bode, W. Frenz, C. Gather, G. Hanekamp, D. Imboden, M. Jahnke, M. Kost, R. Kurz, H. G. Nutzinger, T. H. W. Ziesemer, *Sustainable Development and Innovation in the Energy Sector*, **2005**.
[24] British Petroleum p.l.c., London, **2003**.
[25] A. Wokaun, *Erneuerbare Energien*, **1999**.
[26] DaimlerChrysler AG, Stuttgart, **2004**.

[27] A. F. Holleman, E. Wiberg, *Lehrbuch der Anorganischen Chemie*, 34th ed., **1995**.
[28] A. Coehn, *Ber.* **1910**, *43*, 880.
[29] E. K. Berner, R. A. Berner, *Global Environment - Water, Air, and Geochemical Cycles*, **1996**.
[30] G. J. Kavarnos, *Fundamentals of Photoinduced Electron Transfer*, **1993**.
[31] H. Henning, D. Rehorek, *Photochemische und photokatalytische Reaktionen von Koordinationsverbindungen*, **1988**.
[32] D. Rehm, A. Weller, *Ber. Bunsenges. Phys. Chem.* **1969**, *73*, 834.
[33] J. Sima, *Comments Inorg. Chem.* **1992**, *13*, 277.
[34] E. Amouyal, *Sol. Energy Mat. Sol. Cells* **1995**, *38*, 249.
[35] J. R. Bolton, *Sol. Energy* **1996**, *57*, 37.
[36] P. R. Chitnis, *Annu. Rev. Plant Physiol. Plant Mol. Biol.* **2001**, *52*, 593.
[37] C. Goussias, A. Boussac, A. W. Rutherford, *Phil. Trans. R. Soc. Lond. B* **2002**, *357*, 1369.
[38] K. N. Ferreira, T. M. Iverson, K. Maghlaoui, J. Barber, S. Iwata, *Science* **2004**, *303*, 1831.
[39] M. Kirch, J. M. Lehn, J. P. Sauvage, *Helv. Chim. Acta* **1979**, *62*, 1345.
[40] W. Hieber, H. Fuchs, *Z. Anorg. Allg. Chem.* **1941**, *248*, 256.
[41] R. Alberto, A. Egli, U. Abram, K. Hegetschweiler, V. Gramlich, P. A. Schubiger, *J. Chem. Soc., Dalton Trans.* **1994**, 2815.
[42] W. Hieber, H. Fuchs, *Z. Anorg. Allg. Chem.* **1941**, *248*, 269.
[43] J. C. Luong, L. Nadjo, M. S. Wrighton, *J. Am. Chem. Soc.* **1978**, *100*, 5790.
[44] K. Kalyanasundaram, *J. Chem. Soc., Faraday Trans. 2* **1986**, *82*, 2401.
[45] W. Kaim, S. Kohlmann, *Chem. Phys. Lett.* **1987**, *139*, 365.
[46] D. J. Stufkens, *Comments Inorg. Chem.* **1992**, *13*, 359.
[47] J. Hawecker, J. M. Lehn, R. Ziessel, *J. Chem. Soc., Chem. Comm.* **1983**, 536.
[48] J. Hawecker, J. M. Lehn, R. Ziessel, *Helv. Chim. Acta* **1986**, *69*, 1990.
[49] C. Kutal, M. A. Weber, G. Ferraudi, D. Geiger, *Organometallics* **1985**, *4*, 2161.
[50] C. Kutal, A. J. Corbin, G. Ferraudi, *Organometallics* **1987**, *6*, 553.
[51] C. Pac, K. Ishii, S. Yanagida, *Chem. Lett.* **1989**, 765.
[52] Y. Hayashi, S. Kita, B. S. Brunschwig, E. Fujita, *J. Am. Chem. Soc.* **2003**, *125*, 11976.
[53] O. Ishitani, M. W. George, T. Ibusuki, F. P. A. Johnson, K. Koike, K. Nozaki, C. Pac, J. J. Turner, J. R. Westwell, *Inorg. Chem.* **1994**, *33*, 4712.
[54] H. Hori, J. Ishihara, K. Koike, K. Takeuchi, T. Ibusuki, O. Ishitani, *J. Photochem. Photobiol. A* **1999**, *120*, 119.
[55] G. Calzaferri, K. Haedener, J. Li, *J. Photochem. Photobiol. A* **1992**, *64*, 259.

2. SYNTHESIS AND REACTIVITY OF Tc^{I} / Re^{I} CYANO COMPLEXES

The first part of experiments reported in this thesis was directed towards the development of a $^{99m}Tc^{I}$ cyano moiety that should possess similar advantageous properties like the well-established $[^{99m}Tc^{I}(CO)_3]^+$ core: small size, stability in water, diverse substitution chemistry and a simple access route from $^{99m}TcO_4^-$ using a "kit reaction" in aqueous solution. As the cyano complexes $[M(CN)_6]^{5-}$ of technetium(I) or rhenium(I) had already been prepared around 1960, a study of their synthesis and substitution behaviour seemed to be a promising starting point.

2.1 Synthesis and substitution reactions of $[(Tc,Re)^{I}(CN)_6]^{5-}$

CLAUS and LISSNER first synthesized $[Re(CN)_6]^{5-}$ in 1958[1] for an experimental study aiming at the synthesis of rhenium compounds in low oxidation states. A rhenium(IV) starting material, $K_2[ReCl_6]$ was used and reduced in water to rhenium(I) by potassium amalgam in the presence of a large excess of cyanide (Scheme 2.1). Four years later, SCHWOCHAU and HERR applied a similar method for the preparation of $[Tc(CN)_6]^{5-}$.[2] In this case, the synthesis was possible starting directly from $[Tc^{VII}O_4]^-$. In both cases the analytical data of the complexes is limited to elemental analysis, vibrational spectroscopy, conductivity measurements and X-ray powder diffraction. All are in agreement with a formulation of the complexes as $K_5[M(CN)_6]$, but purity, stability or substitution behaviour of the complexes was not discussed.

$$K_2[Re^{IV}Cl_6] + 3\,K + 6\,KCN \longrightarrow K_5[Re^{I}(CN)_6] + 6\,KCl$$

$$K[Tc^{VII}O_4] + 6\,K + 6\,KCN + 4\,H_2O \longrightarrow K_5[Tc^{I}(CN)_6] + 8\,KOH$$

Scheme 2.1 Original syntheses of $K_5[M(CN)_6]$.

To adapt the original synthesis for possible radiopharmaceutical applications, it was first necessary to find a different reducing agent than the toxic amalgam. As it was known that a very strong, water soluble reducing agent was needed to replace the potassium originally used, sodium dithionite $Na_2S_2O_4$ was chosen for initial experiments. Additionally, it had

been found that the isolation of the very water soluble $K_5[M(CN)_6]$ complexes from a solution containing a large excess of potassium cyanide was very difficult. Probably this was the reason why no pure products could be obtained.[1] For $[Tc(CN)_6]^{5-}$ the thallium salt $Tl_5[Tc(CN)_6]$ could be isolated[2], but as this is insoluble in water and therefore not useful for further studies of the properties.

Different reaction conditions were applied and best results for the synthesis of $K_5[Re(CN)_6]$ (**4**) were obtained for the reaction conditions shown in Scheme 2.2. The use of a water- methanol mixture and a high potassium concentration caused the product to precipitate from the reaction mixture, which greatly simplified purification. The olive- green product obtained showed the characteristic IR spectrum already reported before with a very low cyanide stretching frequency at 1935cm^{-1}.[3] This is among the lowest vibration frequencies reported for cyano complexes[4], indicating that the product is a very electron rich compound.

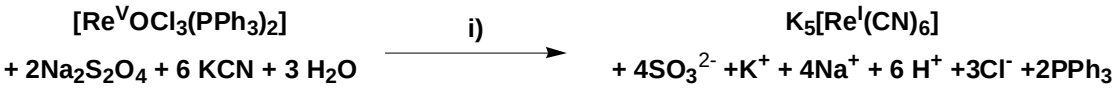

Scheme 2.2 Improved synthesis of $K_5[Re(CN)_6]$ (**4**). i) 0.5M KOH / MeOH, 90°C, 12h.

The dried product is stable in air for weeks and very soluble in water. The compound can be dissolved in nitrogen- or argon- purged water and dried again without changing the IR or mass spectrum. The intense olive green colour of such an aqueous solution changes slightly to a somewhat paler light green over hours. Measurements using a cyanide selective electrode in basic aqueous solution at constant ionic strength showed that the complex slowly loses cyanide when dissolved. When the equilibrium is reached (after ~5h) about 1.4 equivalents of cyanide have been released (Fig. 2.1), so at least three, and possibly more, cyano species must coexist in aqueous solution according to Scheme 2.3. Such equilibria are quite common for cyanide complexes.[5]

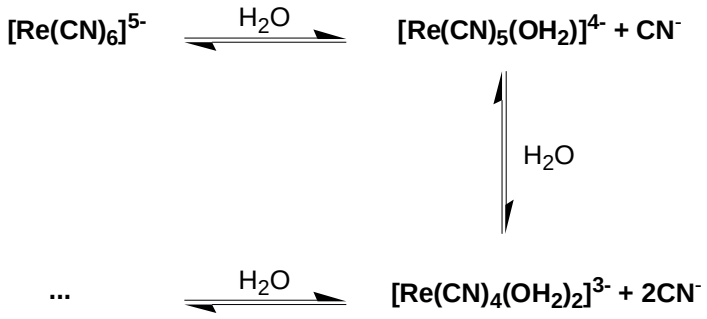

Scheme 2.3 Probable equilibria of **4** when dissolved in basic, aqueous solution.

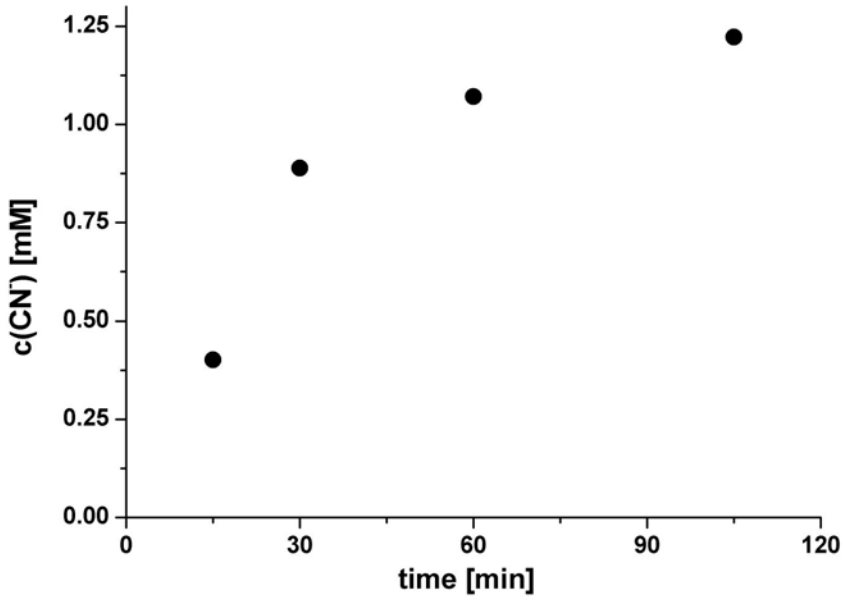

Figure 2.1 Concentration of free cyanide as a function of time for a 1mM solution of **4** at pH≈11, 50mM KNO_3.

The ions $[M(CN)_6]^{5-}$ in aqueous solution were found to be very air sensitive, the technetium even more than the rhenium complex. If an aqueous solution of **4** is exposed to air for some hours the solution becomes bright yellow. The characteristic cyanide IR band at 1935cm^{-1} completely disappears with a new cyanide band appearing at 2088cm^{-1}, the region typical for cyano complexes of rhenium(III) ($\nu_{CN}([Re^{III}(CN)_7]^{4-})$= 2092$cm^{-1}$).[6] So rhenium(III) cyano species seem to form fast when the complex is exposed to air. But follow-on oxidations must also lead to significant amounts of rhenium(V) cyano species: crystals of such compounds were obtained in numerous cases from the many unsuccessful trials to grow crystals of $K_5[Re(CN)_6]$ (e.g. Fig. 2.2).

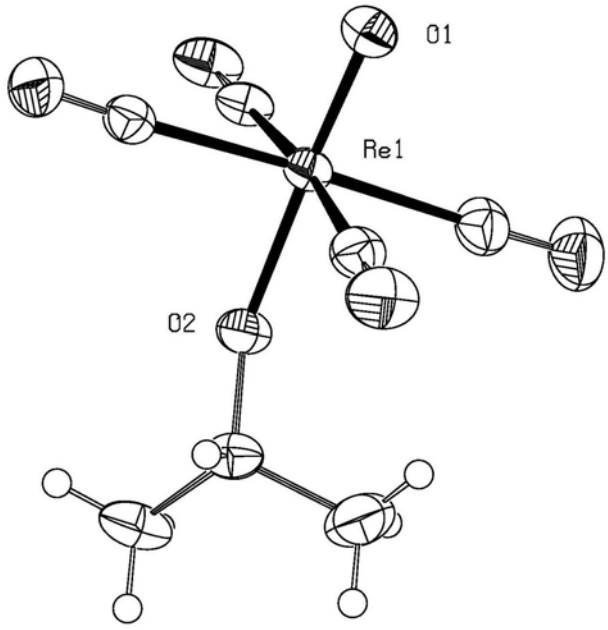

Figure 2.2 Molecular structure of the anion of $[K(Krytofix_{222})]_2[ReO(CN)_4(O^iPr)] \cdot 2$ dioxane, accidentally obtained from a crystallization trial of **4** in the presence of $Krytofix_{222}$.

The same oxidation seems to occur in the technetium case. When a reduction of NBu_4TcO_4 is carried out under the same conditions as for the preparation of **4**, a green solution is obtained, which turns yellow immediately at exposure to traces of air. A ^{99}Tc NMR of this yellow solution showed only one signal, at –1330ppm, the chemical shift reported for $[Tc^{III}(CN)_7]^{4-}$ (the heptacyano complex can form as the solution contains a large excess of KCN from the synthesis).[7] Due to its sensitivity to air and its very good solubility, it was not possible to isolate $K_5[Tc(CN)_6]$ in a similar way as **4**. Similarly, treatment of $^{99m}TcO_4^-$ generator eluate at room temperature with KCN (0.1mM) and $Na_2S_2O_4$ (1mM) resulted in the quantitative conversion of $^{99m}TcO_4^-$ into a new species within 30min according to HPLC, most probably $[^{99m}Tc(CN)_6]^{5-}$.

Substitution reactions of both the rhenium and the ^{99m}technetium cyanides in aqueous solutions were investigated. Reactions with different bi- and tridentate ligands (en, dien, pico, hisam, 9S3, bipy, phen) were investigated, all resulting in the formation of uncharacterised mixtures of many different species according to HPLC analysis.

It can be concluded from these experiments that it is possible to generate $[M(CN)_6]^{5-}$ fragments in water using dithionite as reducing agent in the presence of cyanide. At least two cyanide ligands seem to be quite labile in aqueous solution and the hexacyano species is apparently in equilibrium with complexes containing only five, four and probably even fewer cyanide ligands. It seems possible to use the same method for the formation of a $[^{99m}Tc(CN)_6]^{5-}$ fragment as well.

Nevertheless, the air sensitivity of the complexes is a big disadvantage combined with the fact that no well defined products form in reactions with simple chelate ligands. The $[M(CN)_6]^{5-}$ fragments therefore did not appear to be promising starting points for the development of a new ^{99m}Tc- synthon and the route was not investigated any further.

2.2 Synthesis and substitution reactions of the $[(Tc,Re)^{I}(CN)_4(NO)]^{2-}$ fragment

An important property of the $[M(CN)_6]^{5-}$ fragments is that they are very electron rich, which is apparent from the very low vibration frequency of the cyanide stretch. This also causes the air sensitivity of the aqueous solutions. The reason is the large negative charge of the complexes and the presence of the σ- donating cyanide ligands. It was therefore considered to prepare cyano- complexes of Re(I) and Tc(I) containing good π- acceptors in order to reduce the electron density of the metal. At first, the combination of cyanide and the very strong π- acceptor nitrosyl was investigated.

Scheme 2.4. Original synthesis reported for $K_3[Re^{I}(CN)_5(NO)]$. i) 10eq. KCN, 30eq. KOH, 15eq. $NH_3OH{\cdot}Cl$, H_2O, 90°C, 1h.

A synthesis of the mixed cyano nitrosyl complex $K_3[Re^{I}(CN)_5(NO)]$ in aqueous solution was reported in 1984 by BHATTACHARYYA and ROY (Scheme 2.4), but only limited analytical data of the product was presented.[8] The procedure involves direct reduction of perrhenate by hydroxylamine in the presence of cyanide.

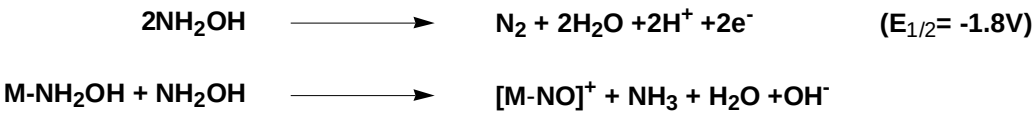

Scheme 2.5. Two of many proposed reactions of hydroxylamine.

Hydroxylamine is known to act both as reducing agent and nitrosyl source in such reactions. There are many proposed mechanisms how this might occur[9, 10]; two examples are given in Scheme 2.5.

In 1995, an additional investigation showed that a reaction similar to Scheme 2.4, but using only four equivalents of KCN, indeed results in the formation of $[Re^{I}(CN)_4(H_2O)(NO)]^{2-}$, isolated and characterised as the $AsPh_4$-salt.[11] A crystal structure analysis of the compound confirmed an octahedral coordination geometry with four linear CN^- and one linear NO^+ ligand *trans* to the coordinated water molecule. Due to the presence of the strong π- acceptor NO^+ and the smaller negative charge, the complex is much less electron rich, reflected in a higher ν_{CN} of 2075cm^{-1} compared to 1935cm^{-1} for $[Re(CN)_6]^{5-}$. Mixed cyano nitrosyl complexes were therefore considered to be promising candidates in the search for new rhenium(I)/ technetium(I) precursors.

The synthesis of $[Re^{I}(CN)_4(H_2O)(NO)]^{2-}$ as reported in 1995 could be reproduced in a similar fashion, and the red potassium salt $K_2[Re^{I}(CN)_4(H_2O)(NO)]$ (**5**) was isolated. In contrast to the cyano complex $[Re(CN)_6]^{5-}$, this compound is stable in water for weeks, even if exposed to air. Additionally, it was found that the synthesis does not even require the exclusion of air. For aqueous solutions of **5**, no free cyanide could be detected by ion selective electrode measurements after 24h.

It was also possible to carry out the similar reaction of hydroxylamine and cyanide with $^{99m}TcO_4^-$ generator eluate, for which HPLC analysis indicated the full conversion of pertechnetate to a single new species after 30min at 90°C.

These initial results were very promising but unfortunately it proved impossible to carry out any substitution reactions on the formed species. The same set of bi- and tridentate ligands as in the case of $[M(CN)_6]^{5-}$ was

tested but instead of mixtures resulting from a set of possible substitutions, no substitution reactions at all could be observed by either HPLC or UV spectroscopy. Instead, the mixed cyano nitrosyl complexes proved to be completely inert. Substitution of the coordinated water by thiourea has been reported for **5** and could be reproduced for rhenium, but no reaction was observed when thiourea was added to a vial containing the ^{99m}Tc cyano nitrosyl complex. Most probably the competition by free cyanide present in the mixture is too strong in this case.

Thus, the introduction of nitrosyl led to the formation of air stable rhenium(I) or technetium(I) cyanides, but their cyano ligands are too strongly bound to allow substitution reactions by chelate ligands. As a consequence, the investigation of the cyano nitrosyl combination was stopped and the combination of cyanide with the slightly weaker π-acceptor ligand carbonyl considered next in order to find a better substitution behaviour combined with oxidation stability.

2.3 Reactions of the $[(Tc,Re)^{I}(CO)_3]^{+}$ moiety with cyanide – investigation of the complexes $[(Tc,Re)(CN)_3(CO)_3]^{2-}$

A different strategy was applied for the synthesis of mixed cyano carbonyl complexes. The synthetic route presented for mixed cyano nitrosyl compounds involved the reduction of the high valent rhenium or technetium precursors in the presence of both ligands to form the mixed compound directly in one step. In a previous work it was found that mixed carbonyl nitrosyl compounds could be prepared in good yield and purity using a stepwise introduction of the ligands.[12] First, the tricarbonyl rhenium(I) precursor $[ReCl_3(CO)_3]^{2-}$ is prepared according to Scheme 1.9. Then, this compound is reacted with NO^{+} resulting in the substitution of only one carbonyl and formation of $[ReCl_3(CO)_2(NO)]^{-}$ according to Scheme 2.6.

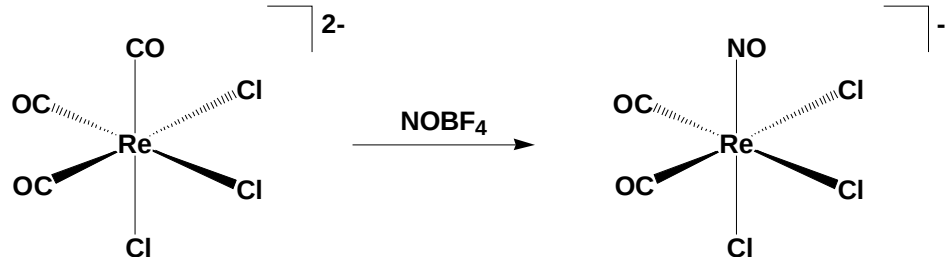

Scheme 2.6 Synthesis of the mixed carbonyl nitrosyl complex $[ReCl_3(CO)_2(NO)]^-$.

Like NO^+, which is able to substitute one CO ligand, CO can also replace itself in M^I carbonyl complexes: under high pressure of ^{13}CO, the exchange of ^{12}CO for ^{13}CO was detected by NMR for $[Tc(H_2O)_3(CO)_3]^+$ in water within days.[13] It therefore seemed possible that the preparation of mixed cyano carbonyl complexes might be achieved by substitution of carbonyl by cyanide in an analogous way.

A reaction of cyanide with rhenium(I) carbonyl had already been reported in 1968 (Scheme 2.7)[14] and it was found that no more than two CO ligands are substituted when $[Re(CO)_5Cl]$ is reacted with CN^- under harsh conditions, thus leaving the '*fac*-$[Re(CO)_3]^+$' core intact. A similar result for the reaction of $[M(H_2O)_3(CO)_3]^+$ with CN^- would demonstrate once again the different reactivity of the ligand CN^- when compared to its isoelectronic counterparts NO^+ and CO.[15]

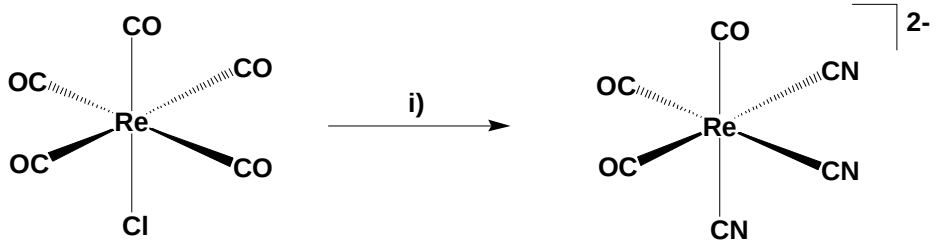

Scheme 2.7 Reported synthesis of the mixed cyano carbonyl complex $[Re(CN)_3(CO)_2]^{2-}$. i) 3eq. KCN, EtOH, 150°C, 3d.

A reaction of $[Re(H_2O)_3(CO)_3]^+$ with an excess of KCN in water at pH≈10 resulted in the formation a white precipitate. A single crystal analysis revealed the product to be the tetranuclear cluster $[(CO)_3(\mu\text{-}OH)Re(\mu\text{-}CN)Re(\mu\text{-}OH)(CO)_3]_2^{2-}$ (**6**) (Figure 2.3). This complex is exceptionally stable: attempts to cleave it with CN^- or strong chelate ligands like bipy were not successful. Treatment of **6** with acid resulted in the decomposition of the tetramer to regain $[Re(H_2O)_3(CO)_3]^+$.

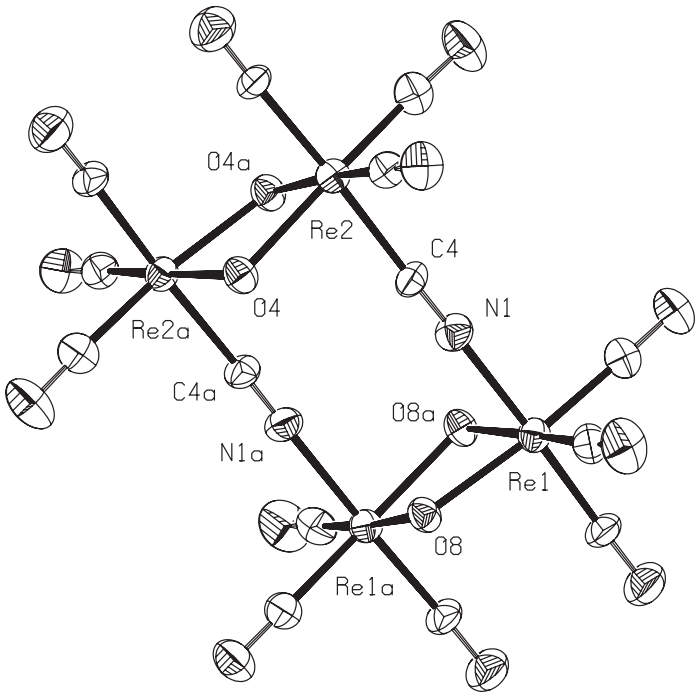

Figure 2.3 ORTEP drawing of the anion of **6**.

To avoid the formation of the unreactive tetranuclear cluster, the same reaction was carried out in methanol. After 2h at room temperature $[Re(H_2O)_3(CO)_3]^+$ was quantitatively converted to one single new species as detected by HPLC. No further change was observed after heating the reaction mixture for another 48h. Addition of $AsPh_4Cl$ to an aqueous solution of the reaction product precipitated the $AsPh_4$- salt of $[Re(CN)_3(CO)_3]^{2-}$ (**8**). The technetium complex $[^{99}Tc(CN)_3(CO)_3]^{2-}$ (**7**) could be synthesized and isolated correspondingly.

Evidence for the facial coordination of three carbonyl and three cyanide ligands in $[M(CN)_3(CO)_3]^{2-}$ was provided by IR spectroscopy. Two strong CO and two weak CN^- bands could be observed, characteristic for C_{3v} symmetry. For products obtained from reactions with isotope enriched $K^{13}CN$ (90% ^{13}C) (**7***, **8***) only the set of bands at higher wavenumbers shifted significantly (Figure 2.4). Thus, they belong unambiguously to the coordinated CN^- ligands. Since this observation indicates decoupling of CN^- and CO vibrations to a great extend, it seemed justified to perform a Cotton- Kraihanzel force field analysis[16] for each set of ligands separately. The calculated vibrational force constants indicate a much stronger bond within the CN^-

ligand (17.5 and 17.2 mdyn/Å for M= Tc and M= Re, respectively) compared to the values for the coordinated CO (16.2 mdyn/Å for both).

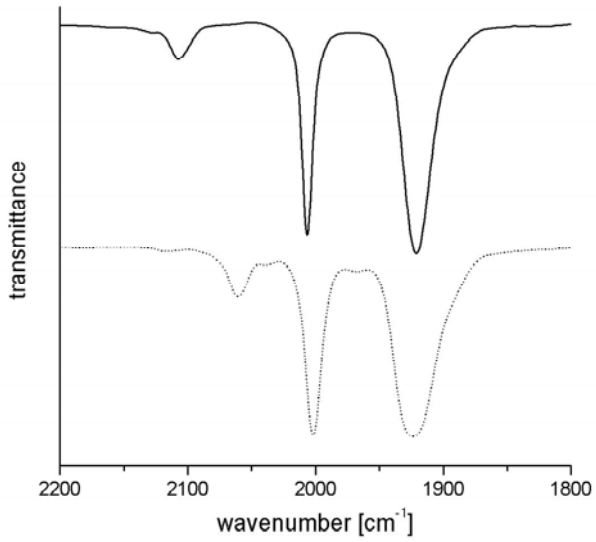

Figure 2.4 IR spectra of **8** (straight line) and the 70% cyanide ^{13}C enriched species **8***.

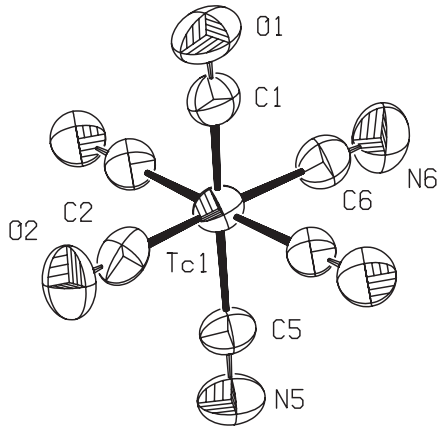

Figure 2.5 Molecular structure of the anion of **7**.

A crystallographic analysis of both $[M(CN)_3(CO)_3]^{2-}$ complexes confirmed the facial coordination of three cyanide and three carbonyl ligands around the metal center in a nearly perfect octahedron (Figure 3). For **7**, one *trans* pair of CO and CN^- ligands was disordered. For the other ligand pairs, CO and CN^- ligands can be crystallographically distinguished. The average metal-carbon bond distances $M\text{-}C(O)_{av}$ is 1.93(1) Å for both $[M(CN)_3(CO)_3]^{2-}$ complexes which is much shorter than the 2.14(1) Å found for $M\text{-}C(N)_{av}$. No significant difference was found for the bond length within the ligands, whereas both complexes show smaller bond angles for NC-M-CN compared to OC-M-CO (Table 2.1).

As expected for a complex with C_{3v} symmetry, the ^{99}Tc NMR spectrum of **7** consists of a sharp singulet signal at –2198 ppm ($\Delta_{1/2}$ = 6.3 Hz), shifted more than 1000 ppm upfield compared to $[Tc(H_2O)_3(CO)_3]^{+}$[13] and therefore indicating a more electron-rich Tc^{I} complex.[7] Due to the coupling of three equivalent cyanide ligands to ^{99}Tc (I=9/2), the ^{99}Tc NMR spectrum of **7*** prepared with ^{13}C enriched $K^{13}CN$ showed a strong quadruplet as well as a weaker triplet and a very weak doublet for the doubly and mono ^{13}C labeled complexes (Figure 2.6). In the ^{13}C NMR spectrum a decet was observed. Due to different relaxation times for the various spin states of ^{99}Tc, the outer lines of the ^{13}C spectrum are sharper than the inner. The $^{1}J_{99Tc,13C}$ coupling constant is 186 Hz, much smaller than the only other $^{1}J_{99Tc,13C}$ coupling constant known to date with 354 Hz for $[Tc(H_2O)_3(CO)_3]^{+}$.[13] The main reason for the smaller coupling constant of the cyano complex might be the longer Tc-C distances for CN^{-} when compared to CO bound to Tc. Addition of 10 equiv of NaCN to the sample at room temperature did not result in any exchange of $^{13}CN^{-}$ for $^{12}CN^{-}$ as evident from the unchanged coupling pattern of the ^{99}Tc NMR spectrum even after several days.

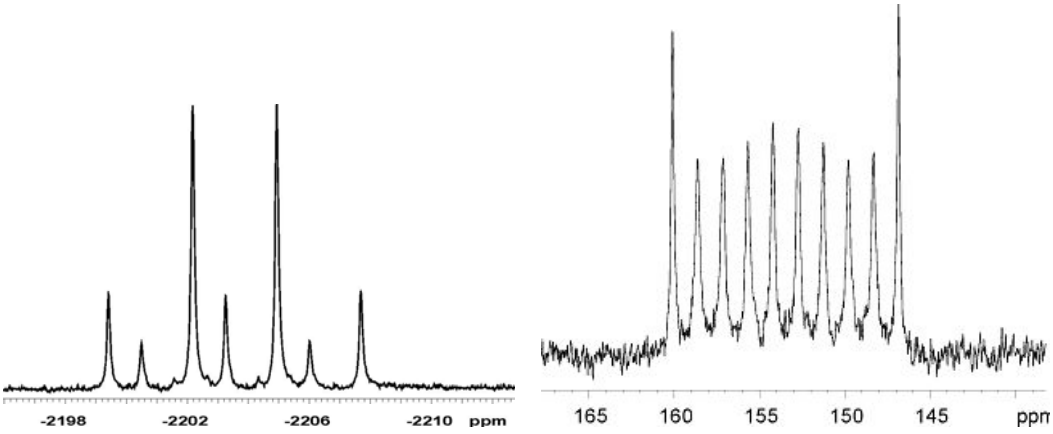

Figure 2.6 NMR spectra for ^{99}Tc (left) and ^{13}C (right) of the ca. 70% cyanide ^{13}C enriched **7*** showing the coupling between ^{99}Tc (I=9/2) and ^{13}C (I=1/2).

Metal complexes containing the two isoelectronic ligands cyanide and carbon monoxide belong to the most fundamental compounds of inorganic chemistry. The first complex containing a combination of both ligands, $[Fe^{II}(CN)_5(CO)]^{3-}$, was reported more than 100 years ago.[17] The recent discovery of $[Fe(CN)_x(CO)_y]$ units as catalytic centers of NiFe and Fe-only hydrogenases[18] has sparked a revival in studies of metal cyano carbonyl

compounds. The analytical data obtained in this work for $[Tc(CN)_3(CO)_3]^{2-}$ and $[Re(CN)_3(CO)_3]^{2-}$ allow comparisons with the data obtained for other compounds in the series $[M(CN)_3(CO)_3]^{n-}$. Therefore **7** and **8** are useful study cases for a deeper understanding of cyano and carbonyl complexes in general but also for the hydrogenase enzymes in particular.

group	VIa		VIIa		VIIIa
	Mo[a]	Mn[b]	Tc	Re	Ru[b]
d_{av}(M – CO) [Å]	[c]	1.79	1.93	1.93	1.96
d_{av}(M – CN) [Å]	[c]	2.01	2.14	2.14	2.07
$\angle_{av}$(OC-M-CO) [°]	[c]	92.7	91.1	91.6	93.7
$\angle_{av}$(NC-M-CN) [°]	[c]	87.7	88.5	87.5	87.8
f_{CO} [mdyn/Å] [d]	14.1	16.0	16.2	16.2	17.8
f_{CN} [mdyn/Å] [d]	16.4	17.0	17.5	17.2	18.1

Table 2.1. Structural data and force constants for complexes $[M(CN)_3(CO)_3]^{n-}$ of groups VIa, VIIa and VIIIa of the periodic table.
[a] data calculated from ref.[19]; [b] data from ref.[20]; [c] no data shown as CN^- and CO were found to be completely disordered in the crystal; [d] calculated from the IR stretching modes according to ref.[16]

The direct neighbours of Tc in the periodic table are of course of special interest. Important data are given in table 2.1. Clear trends in the bonding properties are obvious when comparing the two ligands and the various metals: (i) due to stronger π- backbonding in the case of CO, metal-carbonyl bonds are significantly shorter than metal- cyanide bonds, (ii) stronger repulsions between the more tightly bound carbonyl ligands result in larger cone-angles for the tricarbonyl moieties when compared to the tricyano parts, (iii) comparing metal- ligand distances, the first-row transition metal Mn is significantly smaller than second-row Tc, Ru and the lanthanide-contracted Re (the latter three having very similar sizes), (iv) as the negative charge of the complexes decreases from group VIa to VIIIa, π-backbonding gets weaker, thereby increasing the ligand stretching force constants and decreasing the differences between f_{CN} and f_{CO}.

Concerning a potential use of the cyano carbonyl compounds for radiopharmaceutical applications, the detailed analysis of the properties of the complexes $[M(CN)_3(CO)_3]^{2-}$ showed:

- unlike nitrosyl, cyanide is not able to substitute coordinated carbonyl ligands in tricarbonyl complexes, so only cyano *tri*carbonyl complexes seem accessible.
- in the presence of excess cyanide, the very stable $[M(CN)_3(CO)_3]^{2-}$ complexes form for which no further substitution reactions are possible

2.4 [2+1] Labelling of $[(Tc,Re)^{I}(CO)_3]^{+}$ using bidentade ligands and cyanide

It was apparent from the investigation of the reaction of cyanide with the $[M(H_2O)_3(CO)_3]^{+}$ complexes that very stable complexes are formed. The reason for this stability is most likely a "push- pull" interaction of the good σ- donor CN^{-} and the strong π- acceptor CO coordinated *trans* to each other in the complex. In an additional set off experiments, it was probed whether this strong binding of the small cyanide ligand to the $[M(CO)_3]^{+}$ unit could be used in a so called "[2+1]" labelling approach.

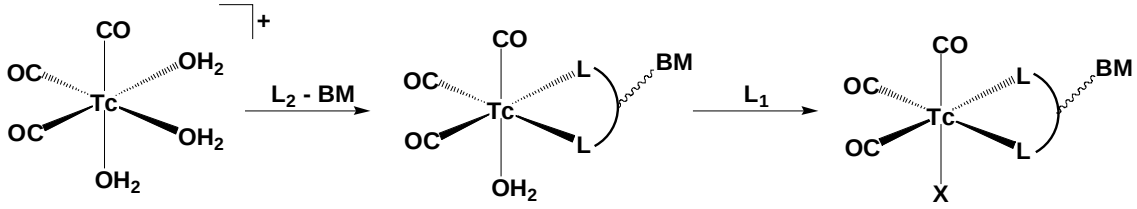

Scheme 2.8 Mixed ligand concept illustrating the [2+1] pathway for linking a biomolecule (BM) to $[^{99m}Tc(CO)_3]^{+}$.

As mentioned above, tridentate ligands are normally used for linking a biomolecule to the $[^{99m}Tc(CO)_3]^{+}$ core (Scheme 1.3).[21] Because the introduction of tridentate ligands on a biomolecule is often difficult, the [2+1] approach was introduced as an alternative (Scheme 2.8).[22] In this method, complexes of the type $[^{99m}Tc(H_2O)(CO)_3(L_2\text{-BM})]$ are generated first by reacting $[^{99m}Tc(H_2O)_3(CO)_3]^{+}$ with a bidentate ligand L_2 connected to a biomolecule. A monodentate ligand X is then introduced to block the last available coordination site on the technetium centre in order to avoid unwanted crosslink reactions otherwise observed for this site in serum. The results of the previous investigation indicated that cyanide might be a very

good candidate for the ligand X, as it is small and binds tightly to $[^{99m}Tc(CO)_3]^+$.

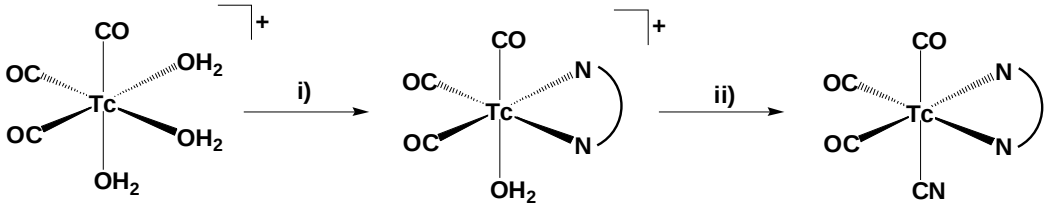

Scheme 2.8 [2+1] labelling of $[^{99m}Tc(CO)_3]^+$ using bidentate nitrogen ligands and cyanide. i) 10^{-4}M L_2, 90°C, 30min. ii) $5{\cdot}10^{-5}$M KCN, 90°C, 30min.

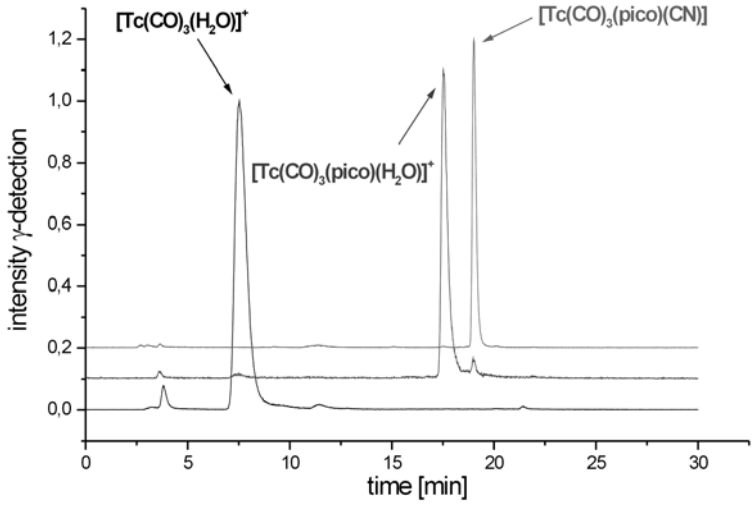

Figure 2.7 HPLC traces (γ- detection) for the [2+1] labelling of $[^{99m}Tc(CO)_3]^+$ using pico and cyanide.

With the aim to obtain neutral complexes as final products (these are most likely to be able to cross the membranes of cells), experiments were carried out using neutral, bidentate nitrogen ligands to probe labelling conditions for a [2+1] approach using CN^-. These first experiments showed that [2+1] labelling is possible for all four L_2 used (en, pico, histam, bipy). Concentrations necessary to obtain the desired $[^{99m}Tc(CN)(CO)_3(L_2)]$ (**9**, **10**) complexes in a yield greater than 90% by HPLC analysis were 10^{-4}M for L_2 and $5{\cdot}10^{-5}$M for KCN. Figure 2.7 shows the stepwise formation of $[^{99m}Tc(CN)(CO)_3(pico)]$ (**9**) in an experiment using pico in an reaction sequence according to Scheme 2.8.

The products of the [2+1] labelling were found to be stable in solution for at least one day. The amount of potassium cyanide needed for 1ml of ^{99m}Tc eluate is only about 3μg, and thus very small compared to a possible toxic

dose of KCN (~100mg), so no problems concerning a possible cyanide poisoning are expected.

In order to obtain additional information about such [2+1] cyanide containing compounds, the rhenium analogue $[Re(CN)(CO)_3pico]$ (**11**) was synthesised following a similar stepwise method (Scheme 2.9) as for technetium, described in more detailed for $[Re(CN)(CO)_3bipy]$ later in parts 2.5 and 3.1.

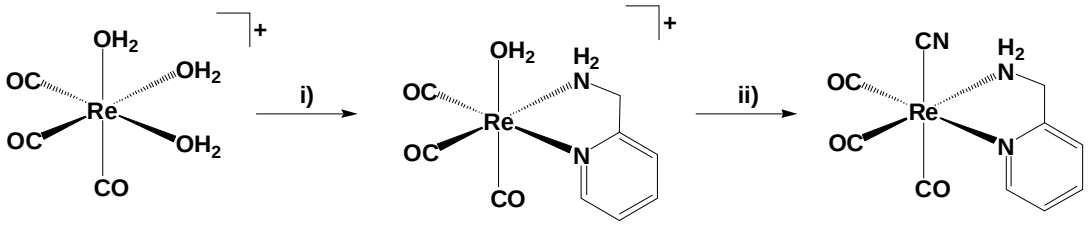

Scheme 2.9 Synthesis of the [2+1] model **11**. i) 1eq. pico, H_2O, r.t., 12h. ii) 3 eq. KCN, r.t., 48h.

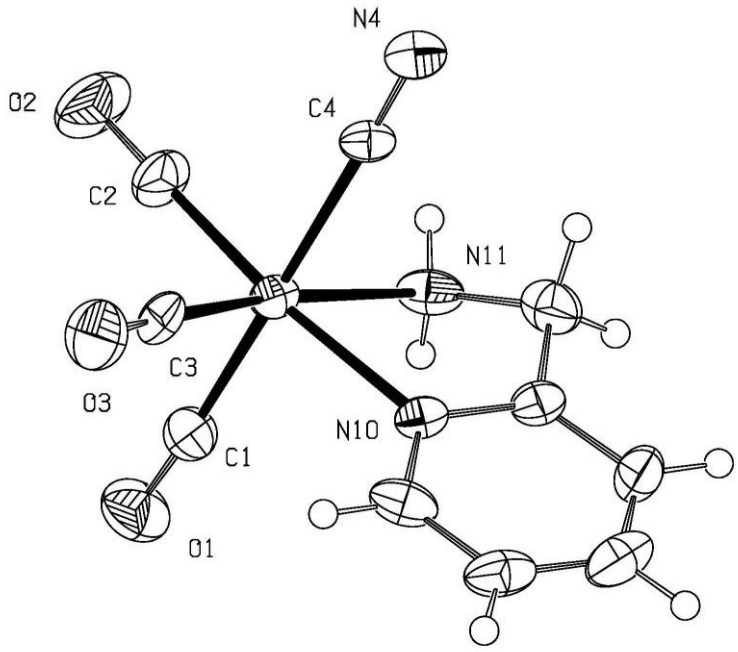

Figure 2.8 Molecular structure of **11**.

Complex **11** is stable in aqueous solutions exposed to air for days. No redox process was detected by voltammetry within the solvent window of water (~-1V < E < 1V). It proved to be difficult to obtain crystals of this compound suitable for a X-ray diffraction study, but after many trials crystals could be obtained and the structure solved (Figure 2.8). The complex shows a nearly perfect octahedral coordination sphere around the

rhenium. The small size of the cyano tricarbonyl part, important for radiopharmaceutical applications of the ^{99m}Tc analogue, is apparent from the structure. Like in the cases of the $[M(CN)_3(CO)_3]^{2-}$ complexes discussed above, the average metal carbonyl bond M-$C(O)_{av}$ is with 1.93Å much shorter than the metal carbon bond for the cyanide (2.14 Å). A comparison of the three M-C(O) bonds shows, that the bond Re-C(1) *trans* to the cyanide is with 1.96 Å slightly longer than the two other rhenium carbonyl bonds (both 1.91Å). This indicates that even though being a much better σ- donor than NO^+ or CO, CN^- is of course still less electron donating than the nitrogen donor sites of pico.

From these results it may be concluded that mixed cyano carbonyl complexes could be attractive alternatives as labelling agents for biomolecules in radiopharmaceutical applications. But for a real application it would first be necessary to develop a procedure to form these complexes in a single reaction instead of using three consecutive steps like in the method presented here.

Even though the preliminary results of the cyano carbonyl experiments for ^{99m}Tc were very promising, further experiments were not carried out because the findings from experiments to synthesise another "[2+1] model compound", $[Re(CN)(CO)_3bipy]$, were quite unexpected. As a consequence, the work changed course and focused on the very different field of inorganic photochemistry, as will be described in the following parts.

2.5 Syntheses of $[Re(CN)(CO)_3bipy]$ and $[(Re(bipy)(CO)_3)_2(\mu\text{-}CN)]^+$ - the "turning point" of the work

The very first experiments for [2+1] model compounds were actually not carried out for the pico but with the bipy ligand. We expected that, if the synthesis succeeded, it might be easier to obtain crystals for an X-ray diffraction study using this rigid, aromatic ligand coordinated to the rhenium than for those containing flexible alkyl chains.

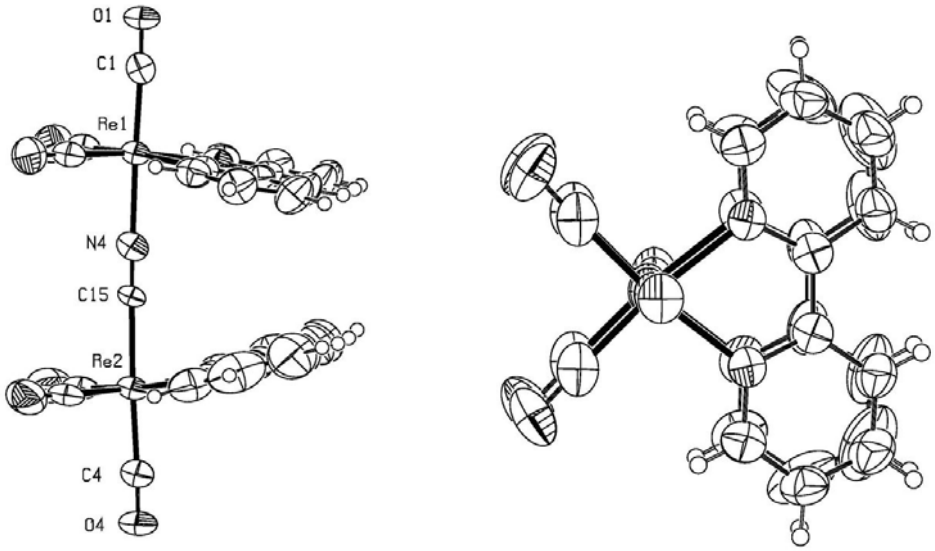

Figure 2.9 Molecular structure of the cation of **16**. View from the side (left) and down from the top (right) of the OC-Re-CN-Re-CO rod.

In a first experiment, stoichiometric amounts of all educts were used. $(NEt_4)_2[Re(CO)_3Br_3]$ (**2**) was dissolved in water and the bromide ligands were removed by the addition of three equivalents of silver perchlorate. AgBr was removed by filtration and one equivalent of bipy was added. After 12 h at room temperature, HPLC analysis confirmed the nearly quantitative formation of $[Re(bipy)(CO)_3(H_2O)]^+$. Now, one equivalent of KCN was added and the mixture was kept at room temperature for two days. HPLC analysis confirmed the nearly quantitative conversion of the educts to a new species, which could be separated from the NEt_4ClO_4 present in the mixture by extraction with THF. An analysis by IR spectroscopy confirmed the coordination of a cyanide ligand, as a weak new band was detected at $2120cm^{-1}$.

Attempts to grow crystals of this compound for an X-ray diffraction analysis were unsuccessful for long until few crystals were found in a sample otherwise containing amorphous powder. The structure could be solved and proved not to be the expected compound [Re(CN)$(CO)_3$bipy] (**15**). Instead, the cyano-bridged, dinuclear complex [(Re(bipy)$(CO)_3)_2(\mu$-CN)](ClO_4) (**16**) was found.

The X-ray data were not of good quality, but as the coincidental isolation of this impurity marks the turning point of the work presented in this thesis, the structure of the dinuclear cation is nevertheless shown in Figure 2.9.

A more thorough literature search than before was carried out, and it was found that both compounds, **15** as well as the accidentally found **16**, had been prepared before in 1992 by KALYANASUNDARAM et al. for a study focussing on fluorescence properties of ruthenium and rhenium complexes.[23] Based on this publication and the experiences from the first synthetic try, it was possible to develop an improved synthesis to obtain both the monomeric [Re(CN)$(CO)_3$bipy] and the dimeric $[(Re(bipy)(CO)_3)_2(\mu\text{-CN})]^+$ complex in pure form, as will be presented in the following chapter.

As the motivation of their work, KALYANASUNDARAM et al. write in the introduction to their paper in 1992:

> *"A long-term goal of these studies is [the] construction of "light harvesting units" capable of absorbing the entire visible light of the solar spectrum and processing the light energy into useful chemical energy."*

The paper contains a long list of references concerning inorganic photochemistry among them also the publications of HAWAECKER et al.[24, 25] dealing with the photochemical properties of [ReX(diimine)$(CO)_3$] complexes and the Strasbourg system for carbon dioxide reduction (Scheme 1.12). All this seemed extremely interesting and caught our attention immediately. More information about rhenium diimine photochemistry, was gathered, which was already presented in parts 1.3 until 1.5.

As a consequence, it was decided to leave the original topic and start the synthesis of different variations of the [ReX(diimine)$(CO)_3$] series of

complexes to obtain variations of the general [ReX(diimine)$(CO)_3$] motive - as shown before in Scheme 1.15.

References

[1] D. Clauss, A. Lissner, *Z. Anorg. Allg. Chem.* **1958**, *297*, 300.

[2] K. Schwochau, W. Herr, *Z. Anorg. Allg. Chem.* **1962**, *319*, 148.

[3] W. Krasser, E. W. Bohres, K. Schwochau, *Z. Naturforsch. A* **1972**, *27*, 1193.

[4] A. G. Sharpe, *The chemistry of cyano complexes of the transition metals*, **1976**.

[5] M. T. Beck, *Pure Appl. Chem.* **1987**, *59*, 1703.

[6] W. P. Griffith, P. M. Kiernan, B. P. O'Hare, J. M. Bregeault, *J. Mol. Struct.* **1978**, *46*, 307.

[7] L. A. O'Connell, R. M. Pearlstein, A. Davison, J. R. Thornback, J. F. Kronauge, A. G. Jones, *Inorg. Chim. Acta* **1989**, *161*, 39.

[8] R. Bhattacharyya, P. S. Roy, *Trans. Met. Chemistry* **1984**, *9*, 281.

[9] K. Wieghardt, *Adv. Inorg. Bioinorg. Mech.* **1984**, *3*, 213.

[10] A. F. Holleman, E. Wiberg, *Lehrbuch der Anorganischen Chemie*, 34th ed., **1995**.

[11] J. Smith, W. Purcell, G. J. Lamprecht, J. G. Leipoldt, *Polyhedron* **1995**, *14*, 1795.

[12] D. Rattat, P. A. Schubiger, H. G. Berke, H. Schmalle, R. Alberto, *Cancer Biother. Radiopharm.* **2001**, *16*, 339.

[13] N. Aebischer, R. Schibli, R. Alberto, A. E. Merbach, *Angew. Chem., Int. Ed.* **2000**, *39*, 254.

[14] H. Behrens, E. Lindner, P. Paessler, *Z. Anorg. Allg. Chem.* **1968**, *361*, 125.

[15] K. R. Dunbar, R. A. Heintz, *Prog. Inorg. Chem.* **1997**, *45*, 283.

[16] F. A. Cotton, C. S. Kraihanzel, *J. Am. Chem. Soc.* **1962**, *84*, 4432.

[17] J. A. Muller, *C. R. Hebd. Seances Acad. Sci.* **1887**, *104*, 992.

[18] A. Volbeda, E. Garcin, C. Piras, A. L. de Lacey, V. M. Fernandez, E. C. Hatchikian, M. Frey, J. C. Fontecilla-Camps, *J. Am. Chem. Soc.* **1996**, *118*, 12989.

[19] S. M. Contakes, T. B. Rauchfuss, *Angew. Chem., Int. Ed.* **2000**, *39*, 1984.

[20] S. M. Contakes, S. C. N. Hsu, T. B. Rauchfuss, S. R. Wilson, *Inorg. Chem.* **2002**, *41*, 1670.

[21] R. Alberto, *Eur. J. Nucl. Med. Mol. Imaging* **2003**, *30*, 1299.

[22] S. Mundwiler, M. Kuendig, K. Ortner, R. Alberto, *Dalton Transactions* **2004**, 1320.

[23] K. Kalyanasundaram, M. Graetzel, M. K. Nazeeruddin, *Inorg. Chem.* **1992**, *31*, 5243.

[24] J. Hawecker, J. M. Lehn, R. Ziessel, *J. Chem. Soc., Chem. Comm.* **1983**, 536.

[25] J. Hawecker, J. M. Lehn, R. Ziessel, *Helv. Chim. Acta* **1986**, *69*, 1990.

3. THE [RE(CO)$_3$BIPYX] SERIES OF COMPLEXES

In the experiments that led to the development of the [2+1] labelling using cyanide, experiences were gathered for the introduction of a sixth ligand X in complexes [Re(CO)$_3$L$_2$X], in this case with cyanide as X. Based on this knowledge, a series of complexes [Re(CO)$_3$bipyX] was prepared for photochemical studies. They all contain bipy, but different monodentate ligands X are coordinated to the complexes' sixth position. Such modifications would change the redox potentials and overall charge of the resulting complexes, without touching the "[Re(CO)$_3$bipy]"- unit itself.

Two such [Re(CO)$_3$bipyX] complexes had already been prepared and tested as catalysts for the Strasbourg reaction, [Re(bipy)(CO)$_3${P(OEt)$_3$}]$^{+}$[1] and [Re(bipy)(CO)$_3$(py)]$^{+}$[2], and they were found to also act as active catalysts for photochemical carbon dioxide reduction. In the case of [Re(bipy)(CO)$_3${P(OEt)$_3$}]$^{+}$, the catalytic rate was enhanced by a factor of 5 compared to the chloride, but the catalyst was found to be less stable. By running catalytisis experiments with more such complexes, it was hoped to clarify the role of the sixth ligand. The original study of HAWAECKER et al. also indicated an influential role for this ligand as the presence of excess halide improved both rate and stability of the catalysis for the cases of [Re(halide)(CO)$_3$bipy].[3]

3.1 Synthetic strategy

The synthetic strategy to obtain [Re(CO)$_3$bipyX] complexes was based on experiences of the experiments mentioned in parts 2.4 until 2.6. The readily available rhenium(I) carbonyl complexes [ReBr(CO)$_5$] (**1**) or (NEt$_4$)$_2$[ReBr$_3$(CO)$_3$] (**2**) were used as starting materials and, for most of the syntheses, the bipy ligand was introduced first, before introducing the sixth ligand X in the final step. Different reaction sequences are possible to obtain the desired products, and it is actually possible to follow any combination of reactions outlined in Scheme 3.1.

For the synthesis of the known compound [ReBr(CO)$_3$bipy] (**12**), the direct reaction of the ligand with **1** proved to be the method of choice. Instead of

the original procedure[4] using toluene as the solvent, syntheses in petroleum benzene of medium boiling range were found to result in better yields. Complex **12** is only soluble in polar organic compounds like acetonitrile, DMF or acetone. It is possible to remove the coordinated bromide in acetone by a precipitation reaction using different silver salts, Ag(anion). In the presence of water, the cationic aqua complex [Re(OH$_2$)(CO)$_3$bipy]$^+$ (**14**) is formed, which can be isolated as a salt with weakly coordinating counterions like OTf$^-$ or ClO$_4^-$.

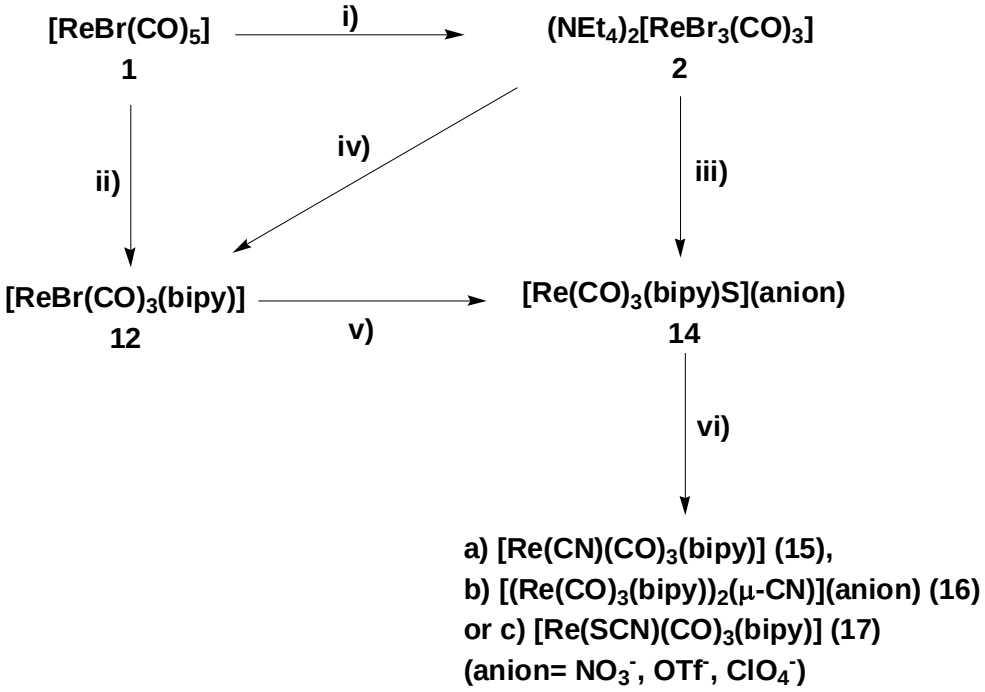

Scheme 3.1 Reaction pathways for the syntheses of different [Re(CO)$_3$bipyX] complexes. i) 2eq. NEt$_4$Br, diglyme, 160°C, 4h. ii) 1.5eq. bipy, petroleum benzene, 100°C, 2h. iii) *1.* 3eq. Ag(anion), solvent S (S= H$_2$O or MeOH), r.t., 30min; *2.* 1 eq. L, r.t., 12h. iv) 1.5eq. bipy, H$_2$O, r.t., 12h. v) *1.* 1eq. Ag(anion), acetone, r.t., 12 h; *2.* H$_2$O, r.t., 2h. vi) a) 3eq. or b) 0.5 eq. KCN; c) 3eq. KSCN.

Complex **14** can also be obtained by a different route in aqueous solution. When **2** is dissolved in water, the coordinated bromides are rapidly replaces by water to form the [Re(OH$_2$)$_3$(CO)$_3$]$^+$ cation. As already mentioned for the first trial to synthesise [Re(CN)(CO)$_3$bipy] (**15**) in part 2.6, the bromides in solution can be removed by the addition of silver salts. If bipy is added to the aqueous solution of [Re(OH$_2$)$_3$(CO)$_3$]$^+$, complex **14** forms slowly in aqueous solution. Besides **1**, all species of Scheme 3.1 can be analysed by reverse phase HPLC using an acidic H$_2$O/MeOH gradient, so it is possible to

follow the progress of reactions. Once **14** has formed in solution, it can either be isolated or also directly reacted further with the strong ligands cyanide or thiocyanate. As the exchange of solvent at the sixth position is known to be quite slow[5], longer reaction times are needed for the complete conversion of **14** to the products [ReX(CO)$_3$bipy] (X= CN, SCN). It also proved to be of advantage to use an excess of cyanide or thiocyanate for this step to reduce the reaction time.

For the case of **15**, the use of excess cyanide also helps to avoid the formation of the bridged species [(Re(bipy)(CO)$_3$)$_2$(μ-CN)]$^+$ (**16**) accidentally found before. can be The synthesis of **16** is achieved by the addition of only half an equivalent of KCN to a solution of **14**. As the result, a first half of **14** reacts within hours with cyanide to form **15** (Scheme 3.2).

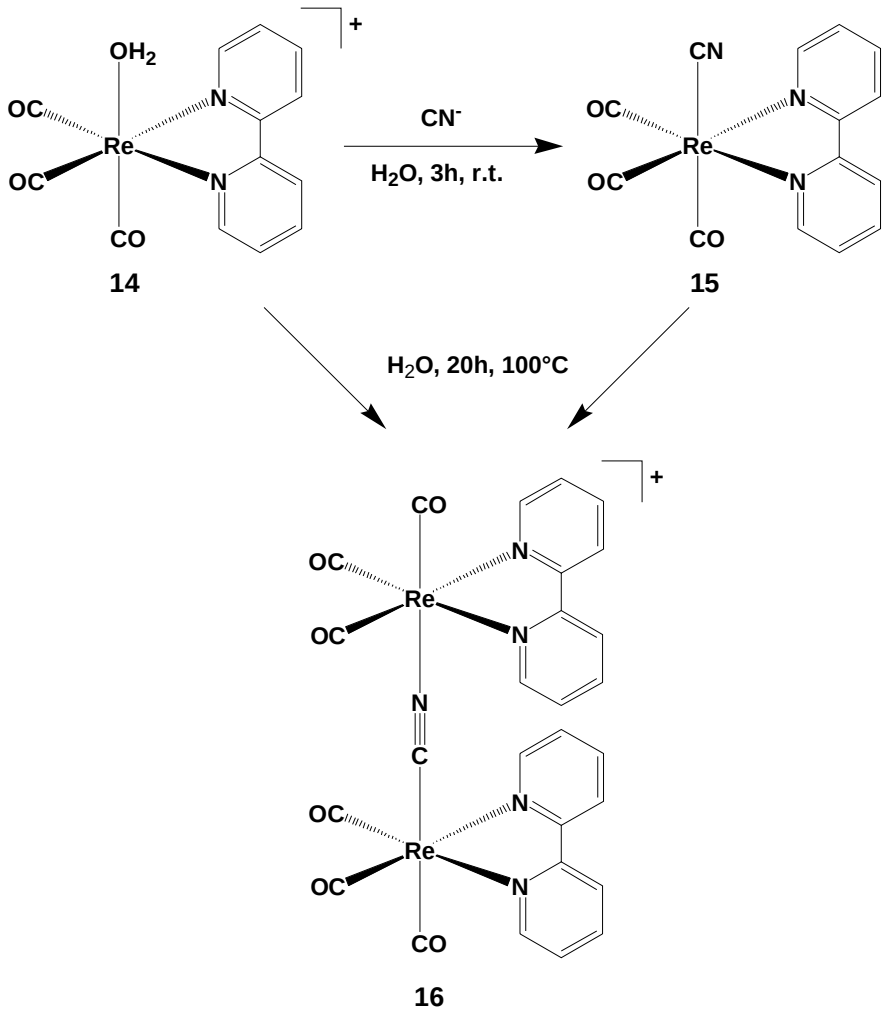

Scheme 3.2 Formation of the cyano bridged dimer **16**.

Unlike terminally coordinated nitrosyl or carbonyl, cyanide can also act as a linear bridging ligand connecting two metal centres. The very first metal cyanide compound ever discovered, Prussian Blue (discovered in 1704), is such a compounds, with iron(II) and iron(III) centres linked by linear bridging cyanides.[6] This ability of the cyanide ligand to coordinate a second metal by its weaker coordinating nitrogen end, is observed here as well for **15**. HPLC analysis shows that the **15** initially formed reacts with the second equivalent of **14** present in solution to form the linear bridged compound **16**. As this involves the combination of two rather big units and coordination of the weakly coordinating end of the cyanide, the process takes a day even at 100°C. If the perchlorate salts are used, the product precipitates from solution, which speeds up the process. For nitrate or triflate counterions, even longer reaction times of up to one week are necessary to obtain the cyano bridged complex.

The monomeric **15** and the cyano- bridged dimer **16** are easily distinguished by their characteristic IR bands found for the cyanide ligand, as the frequency observed for the terminal CN^- (2117cm^{-1}) is much smaller than the one observed for the bridging cyanide (2151cm^{-1}).[7]

3.2 Discussion of spectroscopic and electrochemical data for [Re(CO)$_3$bipyX]

Using the synthetic strategy presented in Scheme 3.1, it was possible to synthesise [Re(CO)$_3$bipyX] bearing bromide, water, cyanide and thiocyanate as sixth ligand X. Additionally, the dinuclear cyano bridged complex **16** could be prepared, which might be considered as a [Re(CO)$_3$bipyX] complex with X= [Re(μ-CN)(CO)$_3$bipy]. Table 3.1 summarises some of the analytical data obtained for these complexes.

Analysing the data of Table 3.1, one can see that the exchange of the sixth ligand bromide causes detectable electronic changes for the complexes, but these are neither very large nor correlated to each other in an obvious way.

A rather clear case seems to be the aqua complex. The exchange of bromide for water results in the formation of a cationic species. As what seems to be simply a result of its charge, this complex appears to have the lowest electron density of the series: its light absorption shifts towards higher energy, as it is more difficult to excite an electron. Less electron density results in less π- backbonding for the carbonyls, so the IR vibrations shift to higher wavelength. The aqua complex is also the one that is most easily reduced electrochemically, as its charge makes it more ready to accept an electron.

ligand X	λ_{max} **[nm]**	λ_{em} **[nm]**	ν_{CO} **[cm^{-1}]**	$E_{1/2, red}$ **[mV]**
Br	370	575	2019, 1905	-1190
CN	355	540	2006, 1878	-1125
SCN	375	580	2020, 1928	-1015
μ- CN- Re	365	535	2025, 1910	-1050
H_2O	350	540	2036, 1918	-1000

Table 3.1 Selected properties of [Re(CO)$_3$bipyX] complexes.

A similar effect of charge is shown in the difference between the terminal- and the bridged cyano complexes. In the bridged complex, the cyano donor is shared between two metal centres. Additionally, the complex has an overall positive charge. This results in higher carbonyl stretching frequencies and a more facile electrochemical reduction.

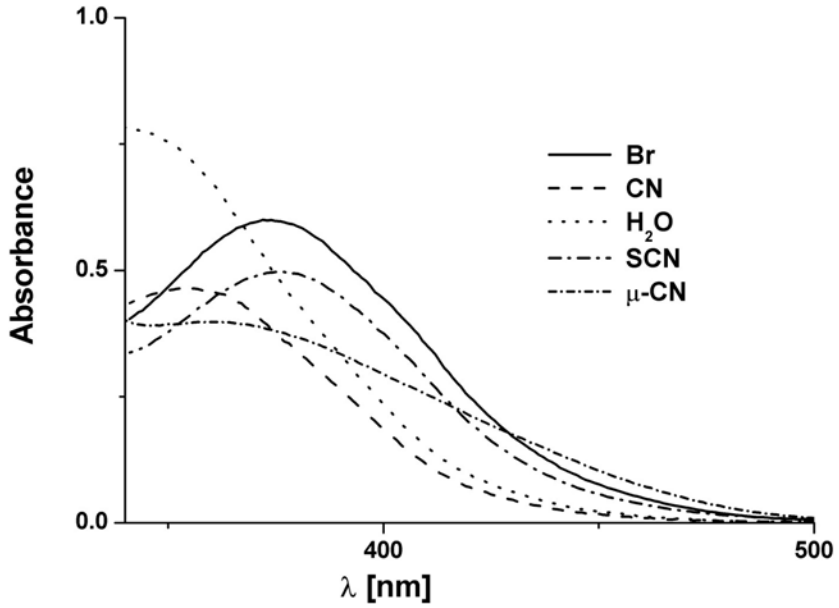

Figure 3.1 Absorption spectra in the visible for different [Re(CO)$_3$bipyX] complexes in DMF solution (all solutions 0.2mM).

For the other complexes, these correlations are less straight forward: considering ν_{CO} and $E_{1/2}$, the thiocyanate complex appears to be about as low in electron density as the cationic aqua complex, yet its visible absorption is shifted furthest towards lower energies. The cyano complex has the by far lowest carbonyl IR bands indicating large π- backbonding for the carbonyls, but than also a low wavelength of UV absorption.

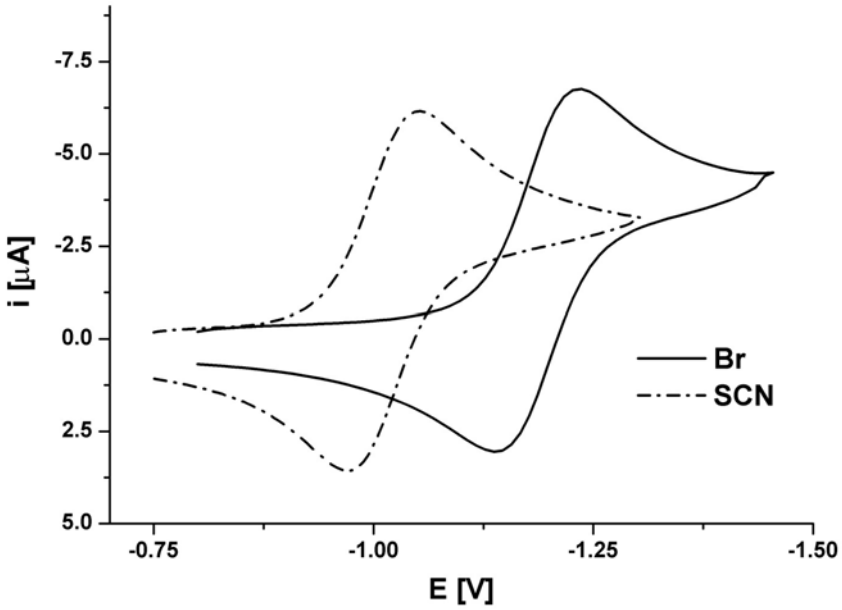

Figure 3.2 Cyclic voltammograms for the complexes [ReBr(CO)$_3$bipy] and [Re(SCN)(CO)$_3$bipy] dissolved in DMF.

The modifications of X influence the potential for the electrochemical reduction but it is found in all cases to be a reversible, one-electron process as shown in Figure 3.2 for two examples. As the reduced complex is the active species for photocatalytic reduction processes, it is of key importance that it is stable and that it can be reoxidised. As the reduced form has mostly the character of a reactive organic radical centred on the ligand, it was not clear beforehand whether the variation of X would influence the reversibility of the redox process.

All five [Re(CO)$_3$bipyX] complexes still show fluorescence when irradiated with visible light around 400nm. However, the intensity of the fluorescence varies by a factor of about 10. For better comparison of the position and shapes of the emission spectra, the *normalised* curves are thus shown in Figure 3.3. The emission spectra show structureless peaks typical for MLCT processes involving aromatic ligands.[8] Some spectra show a main peak with a shoulder or even two peaks, as observed before for series of [ReCl(CO)$_3$(diimine)] complexes containing different substituted bipy-ligands. The positions of the emission maxima shift parallel to the observed UV absorption shifts, with the exception of the cyano bridged dimer which shows an unusually low λ_{em}.

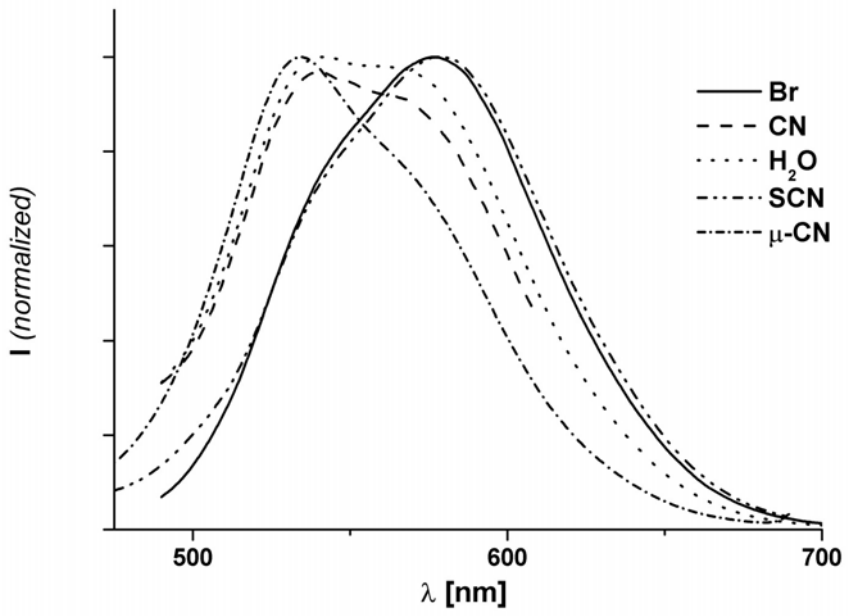

Figure 3.3 Normalised emission spectra for [Re(CO)$_3$bipyX] complexes in DMF.

3.3 Synthesis of the technetium analogue [TcCl(CO)$_3$bipy]

The general synthesis method presented in Scheme 3.1 proved to be successful as described so far in this chapter. So it was decided out of academic interest to expand the series to a technetium(I) complex as well. Of course a radioactive complex is of no use for large-scale photochemical applications, but it seemed nevertheless interesting to see what influence a change of the metal to the lighter homologue of rhenium might have on the photocatalysis.

Unlike rhenium, the $(NEt_4)_2[^{99}TcCl_3(CO)_3]$ (**3**) is used as precursor of choice for the technetium(I) tricarbonyl fragment. As in the case of $[ReBr(CO)_5]$, the synthesis of $[^{99}Tc(Cl,Br)(CO)_5]$ involves a high-pressure carbonylation step to obtain $[Tc_2(CO)_{10}]$[9], which is not practical for a radioactive compound. On the contrary, a ambient pressure carbonylation method has been developed for the synthesis of **3**[10], making this compound readily available for the synthesis of $[^{99}TcCl(CO)_3bipy]$ (**13**) according to Scheme 3.3. The yellow complex **13** could be obtained in good yield via this route. It was possible to confirm the expected structure of the complex by X-ray diffraction (Figure 3.4).

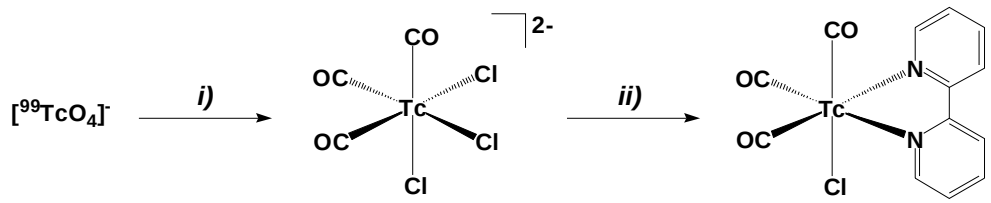

Scheme 3.3 Two-step synthesis of **13** starting from $(NBu_4)[^{99}TcO_4]$. i) 1. 1bar CO, BH_3, THF, r.t., 2h; 2. NEt_4Cl. ii) 1.4eq. bipy, H_2O, r.t., 12h.

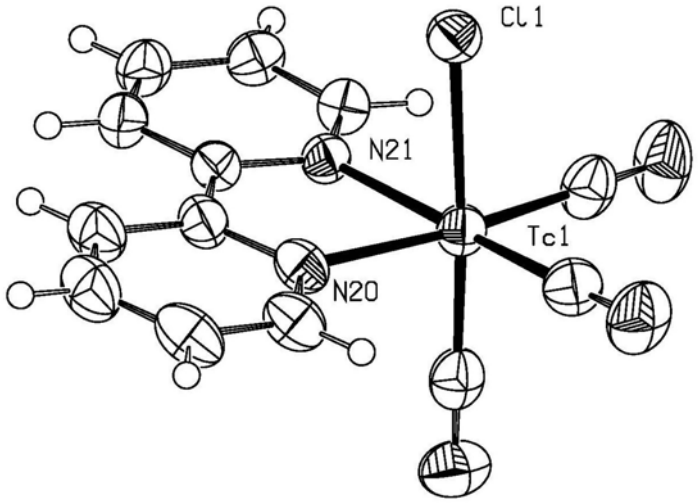

Figure 3.4 ORTEP drawing of the structure of **13**.

As ^{99}Tc is a weak β-emitter, it is not possible to analyse the compound in greater detail in a way similar to the rhenium compounds. Therefore the comparison of data for **13** and its rhenium analogue is limited to the IR and crystallographic data presented in Table 3.2. The geometries of the two homologous complexes are virtually identical, as often found when technetium and rhenium complexes with identical ligand spheres are compared. The only detectable difference can be seen in the IR frequencies for the carbonyl vibrations with the technetium frequencies found at higher wavenumbers. As both the bond lengths and electronegativities of the central metals (Tc:1.4, Re:1.5) are the same, the most likely explanation is that the smaller number of electrons around technetium result in weaker π-backbonding to the carbonyl. Unfortunately, it was not possible to measure fluorescence or electrochemistry for the radioactive technetium complex.

metal	ν_{CO} [cm^{-1}]	d_{av}(M – CO) [Å]	d_{av}(CO) [Å]	d_{av}(M – N_{bipy}) [Å]
Tc	2033, 1930	1.92	1.14	2.18
Re	2019, 1905	1.92[a]	1.14[a]	2.19[a]

Table 3.2 Comparison of IR and crystallographic data for [M(Cl,Br)(CO)$_3$(diimine)] complexes of technetium(I) and rhenium(I).[a] data from the published structure of [ReCl(CO)$_3$terpy].

In conclusion, a series of rhenium(I) carbonyl bipy complexes could be synthesised whose members are very similar to the originally used photocatalyst [ReBr(CO)$_3$bipy] (**12**) from their spectroscopic and electrochemical characteristics. Judging their light absorption, fluorescence and redox properties, they all fulfil the basic requirements to still act as active catalysts for the carbon dioxide reduction reaction (Scheme 1.12). Additionally, the homologous technetium complex [^{99}TcCl(CO)$_3$bipy] (**13**) could be prepared with a molecular structure identical to the rhenium analogue, but slightly different electronics around the metal as indicated by the vibration frequencies of the carbonyl ligands. The differences in the observed properties for all these complexes are however large enough to make one anticipate marked differences in their photocatalytic activity.

References

[1] O. Ishitani, M. W. George, T. Ibusuki, F. P. A. Johnson, K. Koike, K. Nozaki, C. Pac, J. J. Turner, J. R. Westwell, *Inorg. Chem.* **1994**, *33*, 4712.

[2] H. Hori, J. Ishihara, K. Koike, K. Takeuchi, T. Ibusuki, O. Ishitani, *J. Photochem. Photobiol. A* **1999**, *120*, 119.

[3] J. Hawecker, J. M. Lehn, R. Ziessel, *Helv. Chim. Acta* **1986**, *69*, 1990.

[4] A. Juris, S. Campagna, I. Bidd, J. M. Lehn, R. Ziessel, *Inorg. Chem.* **1988**, *27*, 4007.

[5] P. V. Grundler, B. Salignac, S. Cayemittes, R. Alberto, A. E. Merbach, *Inorg. Chem.* **2004**, *43*, 865.

[6] K. R. Dunbar, R. A. Heintz, *Prog. Inorg. Chem.* **1997**, *45*, 283.

[7] K. Nakamoto, *Infrared and Raman Spectra of Inorganic and Coordination Compounds*, 5th ed., **1997**.

[8] H. Henning, D. Rehorek, *Photochemische und photokatalytische Reaktionen von Koordinationsverbindungen*, **1988**.

[9] F. Calderazzo, U. Mazzi, G. Pampaloni, R. Poli, F. Tisato, P. F. Zanazzi, *Gazz. Chim. Ital.* **1989**, *119*, 241.

[10] R. Alberto, R. Schibli, P. A. Schubiger, U. Abram, T. A. Kaden, *Polyhedron* **1996**, *15*, 1079.

4. THE [ReBr(CO)$_3$(diimine)] SERIES OF COMPLEXES

Given the detailed studies carried out concerning the photocatalytic activity of the compounds [Re(Cl,Br)(CO)$_3$bipy] in the 1980s and 90s, it is surprising to see that only one report in the literature about photocatalysis by a rhenium(I) complex of any other diimine but bipy. In this study of 1992, CALZAFERRI et al. synthesised the complex [ReCl(CO)$_3$ptpy][1], shown in Scheme 4.1. Why this ligand in particular was chosen is not clear from the publication. They carried out photocatalytic carbon dioxide reductions and found that [ReCl(CO)$_3$ptpy] was an active catalyst as well, but the catalytic rate was only about one quarter of that of [ReCl(CO)$_3$bipy]. Additionally, the catalyst was only found to be active in DMSO solutions, but not in DMF.

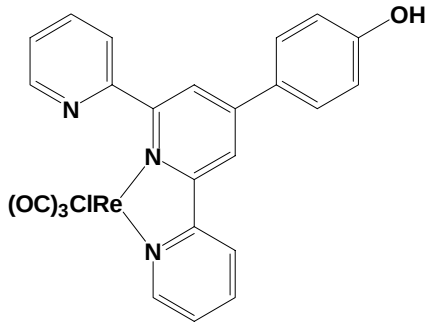

Scheme 4.1 The complex [ReCl(CO)$_3$ptpy], used in the only study of catalytic activity of complexes containing any other diimine but bipy.

As little as can be learned from this isolated study, it seems that the photocatalytic carbon dioxide reduction is not limited to either rhenium bipy complexes nor to DMF solutions, but both apparently have an influence on the catalytic rate. It would be necessary to study more systems to establish some kind of relationship between the type of diimine and the photocatalytic activity of their rhenium complexes.

Consequently, it was decided to synthesise a second series of rhenium carbonyl complexes, this time one with complexes bearing different diimine ligands, but always containing bromide as the sixth ligand. The bromide complexes were synthesised as they are in most cases easily accessible from [ReBr(CO)$_5$] (**1**) (Scheme 3.1) and closest to the well studied complexes [Re(Cl,Br)(CO)$_3$bipy]. The diimine ligands chosen for this work can be divided into two groups:

- *"extended- bipy" diimine*s, which contain a bipy- subunit extended by different numbers of aromatic rings
- *bridging diimines*, that offer one diimine side for the coordination of rhenium and another bidentate coordination site for a second metal fragment as proposed in Scheme 1.15.

4.1 Complexes containing "extended- bipy" diimines

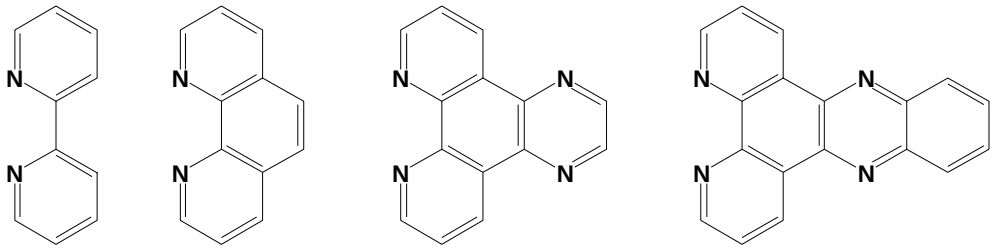

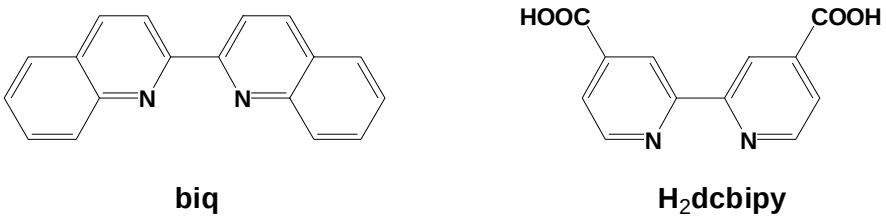

Scheme 4.2 Different diimines used for the preparation of [ReBr(CO)$_3$(diimine)] complexes.

Aromatic diimine ligands like bipy have been used in inorganic coordination chemistry for a long time. As a result, a large number of different ligands has been prepared, many of them are even commercially available. For the synthesis of "extended- bipy" complexes, the ligands shown in Scheme 4.2 were chosen. The ligands bipy, phen and biq are routinely used, commercially available ligands. With dpq and dppz ligands the aromatic system of the ligand is successively enlarged to a total of 5 fused aromatic rings, which was expected to change light absorption and redox properties greatly. Finally, the complex with the commercially available ligand H_2dcbipy was synthesised, as it was known that this complex is soluble in water, in contrast to the other complexes of the series, and would thus allow to probe catalytic activity in aqueous solution.

The complexes containing bipy (**12**) and phen (**18**) have been prepared and extensively studied before.[2, 3] So their syntheses and structures are not discussed in detail here again.

The ligands dpq and dppz were synthesised following published procedures starting from the phd ligand, which will be introduced in part 4.2. In both syntheses the diketone phd is condensed with 1,2-diamines to form a diimine ring (Scheme 4.3).[4, 5] In the case of dppz, this new ring is already aromatic. In the case of dpq, the thermodynamic driving force towards an aromatic system is apparently so large, that the initially formed condensation product looses hydrogen to become an aromatic system.

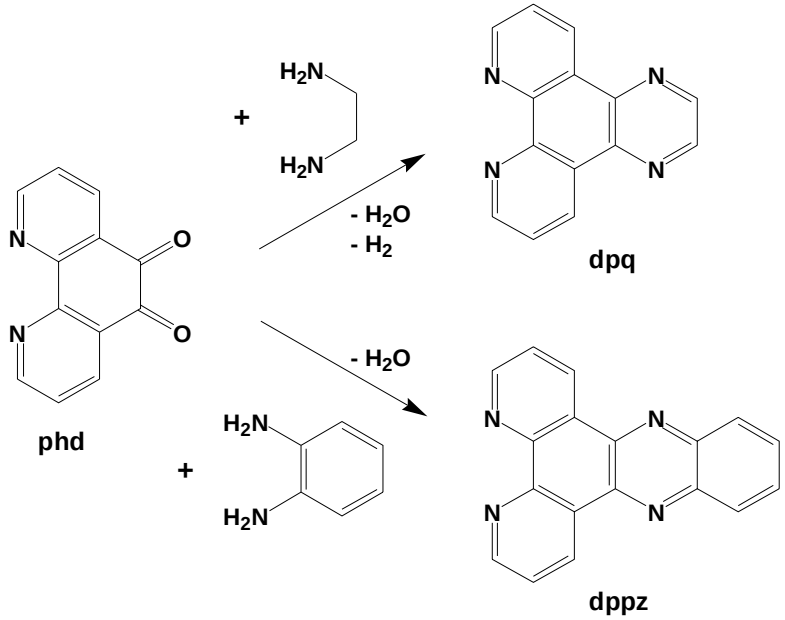

Scheme 4.3 Syntheses of the ligands dpq and dppz.

The reaction of **1** with both dpq and dppz according to Scheme 3.1 allowed the synthesis of the corresponding rhenium complexes **19** and **20** in good yield and purity. For both compound it was possible to obtain crystals suitable for an X-ray diffraction analysis. As expected, both structures show the same octahedral coordination geometry as known for bipy or phen, with all atoms of the aromatic ligand, the rhenium and the two carbonyls *trans* to the diimine in a nearly perfectly planar arrangement. Figure 4.1 shows the dppz complex as an example. Concerning the geometry of the complexes, these complexes are really best described as “extensions” of the known bipy complexes.

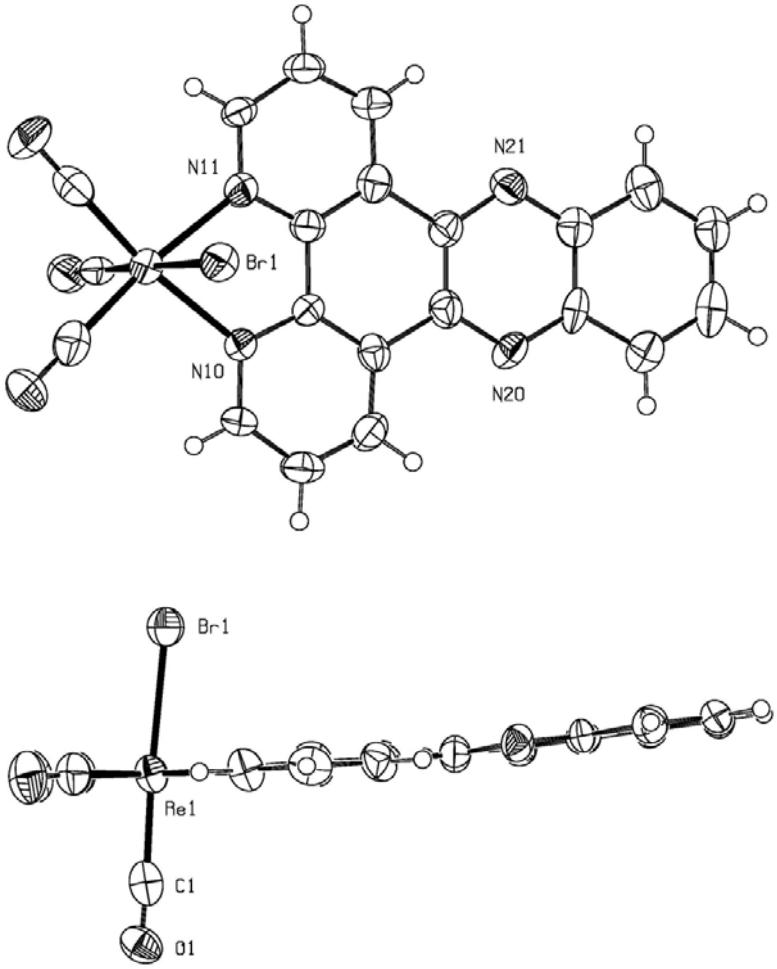

Figure 4.1 ORTEP representation of the molecular structure of diimines **20** showing a view of the molecule from above and from the side.

This planar arrangement of diimine, rhenium and two carbonyl ligands is found for nearly all [ReBr(CO)$_3$(diimine)] complexes. One of the few exceptions is the complex **21** with biq, synthesised as before from **1** and the ligand. As the hydrogen atoms of the outer aromatic rings of the biq ligand get very close to the equatorial carbonyl ligands of the rhenium after coordination, the ligand is pushed out of the otherwise favoured planar arrangement due to steric strain. As a consequence, the two quinoline rings of the biq ligand are not coplanar but twisted 16° away from each other and also tilted out of the Re(CO)$_2$- plane towards the bromide by 23° and 12°, respectively (Figure 4.2). The different twists for the two quinoline rings seem to be only an effect of crystal packing: only six proton signals are observed in the NMR, indicating that the rings are equivalent on the NMR timescale.

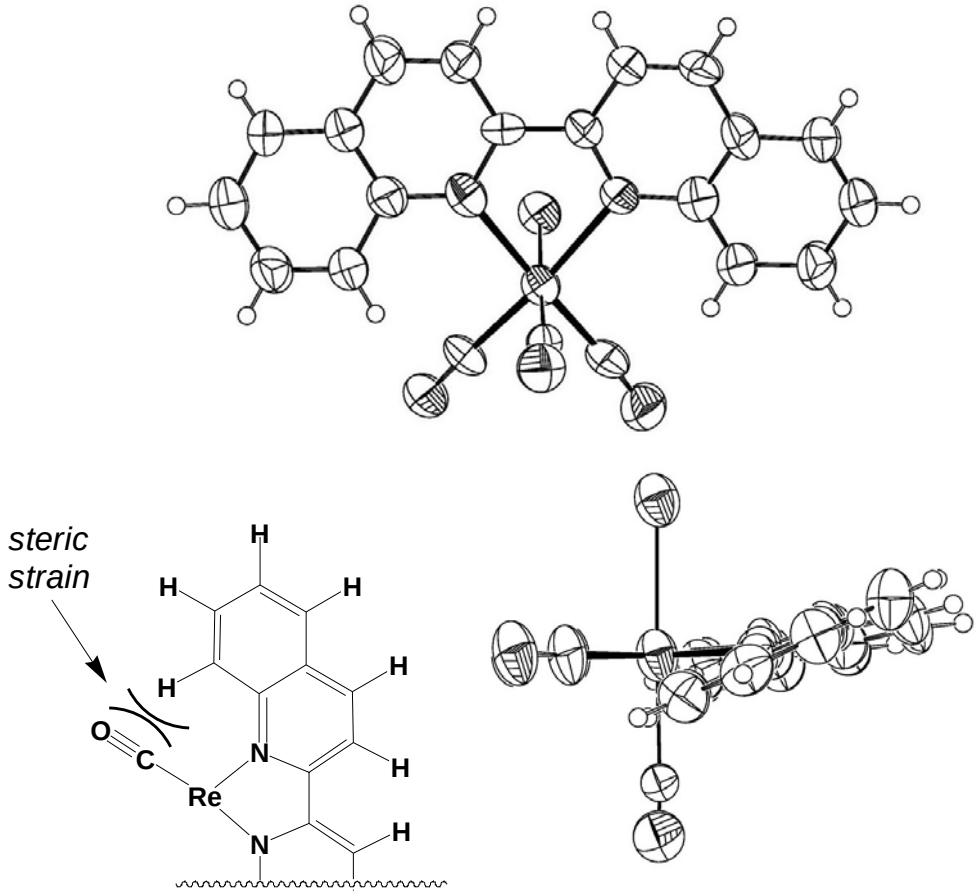

Figure 4.2 ORTEP drawings of a top and a side view of **21** and a sketch illustrating the origin of the steric strain causing the bend geometry of the complex.

The [ReBr(CO)$_3$(diimine)] complexes of this series show much larger differences in their spectroscopic and electrochemical properties than observed for the [Re(CO)$_3$bipyX] series discussed in chapter 3. Again, Table 4.1 offers an overview of the data.

Judging from the carbonyl stretching frequencies, the electron density on the rhenium centre does not seem to be as greatly affected as in the case of the [Re(CO)$_3$bipyX] series. This is understandable as the set of atoms directly bound to rhenium is the same for all these [ReBr(CO)$_3$(diimine)] complexes. The most important feature is rather the more and more decreased energy of the diimine's LUMO as the aromatic system becomes larger. With the metal orbitals at about the same energy, this results in smaller energy gaps for the MLCT. As a result, light absorption shifts towards smaller energies and a larger part of the absorption is in the visible range (Figure 4.3). Consequently, it is also easier to place an additional

electron into the LUMO of the ligand, so the reduction potential of the complexes is increased as the size of the aromatic ligand increases.

diimine	λ_{max} [nm]	λ_{em} [nm]	ν_{CO} [cm^{-1}]	$E_{1/2, red}$ [mV]
Hdcbipy	360	600	2024, 1896	-1250[a]
bipy	370	575	2019, 1905	-1190
phen	370	570	2018, 1933	-1090
dpq	~375[b]	585	2025, 1948	-975
dppz	~425[b]	520	2018, 1918	-705
biq	433	/[c]	2014, 1895	-735

Table 3.1 Selected properties of [ReBr(CO)$_3$(diimine)] complexes. [a] irreversible reduction. [b] absorption shoulder. [c] no fluorescence observed at room temperature.

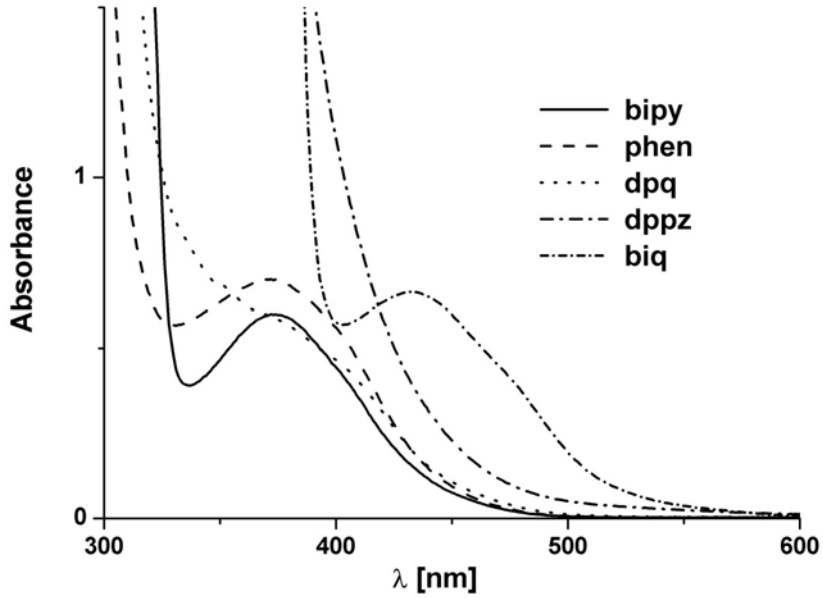

Figure 4.3 Absorption spectra for different [ReBr(CO)$_3$(diimine)] complexes in DMF (all solutions 0.2mM).

For the photocatalytic reactions, these trends should have opposite effects: a red-shift of the absorption is advantageous as a larger range of visible light will be absorbed by the complexes. On the other hand, higher reduction potentials are disadvantageous as the reduced species [ReBr(CO)$_3$(diimine$^{\bullet-}$)] is a less and less powerful reducing agent for substrates.

A special case in this series is the H_2dcbipy complex. The ligand is absolutely insoluble in petroleum benzene, the synthesis starting from **1** was not possible. Instead, an aqueous synthesis starting from $(NEt_4)_2[ReBr_3(CO)_3]$ (**2**) was carried out where the anionic complex $(NEt_4)[ReBr(CO)_3(Hdcbipy)]$ (**22**), containing the mono-deprotonated ligand, precipitated from the neutral solution. The presence of the carboxylate groups on the bipy ligand apparently increases the energy levels of the LUMO even higher than for the unsubstituted bipy resulting in light absorption at lower wavelength and an electrochemical reduction at lower energies. This is also the only case for all diimines used where the reduction was found to be irreversible, which is in disagreement with the literature, where a reversible reduction at –1470mV was reported[6] for the neutral complex [ReBr(CO)$_3$(H_2dcbipy)] (unfortunately, no reference point for this potential is given in the article). The reduction of the ligand probably results in a reduction of one of the carboxylate groups, e.g. to the aldehyde, resulting in an irreversible reduction process.

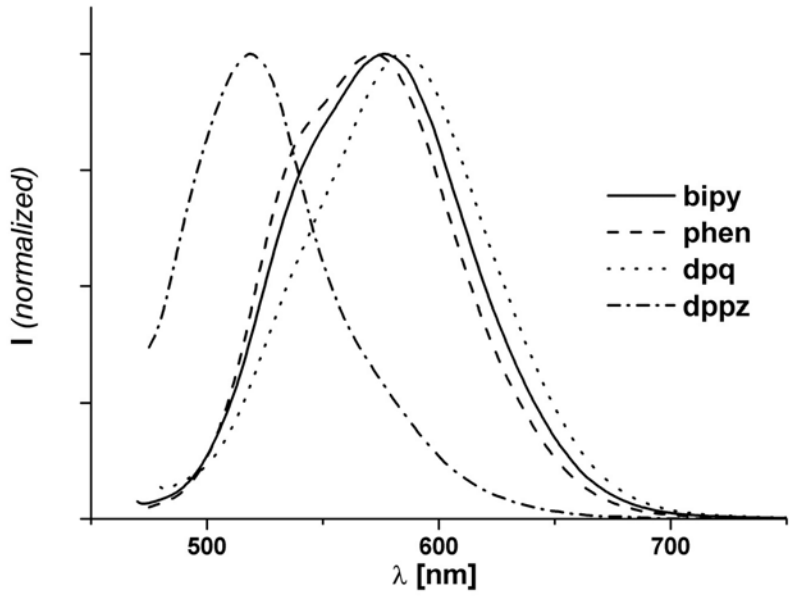

Figure 4.4 Emission spectra for different [ReBr(CO)$_3$(diimine)] complexes in DMF.

With the exception of the biq complex, all complexes of this series fluoresce at room temperature in DMF solution when irradiated with light between 350 and 450nm. The emission maxima are about the same for the Hdcbipy, bipy, phen and dpq complexes (~575nm), but for the dppz complex

it is much lower at 520nm. This is unexpected and not understood, as the light absorption shoulder for this compound is at much higher wavelength compared to the other four fluorescing species.

It is also not clear for which reason the biq complex differs so greatly from the other five complexes of this series. While the other four compounds are orange yellow powders as solids, the biq complex is red and consequently also shows the by far lowest energy absorption maximum for its MLCT band. But the most striking difference is the lack of room temperature fluorescence. An explanation might be the unusual structure of the molecule with the tilted diimine coordination geometry discussed above. This geometry strain might change the electronics of the molecule to such an extend, that light absorption is shifted largely and the fluorescence disappears. Theoretical calculations are necessary to understand this effect better.

4.2 Complexes containing bridging diimines

Another strategy for the modification of the original [ReX(CO)$_3$bipy] system was the use of bridging diimines. The aim was to connect the photoactive rhenium unit directly to a catalytically active second metal centre via the diimine. As the photoelectron ejected from the rhenium centre upon light absorption is known to be located on the diimine, the coordination of a second metal centre to the diimine could make a photoinitiated metal to metal charge transfer possible.

Three well known bridging diimines were investigated for this purpose, that possess very different structures (Scheme 4.4): 2,2'-bipyrimidine (bpm), with a structure very similar to bipy; 1,10-phenanthrolinedione (phd), which is able to act as a bridging ligand in its reduced forms, and the electronically unusual ligand 2,2'-azobispyridine, coordinating both by its aromatic as well as its unusual azo-bridge nitrogen atoms. The rhenium tricarbonyl complexes of both bpm (**23**) and abpy (**27**) have already been prepared.[6, 7] These ligands are known to hold two coordinated metal centres in very short distance from each other, typical distances are around

5.5Å for bpm and even smaller than 5Å for abpy.[8] For a bridging, reduced phd unit these distances are longer[9], but the unusual redox chemistry of the ligand, which will be discussed below, made phd another very interesting candidate for this study.

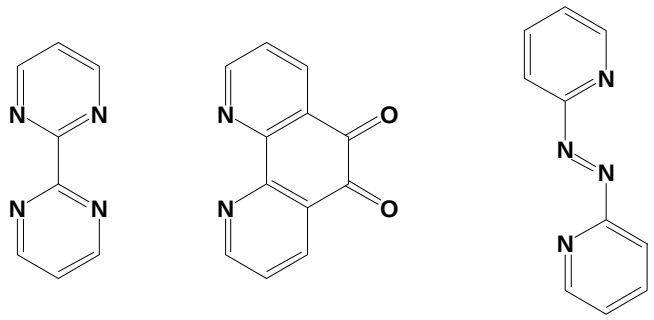

bpm **phd** **abpy**

Scheme 4.4 Bridging diimines used for the preparation of [ReBr(CO)$_3$(diimine)] complexes.

All three bridging ligands are only poorly soluble in petroleum benzene but dissolve well in polar solvents, so the synthesis of the monomeric rhenium complexes was carried out in aqueous or alcohol solutions starting from **2**. A small excess of bpm or abpy has to be used to avoid the formation of bridged dirhenium complexes.

diimine	λ_{max} [nm]	ν_{CO} [cm^{-1}]	$E_{1/2, red}$ [mV]
bpm	385	2030, 1931	-860
phd	375[a]	2033, 1943	-15, -755
abpy	550, 360[a]	2020, 1924	+50

Table 3.2 Selected properties of [ReBr(CO)$_3$(diimine)] complexes containing bridging ligands. [a] absorption shoulder. All three complexes show no fluorescence in DMF at room temperature.

As observed for the series of the non-bridging diimines before, the large differences in electronic properties of the complexes seem to originate mainly from ligand behaviour, as again only small differences for the CO vibration frequencies indicate more or less similar electronics for the rhenium centres. There are also no unexpected influences stemming from the coordination geometry of the complexes, as both the bpm and abpy complexes are known to have the usual coordination mode with the diimine ligand in a Re(CO)$_2$- plane as shown before (Figure 4.1). This is also the case

for the phd complex **29**, which was synthesised here for the first time (Figure 4.5).

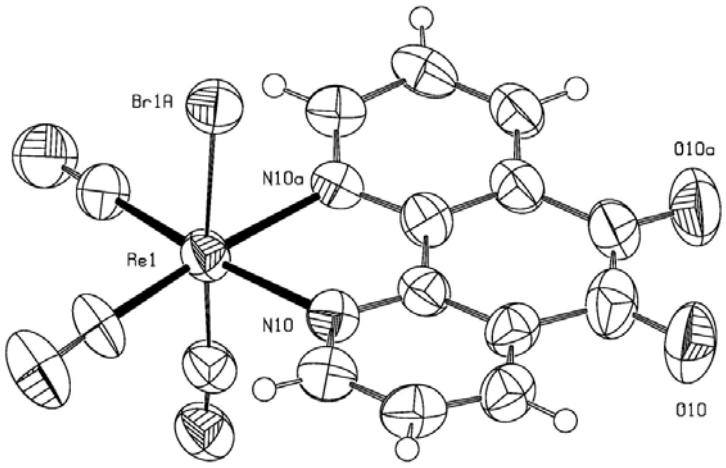

Figure 4.5 ORTEP drawing of the structure of **29**, which contains a mirror plane through Re1, Br1A and bisecting the ligand between the nitrogen atoms.

The electronic properties of **23** are close to the complexes discussed above. The presence of two additional, more electronegative nitrogen atoms in the ligand, reduces the energy of the LUMO, so that the absorption is shifted to slightly smaller energies and the reduction of the complex is more facile when compared to the bipy complex, which otherwise has a ligand π-system of the same size.

For **29**, light absorption is similar to that of the phen complex to which it is most closely related in structure and size. The electrochemical reduction properties are however very different as the ligand is formally a *ortho*-benzoquinone system.[10] Consequently, the first ligand centred reduction is very facile and already occurs at only –15mV. The resulting radical is a strongly stabilized semiquinone (Fig. 4.6). The second reduction to the diolate can be achieved at –755mV. In the presence of increasing concentrations of water, the second reduction occurs at higher and higher potentials, as the diol instead of the diolate is formed in the presence of protons. Ultimately, the two reductions will merge into a single, two electron reduction wave in water, as reported for the reduction of uncoordinated phd in water. As a result the phd complex offers the possibility of reversible two electron storage within a range of accessible

potentials, which is unique for the series of rhenium diimine complexes studied here.

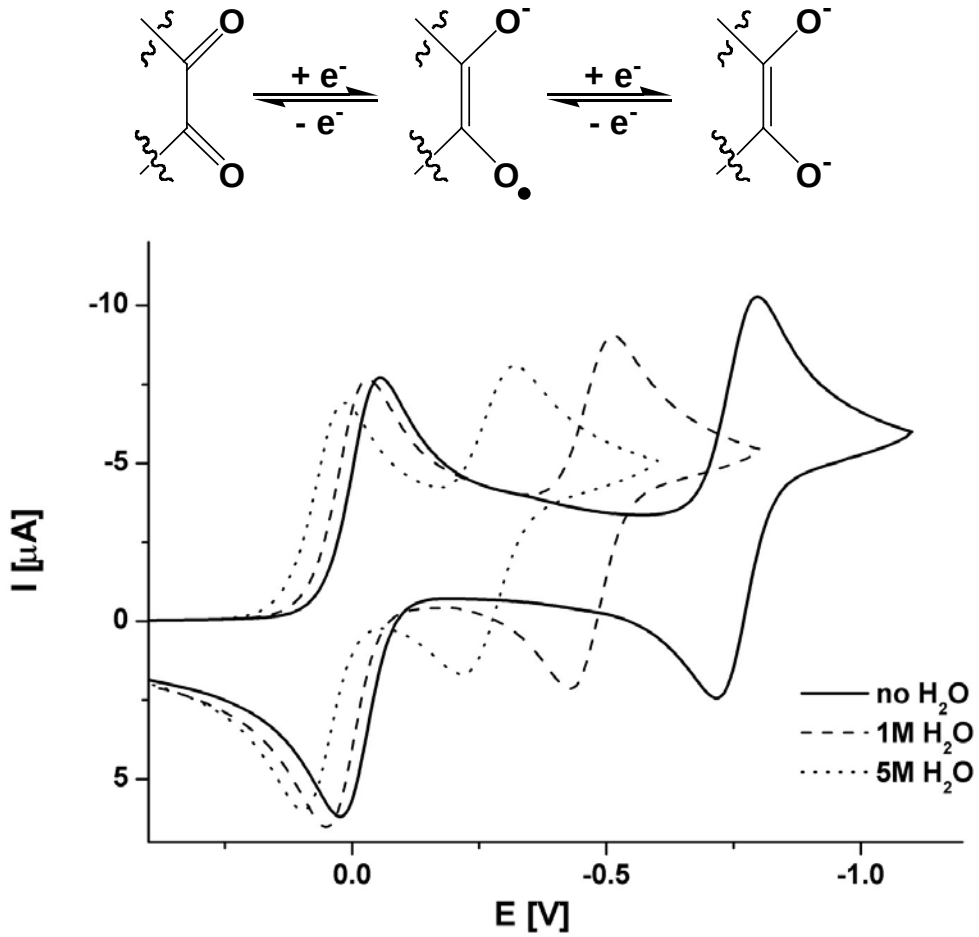

Figure 4.6 Cyclic voltammogram of the two reversible reduction steps observed for the complex **29** in DMF containing increasing concentrations of water. Above, a scheme illustrating the successive reduction of the dione to form the semiquinone and diolate products is shown.

In contrast to the orange complexes of **23** and **29**, the abpy complex **27**, is a dark blue-green powder as a solid and forms deep blue solutions in acetone or DMF. The unusual absorption of this complex is shown in Figure 4.7 in comparison to the absorption spectra obtained for the bpm and phd complexes (which are very similar to the spectra of the non-bridging diimines discussed in part 4.1). The small energies needed for the MLCT transitions of complexes of the abpy ligand are well known and originate from the very low-lying, particularly stabilized LUMO of this ligand which has been calculated to be mainly centred on the azo-function (Figure 4.8).[8] This azo- bridge causes the unusual properties of **27** when compared to the other diimine complexes. As a result, the MLCT absorption band is red-

shifted by over 150nm compared to most other rhenium diimine complexes. Even more striking, the potential needed for the reduction of this complex is only +50mV, as the LUMO is so easily accessible for reduction.

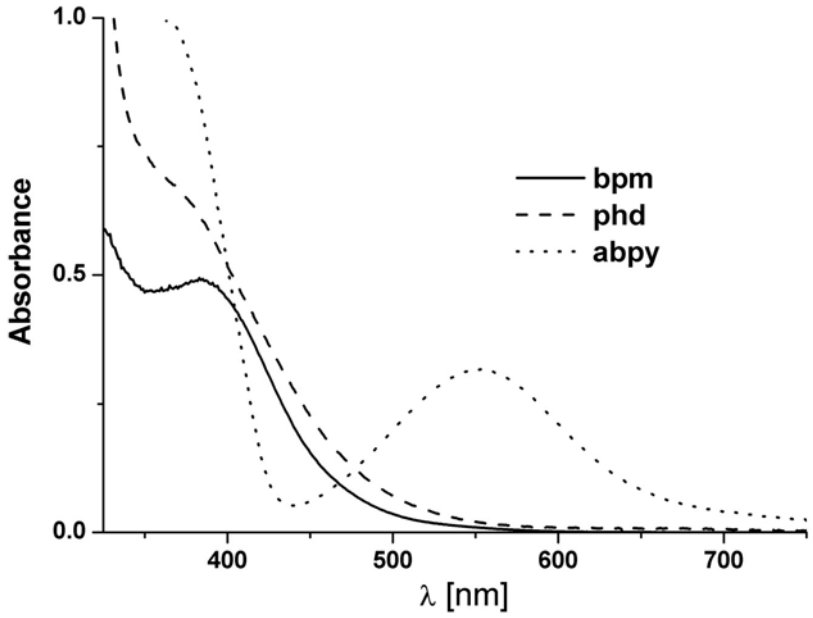

Figure 4.7 Absorption spectra for the different [ReBr(CO)$_3$(diimine)] complexes in DMF (all solutions 0.2mM).

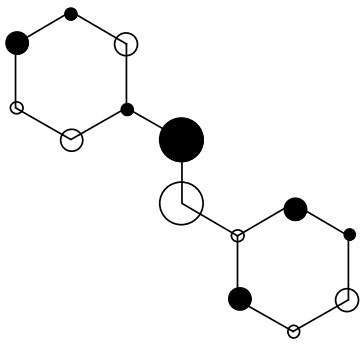

Figure 4.8 Calculated localization of the lowest unoccupied π orbital of abpy (from ref. [11]).

An important difference of the complexes of all three bridging ligands compared to the complexes discussed so far, is the fact that they do not show any room temperature fluorescence in solution. For the known bpm and abpy complexes this has already been reported and it is equally true for the new phd complex. In the cases of **27** and **29** this can be explained by the presence of the low lying acceptor orbitals accessible to the photoelectron. The charge transfer electron will most probably be located on the azo bridge for the abpy and on the quinone moiety for the phd

complex similar to the cases of electrochemical reduction. As the energy gap between these charge transfer states and the ground states is small (like the energies needed for one electron reduction is very small), radiationless transition to the ground state will be fast in accordance with the energy gap law.[12]

But in the case of **23** the absence of fluorescence can not be understood in this way, as the electronic energy gap, judged from the absorption spectrum and the electrochemical reduction, is quite similar to the cases discussed in part 4.1. There is also no strained geometry of the complex like in the case of the biq complex **21**, so the reason for the non- radiative decay of the excited state of **23** remains unclear.

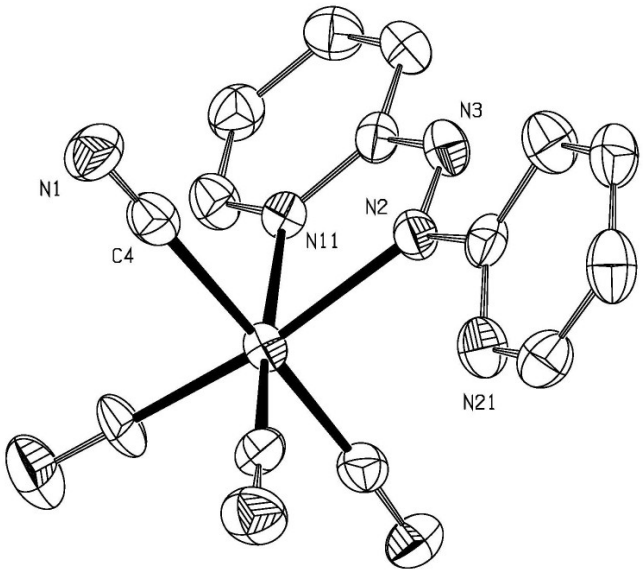

Figure 4.9 ORTEP drawing of the structure of **28**.

Using similar reactions as already described in chapter 3 for the bipy complexes, it is also possible to exchange the sixth ligand X of the complexes containing bridging ligands. In this way the monomeric cyano complexes [Re(CN)(CO)$_3$bpm] (**25**) and [Re(CN)(CO)$_3$abpy] (**28**) were prepared by exchange of the bromide for cyanide ligands. As observed before in the cases of bipy complexes, the electronic effects of the sixth ligand exchanges are rather small, with both the carbonyl frequencies in the infrared and the absorption band in the visible nearly unchanged.

Crystals suitable for a diffraction study could be obtained for complex **28**. The structure was solved and shows the expected coordination geometry for the abpy ligand in plane with the Re(CO)$_2$ moiety *trans* to it. The second pyridine ring of the abpy is slightly bent out of this plane as a result of steric interaction between N21 and the carbonyl ligand next to it. A similar arrangement has been observed for the chloride analogue of this complex, [ReCl(CO)$_3$abpy].[7]

Interestingly, reactions with cyanide are not possible with phd complexes, as the dione functionality of the ligand is attacked by the cyanide nucleophile causing decomposition of the ligand. This phenomenon has been observed and studied in detail before.[13]

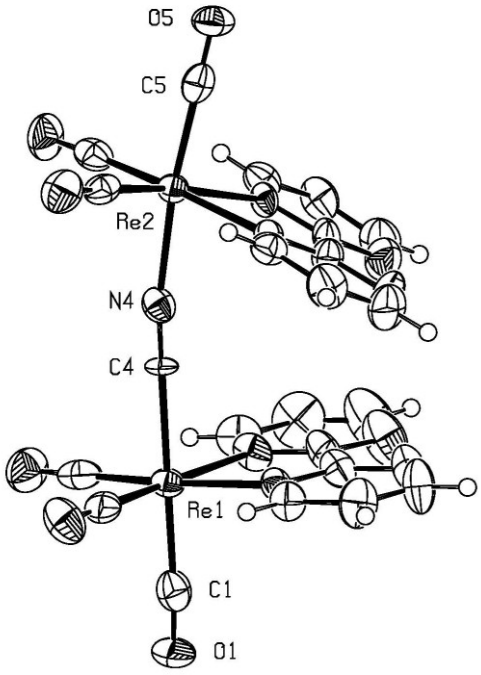

Figure 4.10 ORTEP drawing of the cation of [(Re(CO)$_3$bpm)$_2$(μ-CN)](OTf) (**26**).

Using similar reactions as described for the synthesis of **16**, cyano-bridged dimeric complexes can also be prepared with rhenium bpm or abpy fragments. In the case of bpm, crystals of the OTf$^-$- salt of complex **26** could be obtained for a structure analysis. The coordination geometry of the complex is very similar to the one found for the bipy analogue discussed in chapter 2 (Figure 2.9). The distance between the two rhenium centres is 5.4Å. A strong π-π- stacking interaction between the bpm ligands causes the

two bpm planes to be bent towards each other and the distance at the edges is only 3.7Å. But this bending seems to be merely a phenomenon observed in the solid state – no NOE interaction between the two bpm ligands was observed in NMR, even when a methanol solution of **26** was cooled down to –60°C. Therefore it was concluded that there is free rotation of the two units around the Re-CN-Re axis.

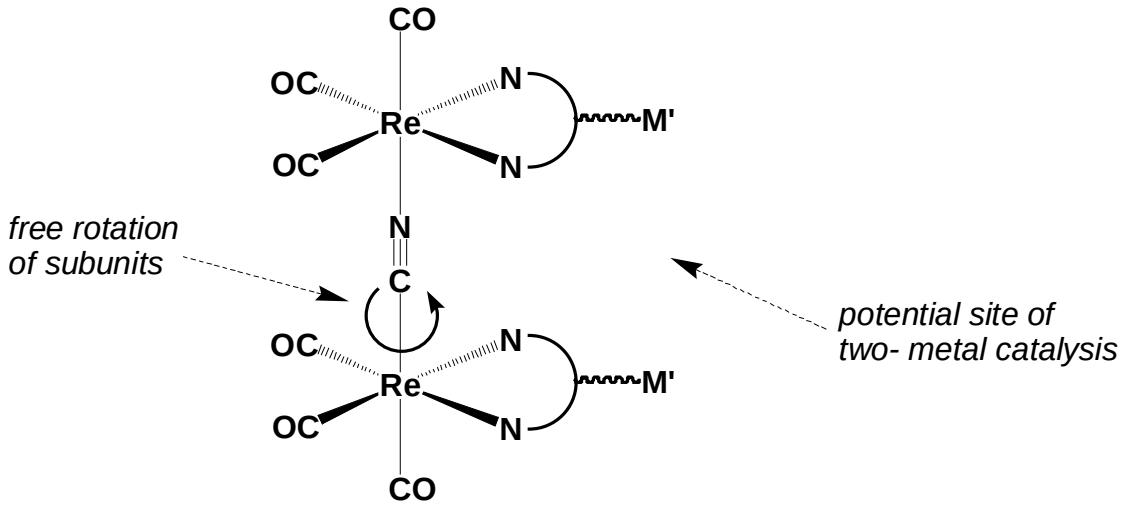

Figure 4.11 Possible use of dimeric complexes as flexible, photoactive ligand scaffolds.

The dimeric complexes containing the bridging diimines bpm and abpy can therefore be seen as unusual, flexible and photoactive ligand scaffold for the complexation of two metals centres M' close to each other. The cyano bridge allows free rotation, the diimine ligands might enable photoinduced metal to metal charge transfer from rhenium to M' and the two additional metals could come into close enough distance to allow two-metal catalysis.

In the case of abpy, the formation of cyano- bridged dimeric species was also possible, but a mixture of stereoisomers was detected by both HPLC and NMR which could not be separated. Unlike all other diimine complexes discussed here (e.g. Figure 4.5), the abpy complex has no mirror symmetry with a plane perpendicular to the diimine ligand. As a result, linking two rhenium abpy fragments by cyanide may result in the formation of stereoisomers according to the simplified representation shown in 4.12: the uncoordinated pyridine rings of the abpy ligand might be on the "same" or

"opposite" sides of the cyano bridge. This could be the explanation for the observed formation of a mixture of products.

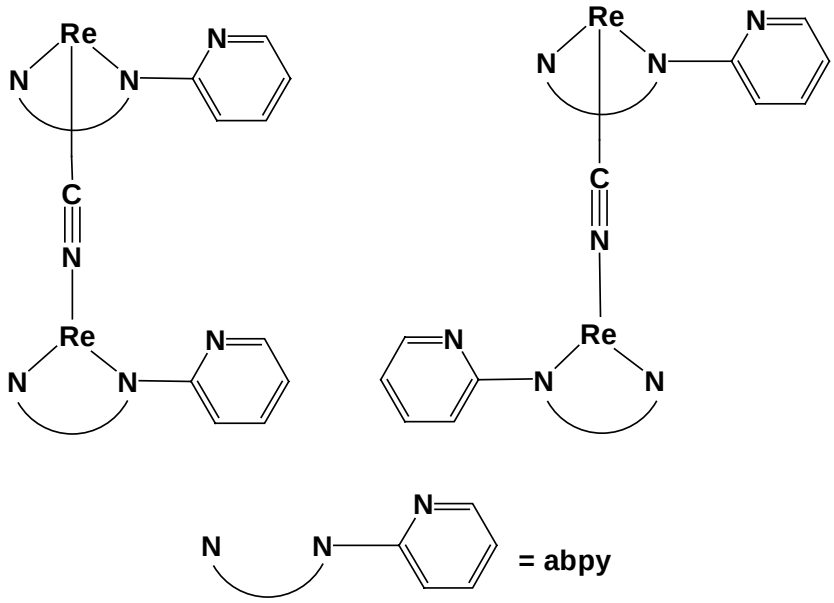

Figure 4.12 Probable formation of stereoisomers as a result of the linkage of two rhenium abpy fragments by a cyanide bridge.

To conclude the results presented in this chapter, it was possible to synthesize [ReX(CO)$_3$(diimine)] complexes using a number of different diimines. In a first series of extended bipy-like systems, diimines larger than bipy offered the possibility to lower the energy level of the LUMO, resulting in smaller energies needed for the MLCT transition and also electrochemical reduction. For the perspective of the photocatalytical application of such complexes this causes absorption of a greater range of wavelength in the visible. On the other hand, the reduced forms of such complexes are less powerful reducing agents when compared to the bipy complex. In a second series, it was also possible to synthesise complexes bearing bridging diimines. These complexes might allow to link the photoactive rhenium tricarbonyl moity to a second metal centre. Cyano- bridged dimers of such complexes might even be used as scaffold ligands for the coordination of two additional metal centres. However, the introduction of the azo- and dione- functionalities in the abpy and phd ligands, respectively, alters the electronic properties of the rhenium complexes to a large extend, especially obvious as the reduction of these complexes becomes very facile and the room temperature fluorescence in solution is not observed. Combined with

the series of complexes already presented in chapter 3, a set of complexes was thus made available for the photocatalytic tests to be presented in chapter 6. Within this set electronic differences from the original [ReX(CO)$_3$bipy] vary greatly, from the subtle effects observed for the exchange of the sixth ligand to the large changes observed for the complexes functionalised diimine. A wide variation of activity was therefore expected for the photocatalysis reactions.

References

[1] G. Calzaferri, K. Haedener, J. Li, *J. Photochem. Photobiol. A* **1992**, *64*, 259.

[2] J. Hawecker, J. M. Lehn, R. Ziessel, *J. Chem. Soc., Chem. Comm.* **1983**, 536.

[3] J. C. Luong, L. Nadjo, M. S. Wrighton, *J. Am. Chem. Soc.* **1978**, *100*, 5790.

[4] R. van Belzen, R. A. Klein, W. J. J. Smeets, A. L. Spek, R. Benedix, C. J. Elsevier, *Recl. Trav. Chim. Pays Bas* **1996**, *115*, 275.

[5] J. E. Dickeson, L. A. Summers, *Austr. J. Chem.* **1970**, *23*, 1023.

[6] A. Juris, S. Campagna, I. Bidd, J. M. Lehn, R. Ziessel, *Inorg. Chem.* **1988**, *27*, 4007.

[7] H. Hartmann, T. Scheiring, J. Fiedler, W. Kaim, *J. Organomet. Chem.* **2000**, *604*, 267.

[8] W. Kaim, S. Kohlmann, J. Jordanov, D. Fenske, *Z. Anorg. Allg. Chem.* **1991**, *598-599*, 217.

[9] G. A. Fox, S. Bhattacharya, C. G. Pierpont, *Inorg. Chem.* **1991**, *30*, 2895.

[10] T. S. Eckert, T. C. Bruice, J. A. Gainor, S. M. Weinreb, *Proc. Natl. Acad. Sci. USA* **1982**, *79*, 2533.

[11] W. Kaim, *Coord. Chem. Rev.* **2001**, *219-221*, 463.

[12] H. Henning, D. Rehorek, *Photochemische und photokatalytische Reaktionen von Koordinationsverbindungen*, **1988**.

[13] H. Kwart, M. M. Baevsky, *J. Am. Chem. Soc.* **1958**, *80*, 580.

5. SYNTHESIS AND REACTIVITY OF HETERONUCLEAR, BIMETALLIC COMPLEXES

The synthetic trials described in part 4.2 showed that it is possible to synthesise monomeric rhenium tricarbonyl complexes containing potentially bridging diimine ligands. With the goal to obtain mixed, heteronuclear species, as proposed in Scheme 1.15, these rhenium complexes were now used for the coordination of a second metal centre. The ideal outcome would be the construction of dimeric systems capable of a photo-initiated metal-to-metal electron transfer, mediated by the bridging diimine.

5.1 Possible metal fragments and synthetic strategy

A study of the literature showed that only very few bridging systems with the bridging ligands bpm, abpy or phd are known were two *different* metal centres are linked by the diimine, while examples of homonuclear species, where the diimine coordinates the same metal fragment on both sides, are abundant. For rhenium tricarbonyl diimines, heteronuclear species are only known for bpm and bptz as bridging ligand. Three complexes of the type $[ReCl(CO)_3(\mu\text{-bpm})(M'L_n)]$ (Scheme 5.1) were prepared in a study by MATHEIS and KAIM in 1991.[1] The bptz complex will be discussed in part 5.3.

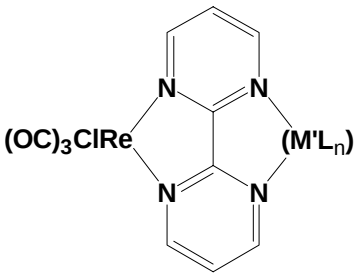

M'Ln:
$Mo(CO)_4$
$Cu(PPh_3)_2^+$
$Ru(bipy)_2^{2+}$

Scheme 5.1 Heteronuclear complexes of the type $[ReCl(CO)_3(\mu\text{-bpm})(MLn)']$ prepared in the study of MATHEIS and KAIM.

The photocatalytic carbon dioxide reduction was never investigated for any of those complexes. For our purpose, only the copper complex from this series seemed to be an attractive choice as it contains phosphine ligands on the second metal centre that might be replaced by a substrate, unlike the carbonyl or bipy ligands of the molybdenum or ruthenium fragments,

respectively, which are expected to be too strongly bound to allow substrate coordination.

As there were no other examples known from the literature for heteronuclear complexes containing rhenium carbonyl, we considered further metal fragments. Possible candidates should contain a metal centre that might undergo one-electron redox chemistry. Additionally, at least one labile coordination position is necessary for the binding of substrates such as CO_2 or H_2O.

At first, we studied reactions of $[ReBr(CO)_3(bpm)]$ (**23**) with salts of first row transition metals like iron(III) chloride, cobalt(II) chloride, nickel(II) acetate or copper(II) tetrafluoroborate in acetonitrile, ethanol, water or mixtures of these solvents. In most of the cases strong colour changes are observed upon addition of the metal salt to solutions of **23**, as deep red, brown or even green solutions were obtained. But HPLC analysis of the solution indicated the formation of mixtures of numerous products. In none of the cases it was possible to isolate a defined, characterised reaction product. The reasons for this behaviour are not clear, but the most likely problem might be the undefined coordination sphere at the second metal, so that dimeric Re-bpm-M' species might form together with Re-bpm-M'-bpm-Re or even $(Re\text{-}bpm)_3$-M' clusters. Additionally, the second metal M' might coordinate a large number of possible ligand combinations on the sites not occupied by bpm, as e.g. acetonitrile, water and halides could compete for vacant coordination sites. This, obviously too simple, synthetic route was therefore not pursued.

Instead, we looked for metal fragments where some of the coordination sites are blocked by strongly bound ligands and the number of possible ligand combinations is therefore reduced. It also seemed a good approach to look for fragments where monomeric complexes with e.g. bipy or phd are known to form, thus making it more likely that such a fragment might form stable complexes with $[ReBr(CO)_3(bpm)]$ (**23**), $[ReBr(CO)_3(abpy)]$ (**27**) or $[ReBr(CO)_3(phd)]$ (**29**) as well. Surprisingly, not too many metal fragments known from the literature meet all these requirements, so that the

synthetic trials of this work were limited to five promising candidates (Scheme 5.2): $[Ru(9S3)]^{2+}$, $[Cu(bipy)]^{+}$, $[IrCp^*]^{2+}$, $[Pt(PPh_3)_2]^{2+}$ and the $[Cu(PPh_3)_2]^{+}$ fragment already discussed above. For these moieties, homonuclear dimeric complexes $[(M'L_n)(\mu\text{-bpm})(M'L_n)]$ or $[(M'L_n)(\mu\text{-abpy})(M'L_n)]$ are known for $[Ru(9S3)]^{2+}$ and $[IrCp^*]^{2+}$.[2,3] The iridium unit is especially interesting because it forms water stable hydrides useful for catalytic reduction processes, as discussed in more detail in part 5.4. The fragment $[Pt(PPh_3)_2]^{2+}$ has been found to form stable complexes with the doubly reduced form of phd as bridge to palladium(II) chloride.[4] The $[Cu(bipy)]^{+}$ seemed interesting as analogue to the known $[Cu(PPh_3)_2]^{+}$ fragment.

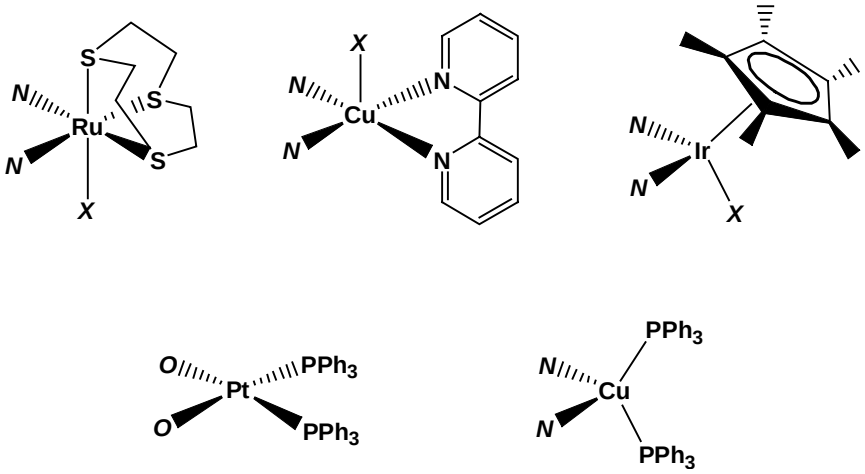

Scheme 5.2 Metal fragments used for the synthesis of complexes of the type Re-μ-diimine-M'L_n. *N* and *O* represent possible coordination sites for nitrogen and oxygen ligand atoms of the bpm, abpy or phd ligands, respectively; X marks the position of weakly coordinated solvent molecules, replaceable by a substrate.

Surproingly, reactions of **23** or **27** with acetonitrile solutions of precursor complexes of the fragments $[Ru(9S3)]^{2+}$ or $[Cu(bipy)]^{2+}$, $[Ru(H_2O)_3(9S3)](OTf)_2$ and $[Cu(MeCN)_2(bipy)](NO_3)$, resulted in the transfer of the bpm or abpy ligands from rhenium to ruthenium or copper. A diimine bridged Re-M' species therefore seems to form temporarily in these reactions, but then the bridged complexes fall apart and the bpm or abpy ligand remains coordinated to the ruthenium or copper fragment. As a result, the $[Re(H_2O)_3(CO)_3]^{+}$ fragment without the diimine ligand can be detected by HPLC in the reaction mixture. Also, crystals of both $[(Ru(9S3)(MeCN))_2(\mu\text{-bpm})](OTf)_4$ and $[Cu(NO_3)(bipy)(bpm)]$ were isolated

from the reaction reaction mixtures, which obviously originate from diimine transfer from rhenium to the other metals.

Facing all these unexpected difficulties and restrictions for the seemingly easy synthesis of heteronuclear μ-diimine complexes, eventually only four examples of such complexes were isolated and properly characterised for this study: the bromide analogue of the known complex from MATHEIS and KAIM, $[(CO)_3BrRe(\mu\text{-bpm})Cu(PPh_3)_2]^+$, a new rhenium analogue of the Pd-(μ-phd)-Pt system described before, and Re - IrCp*- complexes $[(CO)_3(H_2O)Re(\mu\text{-bpm}/\mu\text{-abpy})Ir(H_2O)Cp^*]^{3+}$. Their synthesis and properties will be described in the following parts.

The bridged, heterodinuclear systems seemed to be very interesting compounds, so many synthetic attempts under various reaction conditions were carried out – why only in these few cases well-defined compounds could be isolated (and what happens in all other reactions leading to multi-component mixtures) remains not understood. Even less successful were the equally numerous trials to synthesise an example of the tetranuclear, "horseshoe"-type complex as envisioned in Figure 4.11. Reactions of the $[(Re(CO)_3bpm)_2(\mu\text{-CN})]^+$ "scaffold" complex with the copper or iridium fragments discussed below definitely occurred, as strong changes in colour or HPLC analysis were seen – but the isolation of any tetranuclear complex could not be achieved and remains an interesting challenge for the future.

5.2 $[(CO)_3BrRe(\mu\text{-bpm})Cu(PPh_3)_2]^+$ and $[(CO)_3BrRe(\mu\text{-phd})Pt(PPh_3)_2]$

When it became clear that reactions of **23** or **27** with solutions of transition metal salts did not result in the formation of defined products, one of the first reactions carried out next was the synthesis of $[(CO)_3BrRe(\mu\text{-bpm})Cu(PPh_3)_2]^+$ (**30**), using an analogous procedure as reported for the chloro- analogue by MATHEIS and KAIM. In the original synthesis it was found that this compound is best prepared by a comproportionation reaction starting from a copper(II) precursor and copper metal.[1]

$$\mathbf{2\ [ReBr(CO)_3bpm] + Cu^0 + Cu^{II}(BF_4)_2 + 4\ PPh_3 \longrightarrow 2\ [ReBr(CO)_3(\mu\text{-bpm})Cu(PPh_3)_2](BF_4)}$$

Scheme 5.3 Comproportionation reaction for the synthesis of **30**.

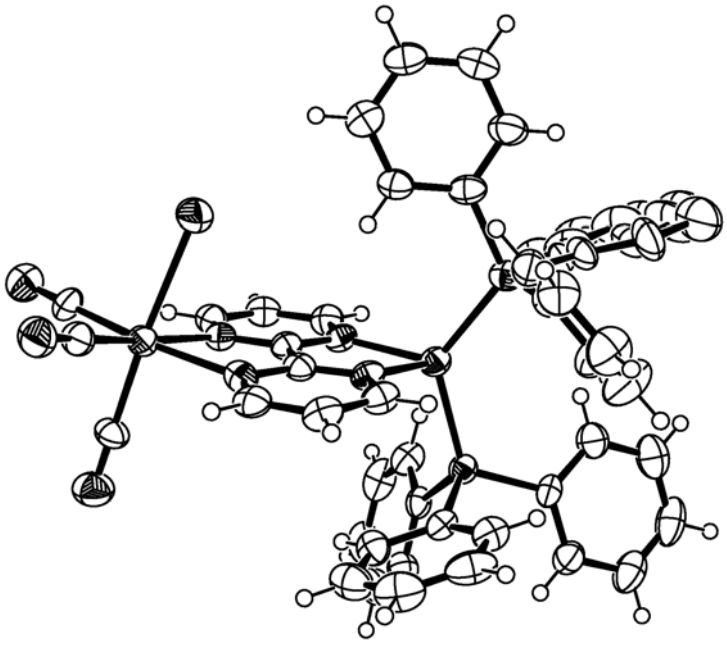

Figure 5.1 ORTEP drawing of the cation of **30**.

Therefore the analogous reaction (Scheme 5.3) was carried out for the coordination of copper to **23** and indeed led to the expected product in good yield. Crystals of good quality of the deep orange substance could be obtained for a X-ray diffraction analysis, which confirmed the expected coordination geometry of the $[ReBr(CO)_3(bpm)]$- unit coordinated to a

tetrahedral copper(I) unit (Fig. 5.1). The only difference for the rhenium fragment to other complexes containing the [$Re(CO)_3$(bpm)] fragment is that the [$ReBr(CO)_3$]-unit is unusually bent towards the bpm plane. The reason for this must be the electronic influence on the molecular orbitals of the bpm by the coordinated copper fragment, as no steric reasons are apparent from the structure. As known for other bpm complexes, the ligand brings the two metals of **30** within a short distance of each other, in this case the distance is 5.8Å.

A comparison of the spectroscopic and electrochemical properties of the complex with monomeric **23** is shown in Table 5.1. The carbonyl frequencies in the IR do not differ significantly; the same is true for the absorption maxima in the visible both in DMF as well as CH_2Cl_2. The latter is surprising, as the appearance of the substance changes from an orange to a deep red powder, but still the absorption maximum remains at the same position. The extinction coefficient is twice as large when compared to **23** which might explain the different appearance. With the IR and UV-Vis spectra more or less unchanged, it was also unexpected to find the first, reversible, electrochemical reduction wave already at –390mV, in agreement with the literature values for the chloro- analogue. MATHEIS and KAIM also measured the EPR spectrum of the reduced chloro- species and found an organic radical best described electronically as $[(CO)_3BrRe^{I}(\mu\text{-bpm}^{\bullet -})Cu^{I}(PPh_3)_2]$.[1]

The reduction potential of **30** indicates an energetically much lower LUMO, which should also influence light absorption - but this is obviously not the case. At lower potentials, a series of irreversible reduction waves is observed, probably due to the formation of instable copper(0) species. No oxidation processes could be observed within the potential range of the solvent up to +1.5V, so the copper(II) species seems not easily accessible for this complex. As a consequence, **30** also allows only one reversible single-electron redox process like the monomeric species. The hope that both the bpm/$bpm^{\bullet -}$ as well as the Cu^{II}/Cu^{I} redox pair might be accessible, was thus not fulfilled.

complex	λ_{max} [nm]	ν_{CO} [cm^{-1}]	$E_{1/2, red}$ [mV]
$[ReBr(CO)_3(bpm)]$	385	2030, 1931	-860
$[ReBr(CO)_3(\mu\text{-bpm})Cu(PPh_3)_2]^+$	385	2031, 1934	-390, -700[b], -900[b], -1250[b]
$[ReBr(CO)_3(phd)]$	375[a]	2033, 1943	-15, -755
$[ReBr(CO)_3(\mu\text{-phd})Pt(PPh_3)_2]$	430[a]	2017, 1910	+785[c], +1420[b,c]

Table 5.1 Comparison of selected properties of monomeric and dimeric $[ReBr(CO)_3(diimine)]$ complexes containing bpm and phd bridging ligands. [a] absorption shoulder. [b] irreversible reduction. [c] oxidation process. All four complexes show no fluorescence in DMF at room temperature.

The synthesis of $[ReBr(CO)_3(\mu\text{-phd})Pt(PPh_3)_2]$ (**33**) could be achieved in a similar way as reported for the complex $[PdCl_2(\mu\text{-phd})Pt(PPh_3)_2]$.[4] As the bridging form of the phd ligand is not the diketone form but the reduced semiquinone or diolate forms, it is necessary to reduce the ligand before the second metal can be coordinated. In the published method this is elegantly achieved by using a stable platinum(0) precursor, $[Pt^0(PPh_3)_4]$, which reacts in an oxidative addition to free or coordinated phd. In this way the platinum complex acts both as reducing agent in its reduced form and as the coordinating metal in its oxidised form. The same strategy could also be applied in the rhenium case, as the reaction of $[ReBr(CO)_3phd]$ with $[Pt^0(PPh_3)_4]$ resulted in the formation of the red compound **33** in good yield (Scheme 5.4).

$$\mathbf{[ReBr(CO)_3phd] + [Pt^0(PPh_3)_4]} \longrightarrow \mathbf{[ReBr(CO)_3(\mu\text{-}phd)Pt^{II}(PPh_3)_2] + 2\ PPh_3}$$

Scheme 5.4 Synthesis of **33** by oxidative addition of a Pt^0 phosphine precursor to **29**.

The result of an X-ray structure analysis proved the structure of the complex to be very similar to the known case of $[PdCl_2(\mu\text{-phd})Pt(PPh_3)_2]$ (Figure 5.2). As in the structure of **30**, the rhenium unit is slightly tilted with respect to the phd plane. The platinum is coordinated to two phosphines and the two diolate oxygen atoms in a square planar geometry typical for platinum(II). The fact that the ligand is really present in its doubly reduced form as a diolate can be seen from IR spectroscopy, where

the strong ketone band at 1700cm^{-1} is not observed for the dinuclear complex. The structural data for **33** supports this as well. For the monomeric phd complex **29**, the average carbon oxygen distance for the phd ligand, $d(CO)_{av}$, is 1.28Å, typical for ketone groups. The carbon-carbon bond length between the two ketone carbon atoms is 1.54Å, so rather matching the bond length of a single than an aromatic bond. On the other hand, the bridging phd between rhenium and platinum shows a longer $d(CO)_{av}$ of 1.34Å, typical for phenolates, and consequently a shorter, carbon- carbon distance typical for an aromatic bond (1.38Å) is found for the two carbons of the diolate.

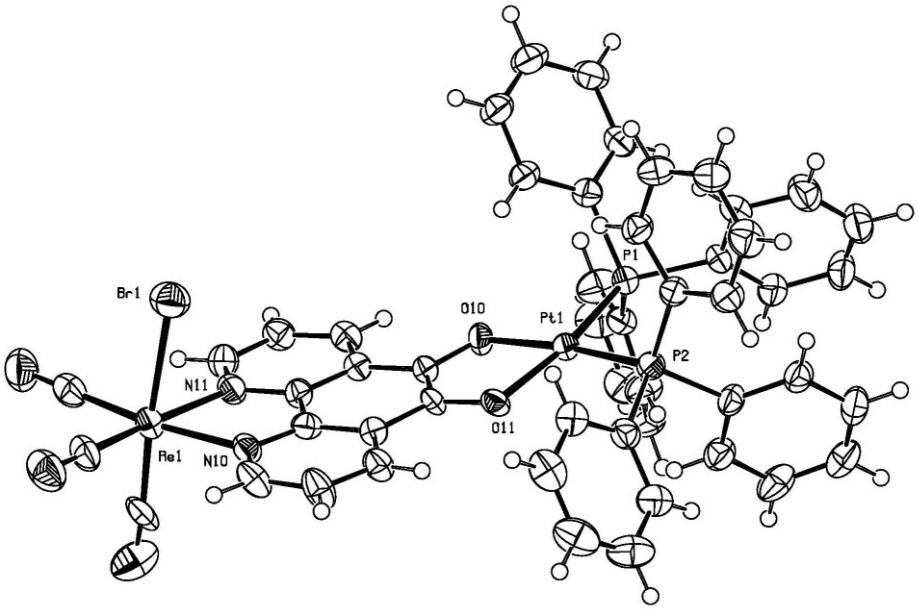

Figure 5.2 ORTEP drawing of the structure of complex **33**.

Judging from the shift observed for the IR vibration frequencies of the rhenium carbonyl ligands, reduction of the ligand and coordination of the platinum moiety increase the electron density on the rhenium markedly. Additionally, the LUMO of the ligand seems to be lowered by the coordination of the platinum, as the visible absorption maximum red-shifts by nearly 50nm. The coordination of the platinum stabilizes the reduced forms of phd greatly against re-oxidation. The difference in potential needed for the oxidations diolate/semiquinone and semiquinone/dione is similarly about 740mV, but the oxidation potentials are more positive for the bridged ligand by 800mV. As the product of the second oxidation is the

dione, which is known not to act as bridging ligand, this second oxidation wave is irreversible (Figure 5.3), as has been observed before the platinum – palladium case.[4] Obviously **33** immediately falls apart when the dione oxidation state is reached. A further reduction of the ligand could not be achieved within potentials down to –1.5V.

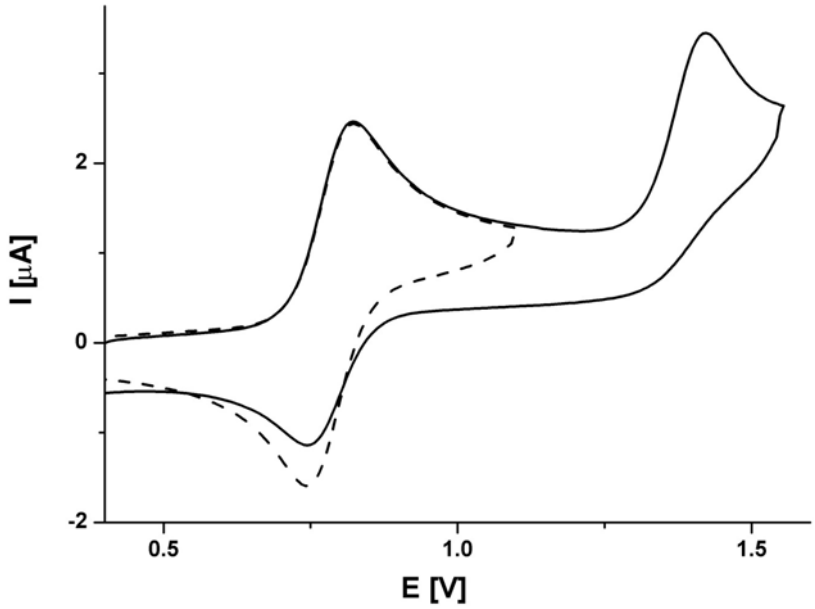

Figure 5.3 Cyclic voltammograms for a solution of **33** in DMF. The oxidation to the semiquinone form (dashed line) is reversible, while the next oxidation step to the dione (solid line) is irreversible.

So similarly to the case of **30**, this dimeric complex also allows only one reversible, one-electron redox process within the possible potential range, in this case the oxidation of **33** to $[ReBr(CO)_3(\mu\text{-}phd^{\bullet-})Pt(PPh_3)_2]$.

For both bridged complexes **30** and **33**, redox potentials are shifted to such high values that their usefulness as reduction catalysts seems doubtful. On the other hand, the complexes might allow direct coordination of substrates if the phosphines are assumed to be reasonably labile to be replaced. This could change the reactivity of these diimine bridged dinuclear complexes significantly.

5.3 The complexes $[(CO)_3(H_2O)Re(\mu\text{-bpm}/\ \mu\text{-abpy})Ir(H_2O)Cp^*]^{3+}$

The rhodium(III) complex $[RhCp^*(H_2O)(bipy)]^{2+}$ was first synthesised in 1987[5] for a study dealing with the reduction of protons to molecular hydrogen in homogeneous solution, where the complex was found to act as an active catalyst. Later studies showed that the unusually stable hydride complex $[RhCp^*H(bipy)]^+$ appears to be the key intermediate in these reactions.[6] The complex hydride was found to be even more stable in the case of the iridium homologue $[IrCp^*H(bipy)]^+$. Since then, a number of reactions catalysed by $[(Rh,Ir)Cp^*(H_2O)(bipy)]^{2+}$ have been found (Scheme 5.5), all involving reductions of different substrates via the hydride intermediate. $[IrCp^*H(bipy)]^+$ is so stable that it was recently possible to isolate it directly from a slightly acidic aqueous solution.[7] This is very unusual for transition metal hydride complexes, often known to lead to a fast formation of H_2 in a acidic aqueous media.

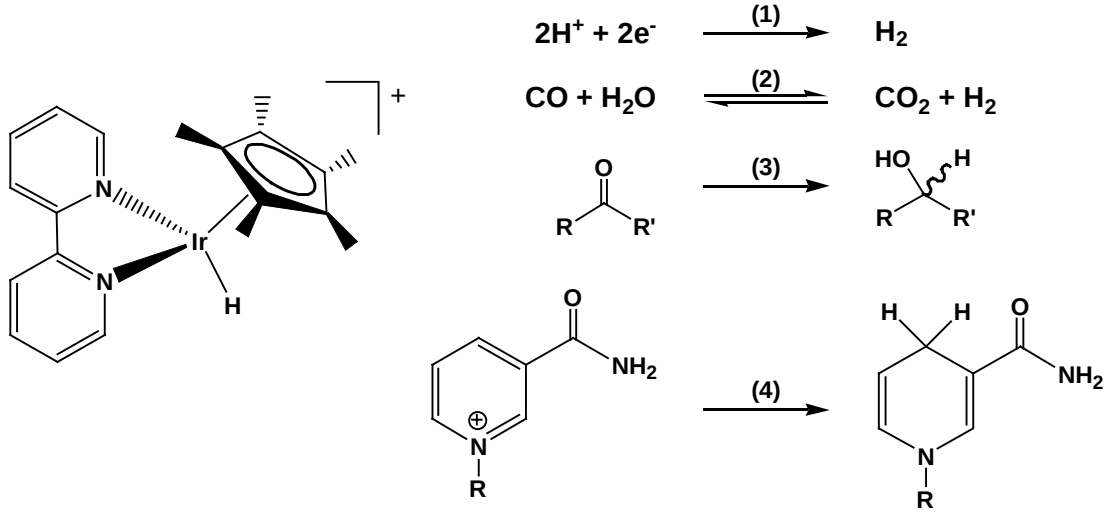

Scheme 5.5 Structure of the water stable hydride complex $[IrCp^*H(bipy)]^+$, the key intermediate in aqueous reduction catalysis by $[IrCp^*(H_2O)(bipy)]^{2+}$ or its rhodium analogue. To the right important examples of reductions catalysed by $[(Rh,Ir)Cp^*(H_2O)(bipy)]^{2+}$ are shown. References: (1) ref. [5]. (2) ref. [6]. (3) ref. [7]. (4) ref.[8].

This metal fragment is of course a very attractive component for a bimetallic catalytic system for reduction reactions. It seemed particularly suitable to be coupled to the photoactive $[Re(CO)_3]^+$ unit. This was already

realised by SCHEIRING et al. in 2001.[9] The complex $[ReCl(CO)_3(\mu\text{-bptz})RhClCp^*]^+$ was synthesised, whose structure is shown in Scheme 5.6. The electrochemical reduction of this complex was studied. Similarly to the the Re-bpm-Cu system presented above, the coordination of the second metal makes the reduction of the bridging diimine ligand more facile. The monomeric $[ReCl(CO)_3(bptz)]$ can be reduced reversibly to $[ReCl(CO)_3(bptz^{\bullet-})]$ at –720mV while the same process occurs already at –180mV for the dinuclear $[ReCl(CO)_3(\mu\text{-bptz})RhClCp^*]^+$. The compound was unfortunately not tested for any catalytic activity neither for one of the reactions shown in Scheme 5.5 nor for the photochemical carbon dioxide reduction following the Strasbourg scheme.

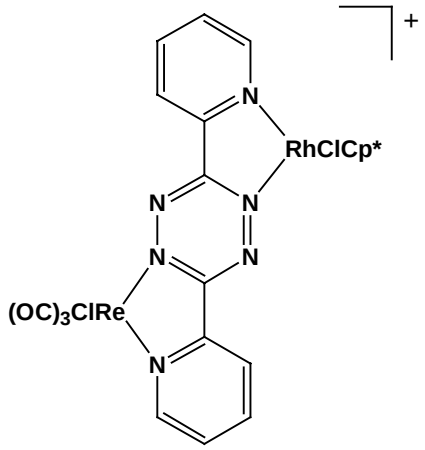

Scheme 5.6 Structure of the dinuclear complex $[ReCl(CO)_3(\mu\text{-bptz})RhClCp^*]^+$ synthesised by SCHEIRING et al..

As the iridium hydride complex had been found to be more stable than the rhodium analogue, it was decided to synthesise the heterodinuclear rhenium-iridium complexes bridged by bpm or abpy. It was of particular interest whether a hydride could be formed of such a dimeric species; therefore the complexes were synthesised as aquo species, as the iridium aquo-complex was considered to be the catalyst of choice for reactions of Scheme 5.5.

The fragment $[IrCp^*(H_2O)_3]^{2+}$ is known to be stable in aqueous solution[10], therefore the synthesis was carried out in water starting from $[Re(H_2O)(CO)_3(bpm/abpy)]^+$ and $[IrCp^*(H_2O)_3]^{2+}$. Indeed, the combination of aqueous solutions of these rhenium and iridium precursors resulted in the

formation of the bridged complexes. However, the products are obtained as a mixture of *cis* and *trans* stereoisomers (Scheme 5.7), easily detected by NMR as two signals for the Cp* protons are observed in a ratio of about 2:1 for both the dinuclear bpm- and the abpy- complex. The formation of isomers was reported for SCHEIRING et al. for the bptz complex as well.[9] For a similar homodinuclear complex, $[(RhClCp^*)_2(\mu\text{-bpm})]^+$, the pure *trans* stereoisomer could be isolated as a solid, but it was found to equilibrate rapidly into a 1:1 *cis*/*trans* mixture in solution.[3] Therefore, a way to separate the isomers was not developed, as it was expected that a solution of the complex, used for catalysis studies, would contain an equilibrium mixture of the isomers anyway, regardless whether a pure isomer or a mixture of *cis* and *trans* forms was dissolved.

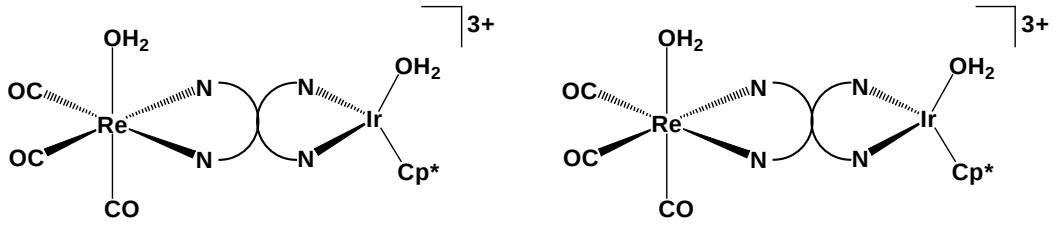

cis ***trans***

Scheme 5.7 Positional isomers of the complexes **31** and **32**.

Most probably due to this mixture of isomers present in solution, it proved to be very difficult to obtain crystals of these complexes for an X-ray structure analysis. A separation of the isomers by HPLC was not possible. Only for the abpy complex it was possible to isolate crystals, but of quite poor quality. Nevertheless the data was good enough to solve the structure of the *cis* isomer of the abpy complex (Figure 5.5), yet a proper refinement of the structure was not possible. But the basic features of the geometry of the complex can be deduced from this analysis: the two metal centres are held in a close distance of 4.9Å to each other, even closer than two metals coordinated to a bridging bpm ligand. Again, the $[Re(CO)_3]^+$ is tilted with respect to the abpy ligand plane but for this complex the ligand itself appears to be unusually bent as well (see especially the side view of Figure 5.4). This has never been reported for the abpy ligand before, and remains

unexplained, as abpy is instead usually found to be planar, even when bridging two metal centres.

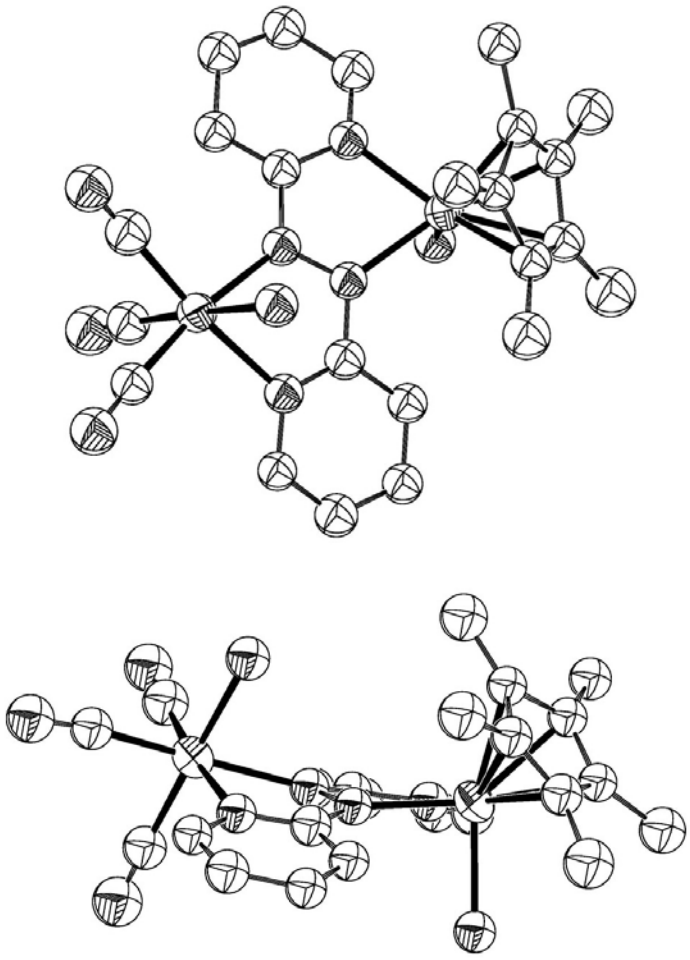

Figure 5.4 ORTEP drawings of the structure of the cation of **32**. Views from the top and side of the abpy ligand are shown.

complex	λ_{max} **[nm]**	ν_{CO} **[cm^{-1}]**
$[ReBr(CO)_3(bpm)]$	385	2030, 1931
$[Re(H_2O)(CO)_3(\mu\text{-bpm})IrCp^*(H_2O)]^{3+}$	425[a], 555	2046, 1936
$[ReBr(CO)_3(abpy)]$	360[a], 550	2020, 1924
$[Re(H_2O)(CO)_3(\mu\text{-abpy})IrCp^*(H_2O)]^{3+}$	450, 510, 700[a]	2028, 1917

Table 5.2 Comparison of selected properties of monomeric rhenium and dimeric Re-μ-diimine-IrCp* complexes containing bpm and abpy bridging ligands. [a] absorption shoulder. All four complexes show no fluorescence in DMF at room temperature.

A large difference in electronic properties is observed when comparing the dinuclear complexes to the mononuclear rhenium species (Table 5.2). The removal of the halide ligands from rhenium and iridium results in the formation of cationic complexes with reduced electron density on the rhenium because of the positive charge. The vibration frequencies of the carbonyl ligands are (with one exception) shifted to higher wavenumbers as a result.

Coordination of the second metal seems to reduce the energy of the ligand LUMO as observed before, because the energy necessary for the MLCT excitation is reduced and the bands of light absorption are shifted to higher wavelength as a result. There is an additional light absorption band present for the bridged complexes, most probably a MLCT band with charge transfer from the iridium instead of rhenium to the ligand. In both cases the MLCT absorption band at smaller wavelength (425nm for bpm, and 510 for abpy) are tentatively assigned as Ir→ligand MLCT, as the iridium(III) centre carrying a double positive charge is expected to be less electron rich than the monocationic rhenium(I) part of the dinuclear complex, making electron transfer more energy demanding as a result.

5.4 Activity of iridium complexes as catalysts for ketone reduction

For catalytic activity, it is of key importance that the hydride complex of the [IrCp*]- unit is formed. To probe whether the new, dinuclear complexes can still form the hydride intermediate, catalysis experiments were performed to compare the catalytic activity of the new assemblies with mononuclear iridium species.

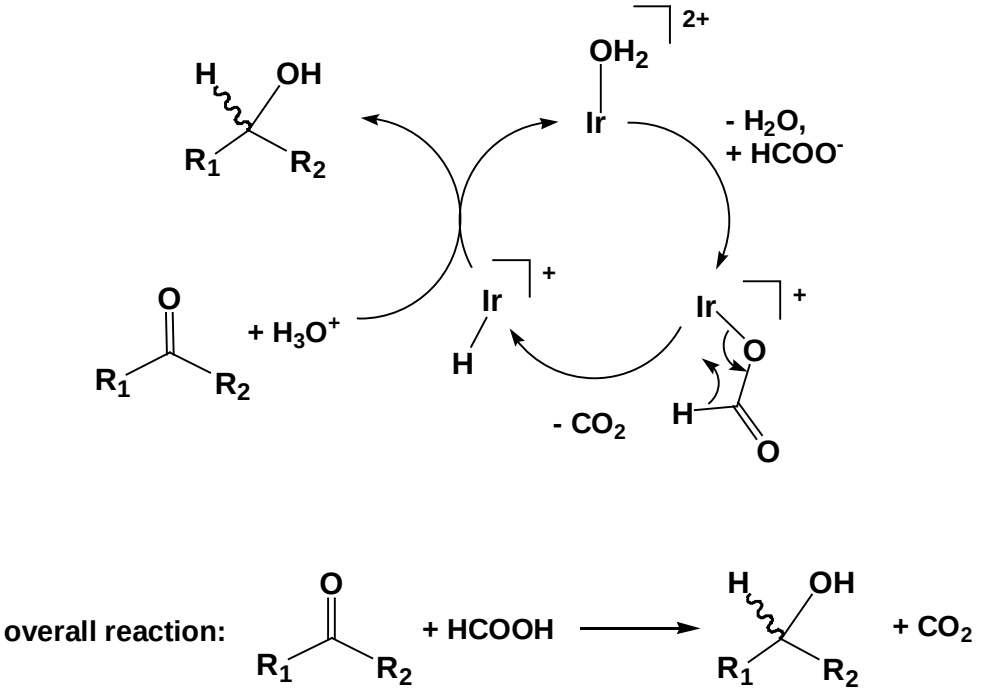

Scheme 5.8 Catalytic cycle for the transfer hydrogenation of ketones catalysed by $[IrCp^*(H_2O)bipy]^{2+}$ in aqueous solution.[7] **Ir** ≡ [IrCp*bipy].

One such a catalytic reactions easily carried out is the reduction of ketones according to reaction (3) of Scheme 5.5. Formate is used as a hydride source in this reaction to form the intermediate $[IrCp^*H(bipy)]^+$ in acidic solution. The ketone than reacts with the iridium hydride and protons to be reduced to a secondary alcohol. The well-established catalytic cycle for this reaction is shown in Scheme 5.8.

In a recent study, catalytic rates were determined for the reduction of various ketones catalysed by $[IrCp^*(H_2O)bipy]^{2+}$ according to Scheme 5.8.[7] The rate of product formation was linear for all seven different ketones and varied between 150 to 525 turnovers per iridium catalyst per hour at 70°C.

A ketone for which fairly average reduction kinetics were determined is cyclohexanone being reduced to cyclohexanol at a rate of 375 turnovers per hour.

To allow a comparison with the reported data, catalytic reduction experiments were run using always cyclohexanone as substrate at the same conditions as reported. But in this study, different iridium diimines were used as catalysts: the dinuclear complexes **31** and **32** described above. All reports in the literature that described the kinetics of ketone reduction according to Scheme 5.8 dealt with $[IrCp^*(H_2O)bipy]^{2+}$ or its rhodium analogue only, so what effects a variation of the [IrCp*]- catalyst might have was unknown.

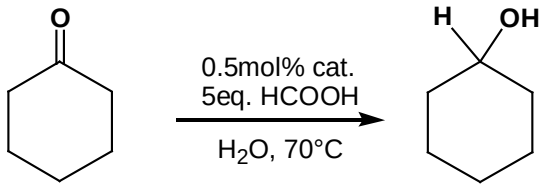

Scheme 5.9 Reaction conditions for the reduction of cyclohexanone to cyclohexanol by formic acid, catalysed by different complexes $[IrCp^*(H_2O)diimine]^{n+}$.

A series of catalysis experiments was carried out with reaction conditions according to Scheme 5.9. The stoichiometry catalyst/substrate/formic acid (1/200/1000) and the temperature of 70°C were the same as in reported in the literature for the cyclohexanone reduction by $[IrCp^*(H_2O)bipy]^{2+}$. From time to time, solution samples were taken from the aqueous reaction mixture, extracted by diethyl ether. The ether phase was analysed by GC to determine the ratio of cyclohexanone/ cyclohexanol. In addition to the bridging diimine compounds a mononuclear reference compound, $[IrCp^*(H_2O)bpm](OTf)_2$ was synthesised following the reported method for the synthesis of the bipy analogue.[10] As this catalysis study was not the main focus of the work, only a limited number of experiments was carried out and many questions had to remain untackled – but still some remarkable effects were clearly observed.

Curves illustrating the formation of the reduction product cyclohexanol with progressing reaction time are shown in Figure 5.6. At first it is striking that replacing the bipy ligand of the original catalyst by bpm reduces the

catalytic rate by a factor of about 6, as only 60 turnovers occur over the first hour compared to the 375 reported for the bipy complex in the literature. For the first 2 hours product formation is found to be linear with time before product formation levels off at about 80% substrate conversion. After 4h, no further reduction of the ketone occurs and the pH of the reaction has risen from the initial value of 2 to a pH≈5. This indicates that, parallel to the consumption of formic acid according to Scheme 5.8, a large fraction of the acid undergoes a disproportionation into molecular hydrogen and carbon dioxide according to Scheme 5.10.

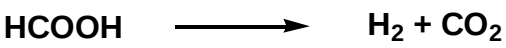

Scheme 5.10 Disproportionation of formic acid.

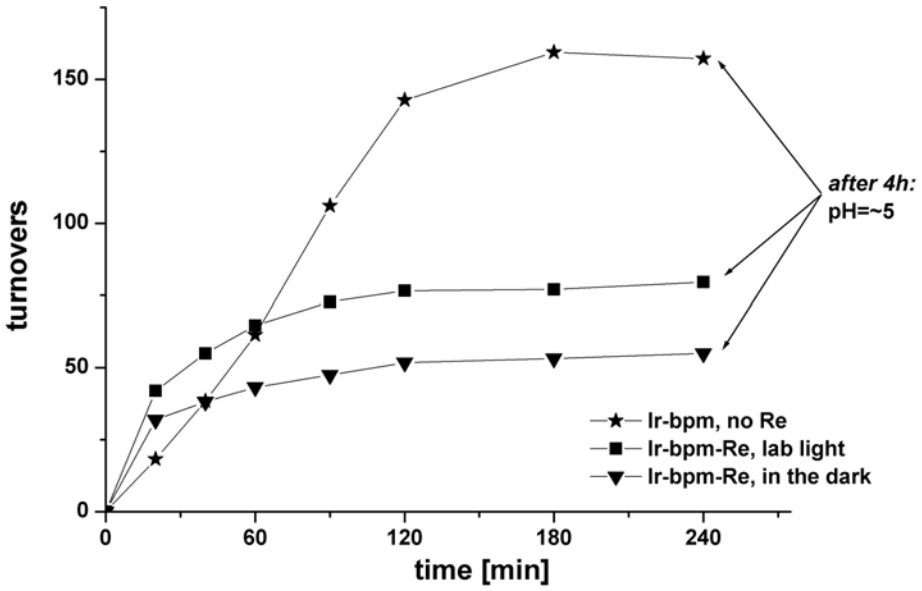

Figure 5.5 Catalytic reduction of cyclohexanone to cyclohexanol. Formation of the product cyclohexanol as a function of reaction time for $[IrCp^*(H_2O)bpm](OTf)_2$ (*Ir-bpm*) or **31** (*Ir-bpm-Re*) as catalysts. Reaction conditions as shown in Scheme 5.9.

It is obvious from Figure 5.5 that the bpm- bridged dinuclear complex **31** is also an active catalyst for the reaction with a slightly higher initial rate of substrate reduction than observed for the mononuclear Ir-bpm species. But **31** appears to be a much more effective catalysts for formic acid disproportionation as well: a strong evolution of gas is observed for reactions using **31** as catalysts together with a much faster rise of the pH, reaching pH≈5 already after 60min. As a result, product formation levels off quickly and substrate conversions of only ≈35% can be achieved.

The different behaviour of **31** proves that the coordination of the rhenium apparently changes the properties of the complex significantly. Even more important, the ability to act as a catalyst is not lost after the coordination of the second metal. This also indicates that **31** is still able to form the iridium hydride intermediate, which was the key question addressed by these catalysis experiments.

The limited time available for the study of this catalytic system did not allow to understand the observed effects in any real detail. Considering the known catalytic cycle, most probably there are different kinetics for the formation of the hydride intermediate in the first step. Once the iridium hydride is formed, two competing parallel reactions might occur as suggested in Scheme 5.11: protonation of the hydride to form H_2 and reaction of the hydride with the ketone to yield the product cyclohexanol.

Both reactions take place in parallel for the compounds investigated, indicated by the rise in pH observed in all reactions, but for **31** both k_1 and k_2 seem to be larger. This could explain that product formation is faster at the beginning for an experiment using catalyst **31**, but also gas evolution is much more intense. The ratio k_1/k_2 for the competing reactions is most probably larger as well, so that the formic acid disproportionates much faster in these cases, resulting in smaller product yields at the end of the experiment, when all the formic acid is consumed. Details of these kinetics remain to be studied to confirm this explanation.

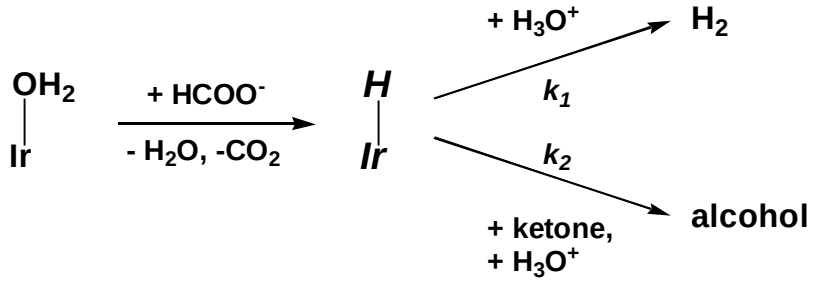

Scheme 5.11 Possible competing reactions for the iridium hydride intermediate.

Another observation that should be studied further is the effect of light for this reaction. Reactions were normally carried out under normal laboratory light. If the catalysis using the Ir-bpm-Re dinuclear catalyst is carried out in the dark, the kinetics of product formation follow a similar

pattern, but the reaction rate is reduced by about one third. For the photocatalytic water-gas shift reaction catalysed by $[IrCp^*(H_2O)bipy]^{2+}$ (Scheme 5.2, reaction (2)), it has been postulated that only the photo-excited state of the iridium hydride intermediate reacts with protons to form H_2, while no H_2 formation is observed in the dark.[6] Here product formation as well as formic acid disproportionation is also taking place in the dark, but it might be that the excited state of the hydride reacts faster than the ground state, so that the ketone reduction catalysed by **31** might be *photo-enhanced* rather than *photo-catalytic* as in the case of the water-gas shift reaction.

It was observed before that the disproportionation of the formic acid results in a rise of the solution's pH. The turnover frequency has been found to be highly dependent on the pH, as the reaction only occurs for a pH between 1 and 4 with pH=2 as optimal acidity. For a second set of reactions the reaction solution was therefore buffered by acidic phosphate buffer at pH=2 to avoid an effect of pH change on the kinetics.

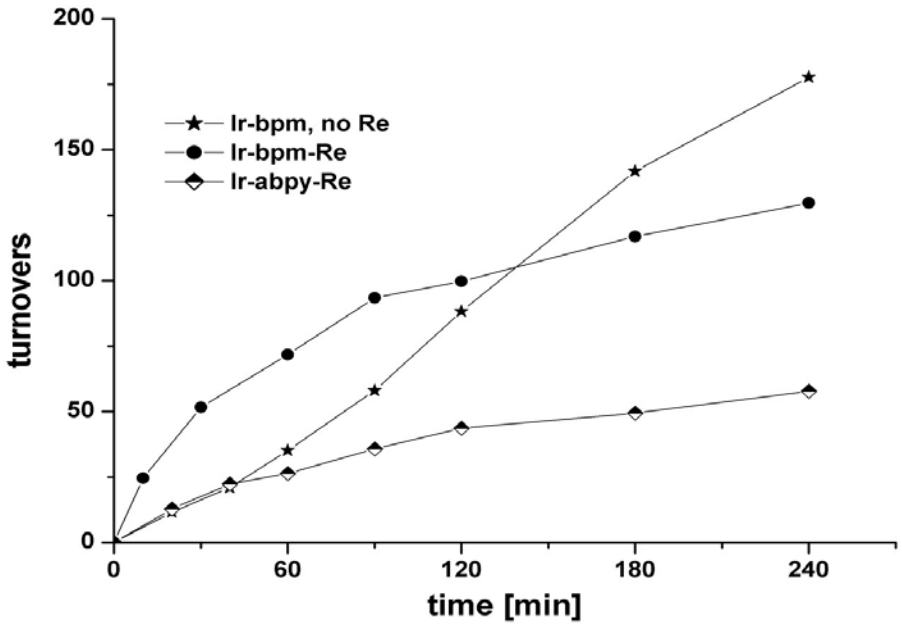

Figure 5.6 Catalytic reduction of cyclohexanone to cyclohexanol in solutions buffered at pH=2. Formation of the product cyclohexanol as a function of reaction time for $[IrCp^*(H_2O)bpm](OTf)_2$ (*Ir-bpm*), **31** (*Ir-bpm-Re*) or **32** (*Ir-abpy-Re*) as catalysts. Reaction conditions as shown in Scheme 5.9 , but in 0.5M H_3PO_4/ 0.5M NaH_2PO_4.

The results of these experiments are shown in Figure 5.6. The features observed for the product formation curves are similar to experiments in non-buffered solutions: a linear product formation is found for the mononuclear iridium catalyst with 45 turnovers h^{-1}, reaching nearly 90% substrate conversion after 4h. For **31**, product formation is initially faster, but again levels off after about two hours. Again, strong evolution of gas is observed from the reaction mixture, indicating fast consumption of the formic acid. Catalysis was also tested for **32**, which was found to be an active catalyst as well. Much slower product formation was detected, accompanied by strong gas evolution which indicates a fast disproportionation of the formic acid.

In conclusion, the synthesis of heterodinuclear complex containing rhenium tricarbonyl diimines proved to be unexpectedly difficult. Given the fact that numerous fragments were studied, it was only possible to isolate and characterise the small number of four examples of such compounds. The many synthetic trials to isolate an example of a tetranuclear "horseshoe"-shaped complex failed. For the four dinuclear examples that could be isolated, large changes of the electronic properties were observed. Coordination of the second metal fragment usually lowers the LUMO energy greatly, resulting in longer wavelength of the MLCT absorption and more facile electrochemical reduction. For complexes **31** and **32** containing the [IrCp*]- moiety, the ability to form the important iridium hydride intermediates could be confirmed for both dinuclear complexes, as the compounds showed activity in standard transfer hydrogenation catalysis reactions. Interesting effects on the reaction kinetics were observed for ketone reductions catalysed by these species, but have to remain unexplained in detail within the scope of this work.

References

[1] W. Matheis, W. Kaim, *Z. Anorg. Allg. Chem.* **1991**, *593*, 147.

[2] C. S. Araujo, M. G. B. Drew, V. Felix, L. Jack, J. Madureira, M. Newell, S. Roche, T. M. Santos, J. A. Thomas, L. Yellowlees, *Inorg. Chem.* **2002**, *41*, 2250.

[3] W. Kaim, R. Reinhardt, S. Greulich, M. Sieger, A. Klein, J. Fiedler, *Collect. Czech. Chem. Comm.* **2001**, *66*, 291.

[4] G. A. Fox, S. Bhattacharya, C. G. Pierpont, *Inorg. Chem.* **1991**, *30*, 2895.

[5] U. Koelle, M. Graetzel, *Angew. Chem.* **1987**, *99*, 572.

[6] R. Ziessel, *Angew. Chem.* **1991**, *103*, 863.

[7] T. Abura, S. Ogo, Y. Watanabe, S. Fukuzumi, *J. Am. Chem. Soc.* **2003**, *125*, 4149.

[8] H. C. Lo, C. Leiva, O. Buriez, J. B. Kerr, M. M. Olmstead, R. H. Fish, *Inorg. Chem.* **2001**, *40*, 6705.

[9] T. Scheiring, J. Fiedler, W. Kaim, *Organometallics* **2001**, *20*, 1437.

[10] L. Dadci, H. Elias, U. Frey, A. Hoernig, U. Koelle, A. E. Merbach, H. Paulus, J. S. Schneider, *Inorg. Chem.* **1995**, *34*, 306.

6. PHOTOCHEMISTRY EXPERIMENTS

After the synthesis and characterisation of the complexes described in Chapters 3 to 5, the photoreactivity of the [$Re(CO)_3$(diimine)] compounds was studied in various experimental set-ups.

It is obvious from the data presented so far that many of the synthesised modifications of the original Strasbourg catalyst cause large differences in spectroscopic, electrochemical and structural properties. The wavelengths of absorbed light causing the MLCT photoexcitation vary between 350 and 550nm, corresponding to largely differing energy gaps of 3.55 or 2.25 eV, respectively. The potentials necessary for electrochemical reduction are also very different: the complex [$ReBr(CO)_3$(abpy)] can be reduced already at +50mV, while a very low potential of –1250mV is needed for the reduction of [$ReBr(CO)_3$(Hdcbipy)]$^-$. Another striking difference is the ability of some complexes to fluoresce in solution at room temperature, while others do not show an emissive excited state. Additionally, there are largely varying sizes of the complexes when very compact complexes like [$ReBr(CO)_3$(bipy)] are compared to bulky dinuclear compounds like the cyano- dimer [$(Re(bipy)(CO)_3)_2(\mu\text{-}CN)]^+$ or the diimine- bridged [$(CO)_3BrRe(\mu\text{-}phd)Pt(PPh_3)_2$]. The complex [$TcCl(CO)_3$(bipy)] even contains a different transition metal centre.

All these differences will most likely affect the photochemical and photocatalytical behaviour of the species. But it was not really possible to make any prediction on the effects, as many factors seem important and, concerning the Strasbourg system photocatalysis, no published data existed for any other catalyst but [$Re(Cl,Br)(CO)_3$(bipy)]. Therefore, even though the experiments carried out to investigate the complexes' photochemistry started from the well- studied [$ReBr(CO)_3$(bipy)], they were really a journey into the unknown.

6.1 Reactions of photo-excited complexes with electron donors

For the original [Re(Cl,Br)$(CO)_3$(bipy)] catalysts it had been established that the primary events of the photocatalytic carbon dioxide reduction reaction are the photoexitation of the complex followed by the reaction of the thexi- state with the electron donor. These events result in the formation of the singly reduced complex in its ground state as the first key intermediate of the catalytic process.[1]

In a first set of experiments it was therefore studied in which way the synthetic modifications of the Strasbourg catalyst influenced the ability of the complexes to react with the standard electron donor TEOA. A second step consisted in finding alternatives to tertiary amines as electron sources.

As already discussed in part 1.5, fluorescence quenching is a good way to probe the reactivity of the excited state of [Re$(CO)_3$(diimine)] compounds towards electron donors. Unfortunately, only a fraction of the compounds synthesised could be tested in this way as all complexes containing bridging diimines do not show fluorescence in solution at room temperature and can therefore not be studied.

Thus, fluorescence quenching experiments could only be carried out for the complexes of the "extended bipy"- series and bipy- complexes containing different sixth ligands. In the experiments, the fluorescence intensity is measured for different concentrations of electron donors present in solution and then analysed assuming STERN- VOLMER kinetics as discussed in part 1.5, using the equation:

$$\mathbf{I_0/I = 1 + k_q \tau\,[Q] = 1 + K_{SV}\,[Q]}$$

STERN- VOLMER constants K_{SV} can be determined from plots of (I_0/I)-1 versus the quencher concentration, in this case TEOA.[2] Figure 6.1 shows the STERN-VOLMER plots for different complexes undergoing reductive quenching by TEOA in DMF solutions. The conditions were chosen to mimic the original CO_2 reduction experiments.

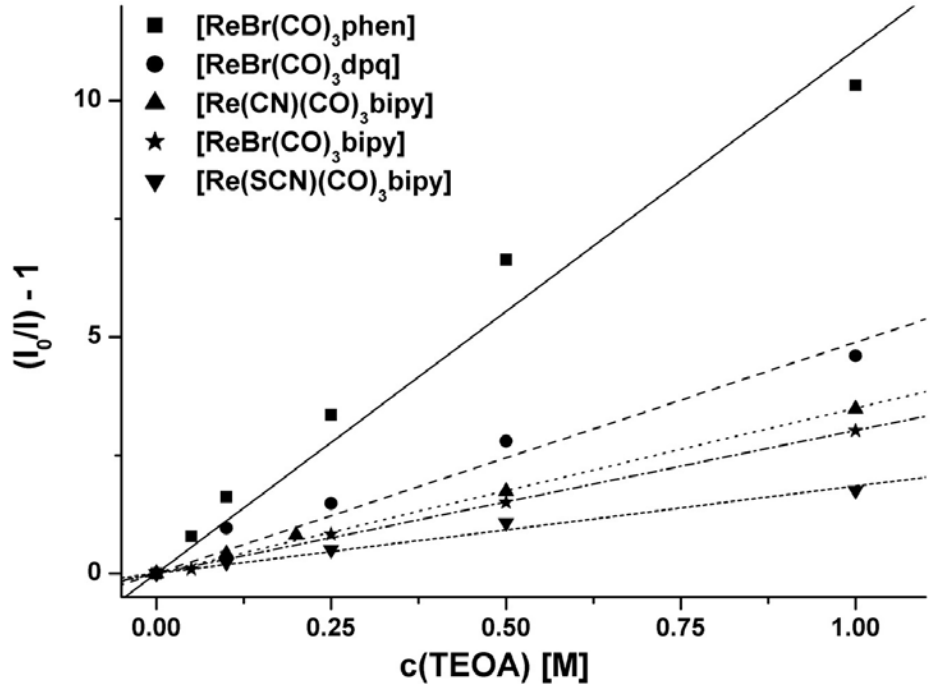

Figure 6.1 STERN- VOLMER plots for the fluorescence quenching of the excited states of different $[Re(CO)_3(diimine)]$ (c=1mM) complexes by TEOA in DMF.

complex	K_{SV}	$E_{1/2,\ red}$ [mV]	λ_{em} [nm]	τ [ns][a]
$[ReBr(CO)_3(phen)]$ **18**	**11.08** ± 0.60	-1090	570	288
$[ReBr(CO)_3(dpq)]$ **19**	**4.89** ± 0.31	-975	585	
$[Re(CN)(CO)_3(bipy)]$ **15**	**3.50** ± 0.06	-1125	540	
$[ReBr(CO)_3(bipy)]$ **12**	**3.02** ± 0.04	-1190	575	50
$[Re(SCN)(CO)_3(bipy)]$ **17**	**1.85** ± 0.08	-1015	580	

Table 6.1 STERN- VOLMER constants determined from the plots of Fig. 6.1 by linear fits of the data forced through zero related to the corresponding values of $E_{1/2,\ red}$ and λ_{em}. [a] in CH_2Cl_2, from Ref. [3]

Table 6.1 summarises the values determined for K_{SV}. The wavelengths of emission and the reduction potentials are also given for comparisons. It is obvious that there is no correlation between either of these two parameters and the trends in values for K_{SV}. A way to explain this result is to assume similar values of k_q (the rate constant for the bimolecular reduction reaction) for all complexes, independent of the complexes' redox potentials and emission/ absorption wavelengths. The differences in K_{SV} would consequently originate mainly from differences in the second component influencing K_{SV}, the excited state lifetime τ. Unfortunately, no apparatus for

time-resolved spectroscopy was at hand to determine τ for the complexes. Only for two complexes values for τ have been reported[3] (Table 6.1) and these values match reasonably well to explain the differences in the corresponding K_{SV}. Assuming similar values for τ in DMF, k_q is expected to be in the range of $5 \cdot 10^7 s^{-1}$ in both cases, thus approaching diffusion control.

These results indicate two properties of the system. Variation of the diimine or the sixth ligands causes K_{SV} to vary by a factor of up to five. K_{SV} is an indicator for the "success rate" of forming the reduced complex after photoexcitation in the presence of quencher. If the photoreduction step was rate-determining for the overall photocatalysis, one would expect [$ReBr(CO)_3(phen)$] **18** to be the five times faster catalyst when compared to [$Re(SCN)(CO)_3(bipy)$] **17**.

Secondly, it seems most likely that the electron transfer taking place is an outer-sphere reduction. The estimated values for k_q are well below the limit of diffusion control, so too small to indicate a coordination of the amine before reduction. Also, the most likely site for pre-coordination would be the sixth position. If coordination of the amine was important, one would expect great differences in K_{SV} between the complex [$ReBr(CO)_3(bipy)$] **12**, with a substitution labile sixth ligand, and the cases of the cyano and thiocyanato complexes **15** and **17**, where the sixth ligand is expected to be much more strongly bound.

All catalytic reactions reported in the literature have been carried out in DMF solutions containing the ternary amines TEOA or TEA as electron donors. A number of experiments was carried out to probe the possibility of finding a different solvent/ donor combination for which reductive fluorescence quenching is observed. Fluorescence quenching of **12** by these amines is also found to occur in acetonitrile or acetonitrile/water solutions, as can be seen in Figure 6.2, but the K_{SV} found in these systems are much smaller than in DMF (Table 6.2). This observation might again be explained by the influence of τ on K_{SV}, as it is reported that the excited state lifetime is only half as long in MeCN (25ns) when compared to CH_2Cl_2 solutions

(50ns).[3] The results presented in Table 6.2 also show that it is possible to replace the electron donor TEOA by TEA.

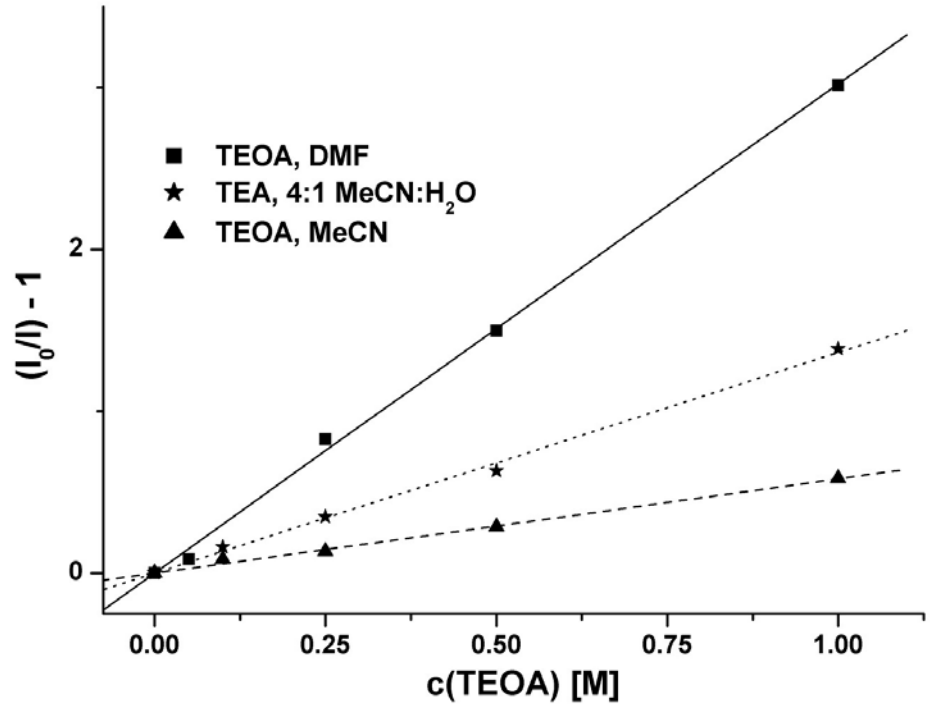

Figure 6.2 STERN- VOLMER plots for the fluorescence quenching of the excited states of **12** (c=1mM) in three different solvent/electron donor systems.

solvent	electron donor	K_{SV}
DMF	TEOA	**3.02** ± 0.04
MECN/H_2O (4:1)	TEA	**1.36** ± 0.03
MeCN	TEOA	**0.58** ± 0.01

Table 6.2 STERN- VOLMER constants determined from the plots of Fig. 6.2 by linear fits of the data.

In general, the use of ternary amines as electron donors restricts the reactions to be studied to alkaline conditions. This is especially disadvantageous for the goal of shifting the reactivity of the system from CO_2 to H_2O reduction, as it is thermodynamically much more difficult to achieve water reduction in basic than neutral or acidic solutions.

Therefore other, non-basic electron donors were looked for, which should show irreversible oxidation within a range of about +0.5 to +1V and solubility in DMF, MeCN or H_2O. Candidates found in the literature were oxalic acid, vitamin C, cystamine or EDTA. None of these donors was found to cause any quenching of the [$Re(CO)_3$(diimine)] fluorescence in solution,

even though all meet the requirements of a thermodynamically accessible, irreversible oxidation.

Even though not mechanistically understood, this result is in agreement with the literature: a thorough screening of possible reductive quenchers revealed in one study that only 25 out of 80 possible donors were able to reduce the photoexcited organic dye proflavin.[4] All active donors were either amines or thiols. It seems that only the amine and thiol radical cations formed after oxidation decompose fast enough to make a recombination with the reduced complex, a radical anion, impossible. It is therefore not surprising that an alternative to the ternary amines was not found in the small screening done here. The resulting restriction to work in alkaline solution is nevertheless a severe limitation of the presented photochemical system.

6.2 Activity of the complexes as photocatalysts for the reduction of CO_2 to CO

The preliminary experiments on the photochemical behaviour of the [$Re(CO)_3$(diimine)] complexes presented so far indicated that the various complexes show properties differing from the original [$ReBr(CO)_3$(bipy)] catalyst, but fundamental features such as reductive quenching, fluorescence or reversible electrochemical reduction were found to be common to a number of the complexes at different solution conditions.

So the stage was set for the "real" tests: experiments to study the ability of the complexes to act as photocatalysts in the Strasbourg reaction. In order to allow a comparison of the results with the original catalysis experiments performed by the Strasbourg group, the conditions for the initial experiments were chosen similar to the reported set-up (Scheme 6.1).

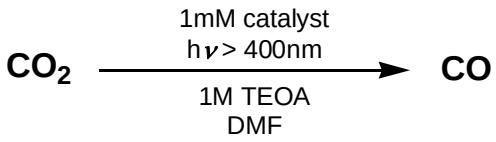

Scheme 6.1 Reaction conditions for photocatalytic carbon dioxide reduction, similar to the original Strasbourg system.[5]

For the experiments, catalyst and TEOA were mixed in DMF in a Schlenk tube in the dark and the solution was degassed under CO_2. The vigorously stirred mixtures were equilibrated under a pressure of 1.5bar of CO_2 for 15min, as it was found that the CO_2 dissolves in DMF rather slowly. Now the samples were transferred to a dark room and irradiated by a commercial 250W slide projector through a 400nm cut-off filter as a simple way to simulate solar irradiation. The gas above the solution was sampled every 15 to 30 min and analysed by GC-TCD able to detect carbon monoxide, nitrogen, oxygen and hydrogen. The amount of residual air left in the headspace was less than 1% according to GC analysis.

The only detected product in the gas phase for all reactions carried out according to Scheme 6.1 was carbon monoxide. In no cases any measurable quantities of hydrogen were found. The amount of nitrogen in the gas phase is constant, indicating that the apparatus is sufficiently gas tight for the duration of the measurements (2 hours). In some cases a slight decrease of the oxygen concentration was observed, which will be discussed below.

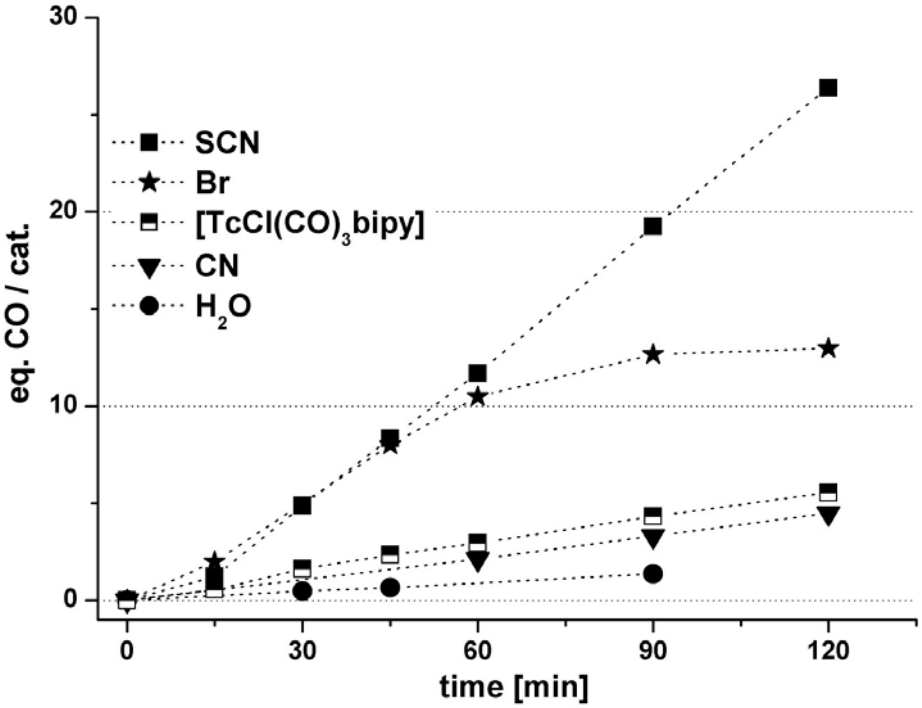

Figure 6.3 Formation of carbon monoxide over time. Reactions according to Scheme 6.1 with different catalysts $[ReX(CO)_3(bipy)]$ as well as $[TcCl(CO)_3(bipy]$.

Figure 6.3 shows the amount of carbon monoxide per mole of rhenium catalyst detected in the headspace above the catalyst solution over time.

Curves of CO production for complexes of the [ReX(CO)$_3$(bipy)] series containing different sixth ligands X are shown together with the technetium analogue [TcCl(CO)$_3$(bipy] **13**. All complexes of this series were found to be active catalysts, though at very different rates (Table 6.3).

catalyst	CO produced after 30min. [eq./cat.]	CO produced after 120min. [eq./cat.]
[Re(SCN)(CO)$_3$(bipy)] **17**	4.9	26.4
[ReBr(CO)$_3$(bipy)] **12**	4.0	13.0
[TcCl(CO)$_3$(bipy)] **13**	1.6	5.5
[Re(CN)(CO)$_3$(bipy)] **15**	1.1[a]	4.5
[(Re(CO)$_3$(bipy))(μ-CN)]$^+$ **16**	0.6[a]	2.6
[Re(OH$_2$)(CO)$_3$(bipy)]$^+$ **14**	0.5	1.8[a]

Table 6.3 Rates of CO formation for the graphs shown in Figure 6.3. [a] extrapolated values.

Similar observations about the reduction of CO_2 to CO could be made concerning the "extended bipy" series with catalysts of the type [ReBr(CO)$_3$(diimine)], shown in Table and Figure 6.4. The complexes of phen, Hdcbipy and dpq all show activity as photocatalysts, but all at smaller rates when compared to the original Strasbourg catalyst **12**.

catalyst	CO produced after 30min. [eq./cat.]	CO produced after 120min. [eq./cat.]
[ReBr(CO)$_3$(bipy)] **12**	4.0	13.0
[ReBr(CO)$_3$(phen)] **18**	4.8	11.5
[ReBr(CO)$_3$(Hdcbipy)]$^-$ **22**	2.2	7.7
[ReBr(CO)$_3$(dpq)] **19**	0.5	1.1

Table 6.4 Rates of CO formation for the graphs shown in Figure 6.4.

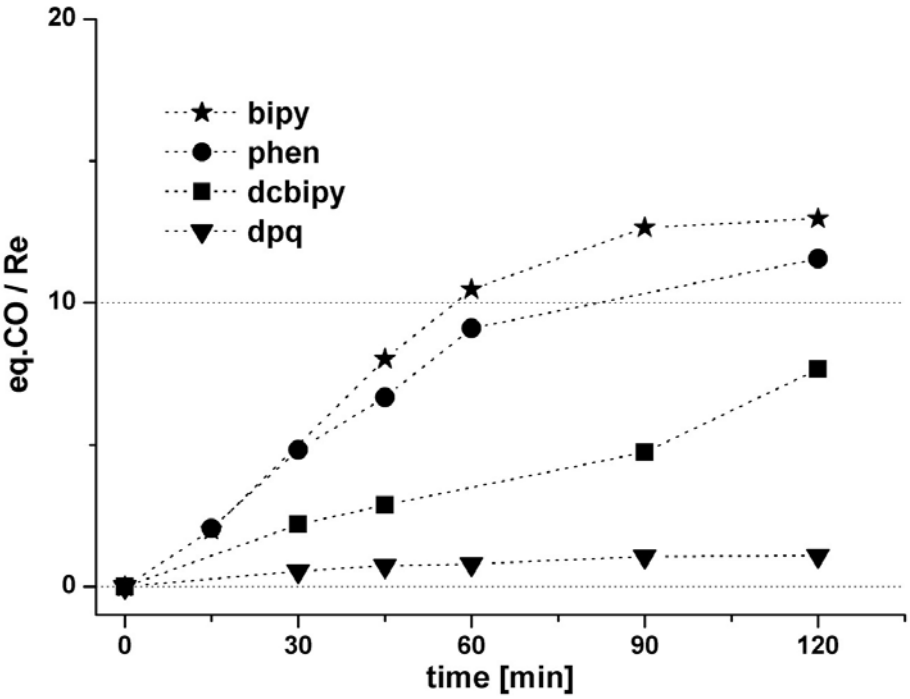

Figure 6.4 Formation of carbon monoxide over time for reactions with different catalysts from the "extended bipy" series, $[ReBr(CO)_3(diimine)]$.

An interesting observation is made for the case of complex **18** acting as catalyst, as the solution turns deep blue after a few minutes of reaction time, while reaction mixtures of all other catalysts keep their yellow to orange colour during catalysis. This was studied in more detail: a solution containing **18** and TEOA was illuminated with the same light source as used in the photocatalysis experiments. Within minutes the formation of a new absorption band with a maximum at 570nm was observed (Fig. 6.5). The amount of this new species present in solution levels off after about 30 min of irradiation (Fig. 6.6). If air is excluded, the solution keeps its colour for at least a day at room temperature in the dark. On the other side, immediate decolourisation to the original yellow colour is observed if air is bubbled through the solution for only one minute. This could also explain the slight drop in oxygen concentration observed for the headspace for these reactions. As $[ReBr(CO)_3(phen^{\bullet-})]$ $\mathbf{18^{\bullet-}}$ is a strong reducing agent ($E_{1/2}$= -1090mV) it is able to reduce O_2 to superoxide $O_2^{\bullet-}$ ($E_{1/2}$= -750mV in DMF), which will react further rapidly, thus decreasing O_2 concentrations in the headspace. All these results make it very likely that the blue species observed is the reduced complex in its radical anion form $\mathbf{18^{\bullet-}}$. Additionally,

a similar absorption maximum of 560nm has been found for the analogous reduced form of the bipy complex, [ReBr(CO)$_3$(bipy$^{\bullet-}$)], in THF solution.[6]

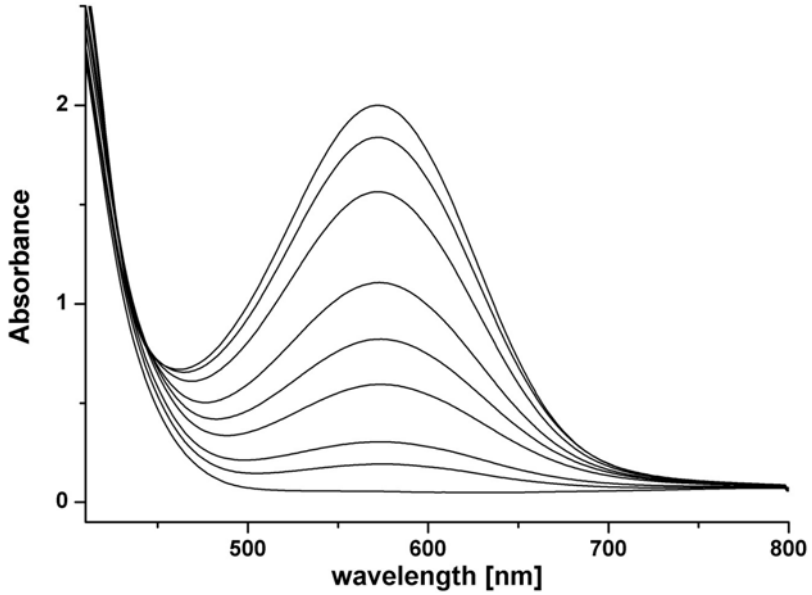

Figure 6.5 Spectral changes observed for a CO_2- saturated solution of **18** (0.2mM) and TEOA (1M) in DMF upon irradiation (hν>400nm).

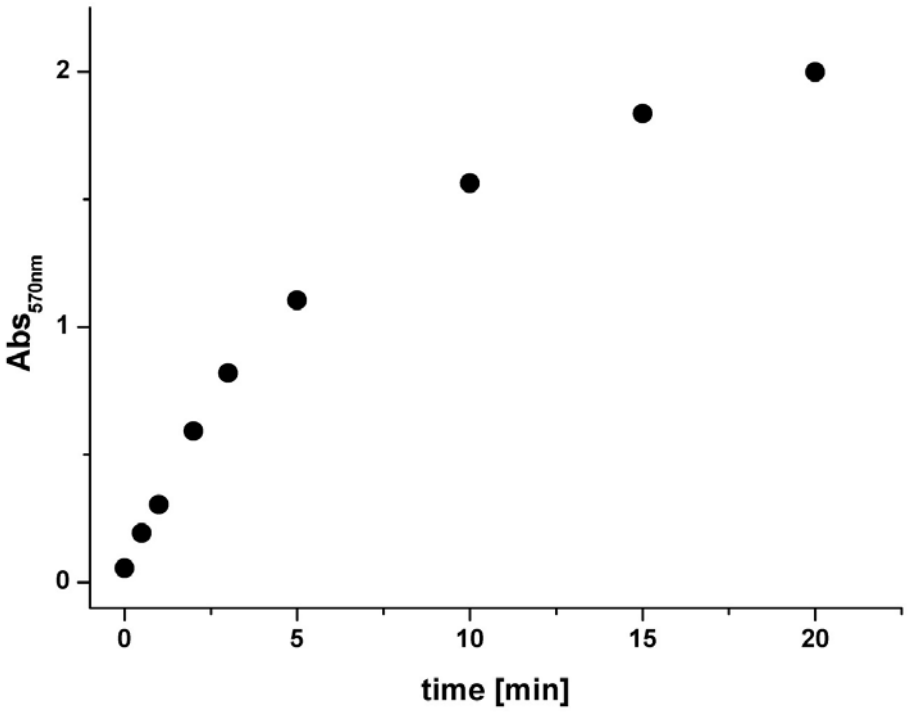

Figure 6.6 Plot of the absorbance measured for the new absorption maximum at 570nm vs. time for the spectral changes shown in Figure 6.5.

Experiments probing the photochemical reduction of CO_2 according to Scheme 6.1 were carried out for all [Re(CO)$_3$(diimine)] complexes described in chapters 3 to 5. Only the seven rhenium complexes listed in Tables 6.3

and 6.4 and the technetium analogue **13** were found to show catalytic activity for this reaction. In particular, no CO or any other gaseous products were detected for all mono- and dinuclear complexes containing bridging diimines (bpm, abpy or phd). The same is true for the "extended bipy" complex [ReBr(CO)$_3$(biq)] **21**. There seems to be a strict correlation between room temperature fluorescence and catalytic activity: all fluorescing complexes are active catalysts for the photocatalytic CO_2 reduction, while all others are not.

As mentioned before, one group had claimed that the system would switch from CO_2 to H_2O reduction if the reaction according to Scheme 6.1 was carried out in a THF/water mixture instead of DMF as solvent.[7] This reaction was carried out multiple times, using both **12** and **18** as catalysts, but the reported formation of H_2 could not be reproduced. No products at all, neither H_2 nor CO, were detected for reactions carried out in THF/water (4:1).

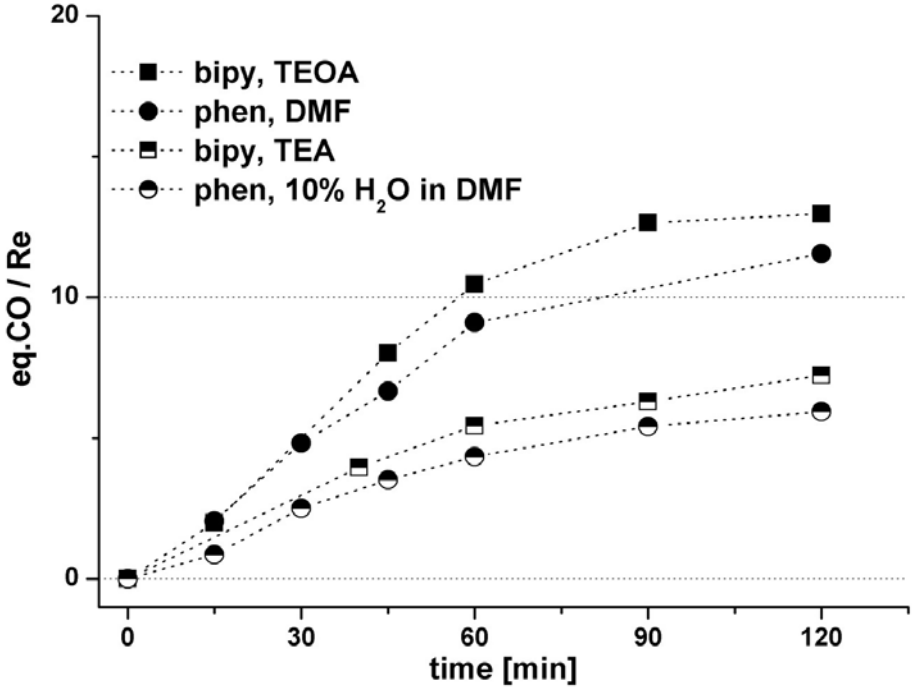

Figure 6.7 Formation of carbon monoxide over time for reactions of **12** and **18** in the different solvent/electron donor systems listed in Table 6.5.

As an aim of the work was to change both electron donors and substrates of the Strasbourg system, other combinations of solvents and donors were tested as well. In DMF, only the triamine donor molecule TEA was found to

be an alternative to TEOA, with the catalytic system still active, even though only at about half the catalytic rate (Figure 6.7, Table 6.5). For experiments using the possible donor molecules cystamine and vitamin C in DMF no products were observed. This is in agreement with the fluorescence quenching experiments described in part 6.1, where these molecules were found to be inactive as quenchers as well. It can be seen in Figure 6.7 that the addition of water to the system slows down catalysis, but does not inhibit the reaction completely. For reactions using **18** as catalyst, the colour change to blue, taken as an indication of the formation of the radical **18$^{\bullet-}$**, is still observed. This also suggests that the reduced species **18$^{\bullet-}$** is stable in the presence of water and does not react with water directly.

catalyst	electron donor	solvent	CO produced after 120min. [eq./cat.]
[ReBr(CO)$_3$(bipy)] **12**	TEOA	DMF	13.0
[ReBr(CO)$_3$(phen)] **18**	TEOA	DMF	11.5
[ReBr(CO)$_3$(bipy)] **12**	TEA	DMF	7.2
[ReBr(CO)$_3$(dpq)] **19**	TEOA	DMF/10% H_2O	5.9

Table 6.4 Rates of CO formation and solvent / electron donor combinations for the experiments of Figure 6.7.

Taking these new results into account together with the work presented in the literature (see esp. part 1.5), a catalytic mechanism slightly different than the originally presented one[5] is suggested (Scheme 6.2).

The well- established initial step ① is the absorption of a visible-light photon by the catalyst [Re^{I}(CO)$_3$(diimine)X] and the resulting MLCT to form the charge-transfer excited state [Re^{II}(CO)$_3$(diimine$^{\bullet-}$)X].

Step ② following this reaction is already not really accessible to analytical measurements and therefore less easily identified. It can be deduced from the fluorescence quenching experiments that the reaction of the MLCT thexi-state with the amine electron donors is rapid while no reaction of the excited state with the CO_2 substrate seems to occur. Additionally, it can be concluded from the experiments with $^{13}CO_2$ as substrate that the substrate CO_2 is reduced to CO while coordinated to the

metal: ^{13}CO rhenium complexes are formed during the catalysis and exchange of coordinated CO for ^{13}CO from the solution is known to be very slow.[5] The results of the catalysis experiments for the $[Re(CO)_3(bipy)X]$ series (Fig. 6.3) indicate that the sixth ligand stays coordinated to the rhenium throughout the entire catalysis cycle, as otherwise the strong effects on the catalytic rate caused by the different X can not be explained.

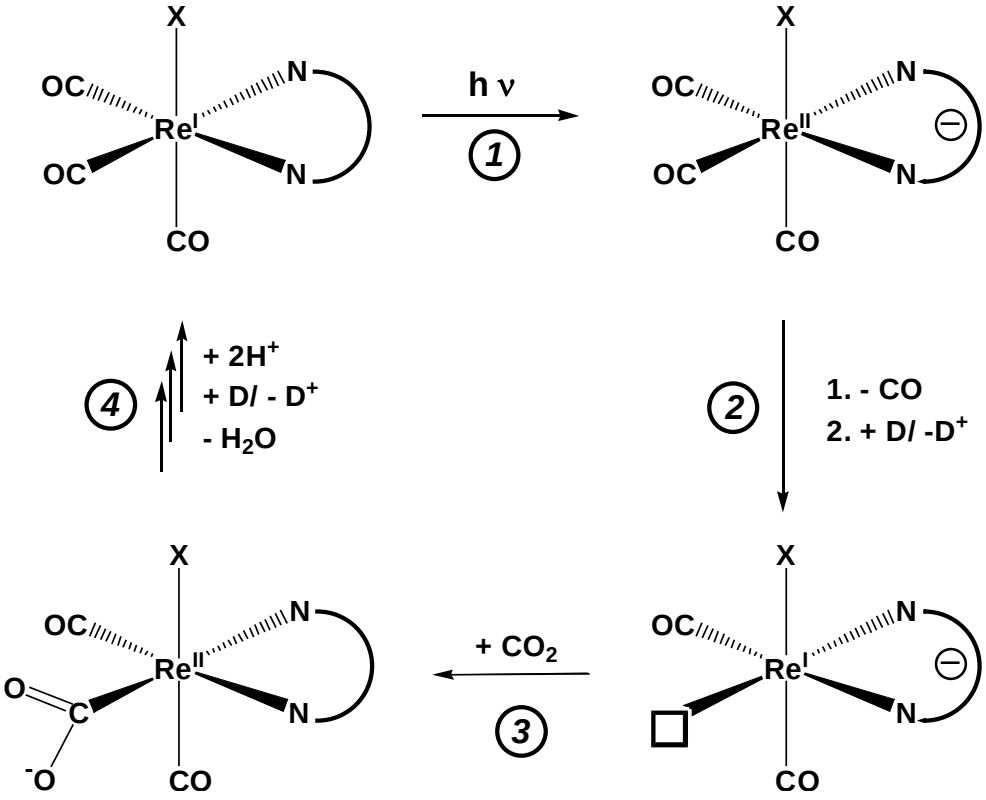

Scheme 6.2 Suggested mechanism for the Strasbourg system for the photocatalytic carbon dioxide reduction.

Given the fact that a coordinated CO has to leave the complex at one step of the cycle, the rhenium(II) species is the most likely candidate, as the carbonyl ligands will be less tightly bound to the oxidised rhenium centre. It seems unlikely that the loss of CO occurs after reduction by the donor, as the $[Re(CO)_3(diimine^{\bullet -})X]$ radicals formed are stable in solution for extended periods of time. Additionally, it is known that $[ReBr_3(CO)_3]^{2-}$ looses one CO ligand upon oxidation to rhenium(III) forming rhenium biscarbonyl species.[8] It has also been found that rhenium(I) biscarbonyl species are formed by photoreactions of $[Re(CO)_3(diimine)X]$ complexes in the presence of different excess phosphines P[9], where the complexes of the type

$[Re(CO)_2(diimine)P_2]$ isolated from such reactions might be seen as trapped forms of the intermediate $[Re(CO)_2(diimine)X]$ postulated here. Therefore it seems justified to assume that step ② corresponds to the loss of a carbonyl ligand, followed by the outer sphere reduction of the catalyst by the electron donor D to produce a reduced intermediate complex with a vacant coordination site. But of course it can not be entirely ruled out that step ② occurs in the opposite sequence: reduction by D first, followed by CO loss of the reduced species later.

Compared to the other steps involved, the loss of a carbonyl ligand is most likely the energetically most demanding event of the catalytic cycle. This might cause ② to be the rate determining step of the overall reaction. If this is the case, the different rates found for the $[Re(CO)_3(bipy)X]$ series (Fig. 6.3) might be explained by the *cis*-labilising influence of the different sixth ligands X, as thiocyanate and halides, for which the fastest rates were observed, are also known to be the most *cis*-labilising ligands of the series.[10, 11] Therefore, the CO ligand leaving the complex in step ② has been tentatively assumed to be an equatorial CO *cis* to the sixth ligand X.

The substrate CO_2 can now coordinate to this vacant coordination site in the following step ③. A rhenacarboxylate is formed after one-electron reduction of CO_2 by the unpaired electron residing on the diimine ligand before. Under the very alkaline conditions of the catalytic reaction, this species will most probably be present in its deprotonated form.

Up to step ③ the proposed mechanism follows established chemistry and experimental data is available to support the argumentation for each step involved. But details about the last step ④ remain elusive. A second electron has to be transferred from another donor molecule to achieve the two-electron reduction of CO_2. Additionally, a double protonation of the carboxylic acid group is necessary to release the second reaction product H_2O. How and in which order these steps might occur remains unclear.

For steps ① and ③ the mechanism is in agreement with the one originally proposed by the Strasbourg group.[5] For step ②, the additional

information gained by the study of the [$Re(CO)_3$(bipy)X] series, allows to present more details. On the other hand, there is no evidence to support a carboxylate-bridged rhenium dimer as key intermediate, as proposed in a recent study. Also, the rhenium compounds act both as photoactive and catalytic centres for the reduction of CO_2, but show no reactivity to reduce water, as was claimed before.

If one accepts the proposed mechanism and assumes step ② to be rate determining, some other results can also be explained: as the reaction of the excited state with the electron donor is not the rate-limiting step, there is, as observed, no correlation between the STERN-VOLMER constants and the catalytic rates. The same is true for a possible effect of the redox potential necessary for the reduction of the complexes. If the reaction of the reduced complex with CO_2 was rate determining, the most strongly reducing complex, **22**, should show the fastest catalytic rate, which it does not. Also the step of light absorption seems to be of no significant influence: complex **19** with a larger absorption in the region of interest (λ>400nm) shows a small catalytic rate. Furthermore, there is no obvious reason for this catalytic cycle to be limited to rhenium - and indeed, the analogous technetium complex was found to be an active catalyst as well.

Nevertheless, with a catalytic cycle consisting of many steps and many potentially important influences to be considered, some puzzling questions remain:

- Why are the complexes containing the ligands abpy, bpm, biq and phd inactive for the catalysis despite their good light absorption? Does the lack of fluorescence for these complexes indicate that the back- reaction of ① (the MLCT step) is so fast that the important step ② does not occur?
- Is the reason for the different rates found for the [$Re(CO)_3$(bipy)X] series only their difference in *cis*-labilisation mentioned above?

- Which effect causes the accumulation of the blue phen complex **18**$^{\bullet-}$, while something similar does not occur for the other diimine complexes?
- A significant amount of catalyst will be reduced after excitation to form [Re(CO)$_3$(diimine$^{\bullet-}$)X] species as the quenching constants k_q are large. What is the fate of these reduced forms as they seem to accumulate only in the case of **18**$^{\bullet-}$?
- Why does catalysis stop when the reaction is carried out in THF/water?
- What is the reason for the much slower catalysis observed for **19**? Does the fact that the substance is a much weaker reducing agent have an effect after all?
- And, most unclear: in which sequence might the reaction steps of ④ work?

Even as all these questions remain unanswered, it could be shown by the experiments in this part that it is possible to modify the Strasbourg system to some extend and conserve catalytic activity. One of the new compounds, complex **17**, was found to be a better catalyst than the original **12** as it combines a rate as fast as the original catalyst with improved long term stability. While the rate of conversion decreases for **12** after about one hour, for **17** the turnover rate does not change over the first two hours. The reason might be that the catalytically inefficient formato complex [Re(HCOO)(CO)$_3$(bipy)][5], formed as undesired side product in reactions catalysed by **12**, cannot form here.

On the other hand, most complexes show significantly worse catalytic performance when compared to the Strasbourg catalyst and many do not work at all. Especially the fact that all dinuclear compounds showed no reactivity towards CO_2 at all is quite disappointing.

6.3 Photogeneration of H_2 in the presence of co-catalysts

Hydrogen formation was not observed for any of the systems discussed in part 6.2. As it was a key motivation of this work to find a rhenium based photoreaction resulting in the reduction of water to hydrogen, some additional experiments were carried out to approach this goal.

It was found that the reduced rhenium species $[Re(CO)_3(diimine^{\bullet-})X]$ form photochemically in the presence of an electron donor. These radicals do not react directly with water, despite their strongly reducing potentials in the range of $-1250mV \leq E_{1/2} \leq -700mV$. The reason for this is might be that only one electron is available from each reduced rhenium species, while two electrons are necessary for the reduction of two H^+ to H_2, for which the redox potential in alkaline solution is accessible at $E_{1/2} \approx -800mV$. In comparison, the reduction of a single proton to $H^{\bullet}$, atomic hydrogen, is thermodynamically not feasible, as the redox potential for this process is $E_{1/2} \approx -2900mV$.[12]

For the case of the two-electron reduction of CO_2, this problem seems to be solved by the formation of the mono-reduced rhenacarboxylate intermediate (Scheme 6.2). For the substrate water a similar pathway does not exist. As a result the $[Re(CO)_3(diimine)X]$ complexes might be used as photosensitisers for water reduction, but can not act as water reduction catalysts as well. Therefore, if water reduction is to be achieved, co-catalysts are needed, which accumulate electrons from the reduced $[Re(CO)_3(diimine^{\bullet-})X]$ and transfer them to water in a two-electron reduction step.

A commonly used compound to act both as electron acceptor and as water reduction catalyst is Adams' catalyst (PtO_2), which has already been used for water reduction in different photochemical systems.[13, 14] If PtO_2 is added to the standard photochemical set-up (Scheme 6.1) in a DMF/H_2O (4:1) mixture under nitrogen, no formation of hydrogen was observed. With **18** used as catalyst under a CO_2 atmosphere and PtO_2 added, the formation

of CO at the same rate as found before (Table 6.4) was detected. The dark blue colour indicative of the formation of **18**$^{\bullet-}$ is also observed. From this it can be concluded that a direct electron transfer from [Re(CO)$_3$(diimine$^{\bullet-}$)X] to PtO_2 does not occur and that another electron relay is needed.

Such a relay has been reported in the literature in the form of bipy complexes of cobalt(II).[15, 16] The complete electron transfer chain, shown in Scheme 6.3, was already successfully used for water reduction using $[Ru(bipy)_3]^{2+}$ as photosensitiser. Cobalt(II) is known to form different complexes in equilibrium with each other in the presence of bipy, so the solution of Co^{2+} and two equivalents of bipy used for the reactions here is known to contain a mixture of different species $[Co^{II}(bipy)_n]^{2+}$, with n = 1,2 or 3.[17]

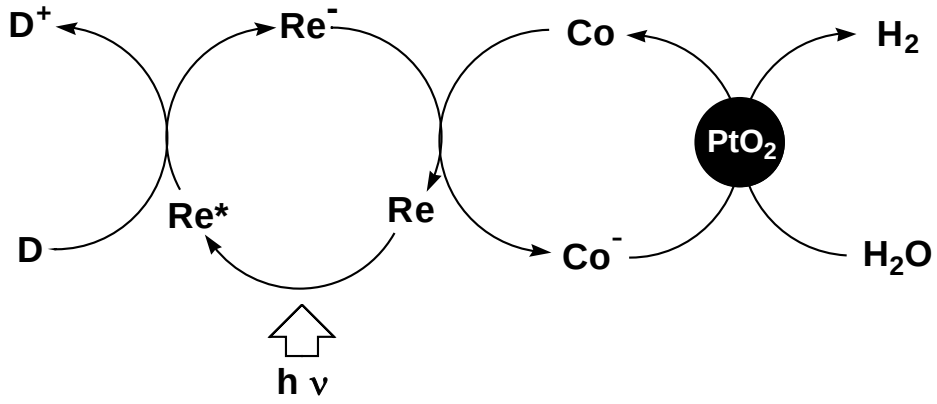

Scheme 6.3 Electron transfer system for water reduction using [Re(CO)$_3$(diimine)X] as photosensitiser. **D**: electron donor, **Re**: **12**, **Co**: $[Co^{II}(bipy)_n]^{2+}$

The reaction according to Scheme 6.3 does occur using the rhenium catalyst, but at a very slow catalytic rate: about two equivalents of H_2 are formed per rhenium catalyst (only **12** was used as sensitiser) over a reaction time of 20h(!). This rate is similar to the one reported before for the system using $[Ru(bipy)_3]^{2+}$ as light absorbing dye.[16] All three components, [Re(CO)$_3$(diimine)X], $[Co^{II}(bipy)_n]^{2+}$ and PtO_2 are necessary to achieve water reduction. No hydrogen formation is detected if any of the three substances is lacking.

It could be demonstrated in two ways that a rhenium- mediated electron transfer from the TEOA donor to $[Co^{II}(bipy)_n]^{2+}$ does indeed occur: if a solution containing **12**, $[Co^{II}(bipy)_n]^{2+}$ and TEOA under nitrogen is exposed to visible light, the solution turns blue with a new absorption maximum emerging at 610nm after about 20min. of irradiation (Figure 6.8). This is the region of absorption reported for electrochemically reduced species $[Co(bipy)_n]^{+}$, which are strong reducing agents with an $E_{1/2}$ measured to be around –1000mV.[17] The blue solution is very air sensitive and looses its colour when exposed to air for some seconds only. The lag phase of about 20min. might therefore correspond to the time needed to consume all dissolved residual oxygen in solution.

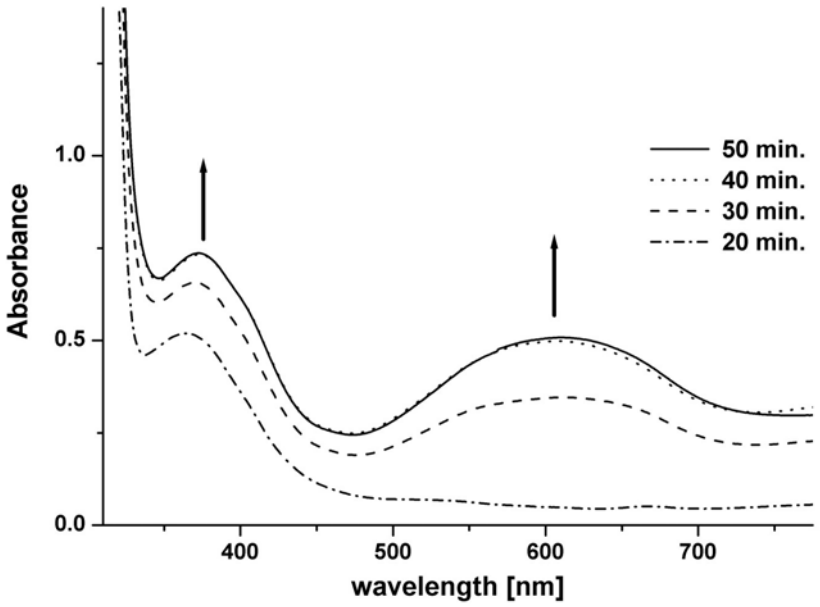

Figure 6.8 Spectral changes observed for a solution of **12** (0.1mM), $[Co^{II}(bipy)_n]^{2+}$ (0.5mM $Co(ac)_2$, 0.1mM bipy) and TEOA (0.1M) in DMF exposed to visible light (λ>400nm).

Secondly, a photocatalytic CO_2 reduction experiment was carried according to Scheme 6.1 in a mixture of DMF and water (4:1). As found before (Fig. 6.7), CO_2 reduction does occur when water is present in the system, but at a reduced rate. About 3 equivalents of CO per rhenium did form after 30min. Now a small volume of a DMF solution containing $[Co^{II}(bipy)_n]^{2+}$ was added to the reaction mixture. The formation of CO stopped immediately (Fig. 6.9) and after about 30min. the solution turned

blue. This result indicates that the $[Co^{II}(bipy)_n]^{2+}$ added competes successfully with the substrate CO_2 for the available reduction equivalents. As a result the CO_2 reduction stops and the blue $[Co(bipy)_n]^{+}$ is formed.

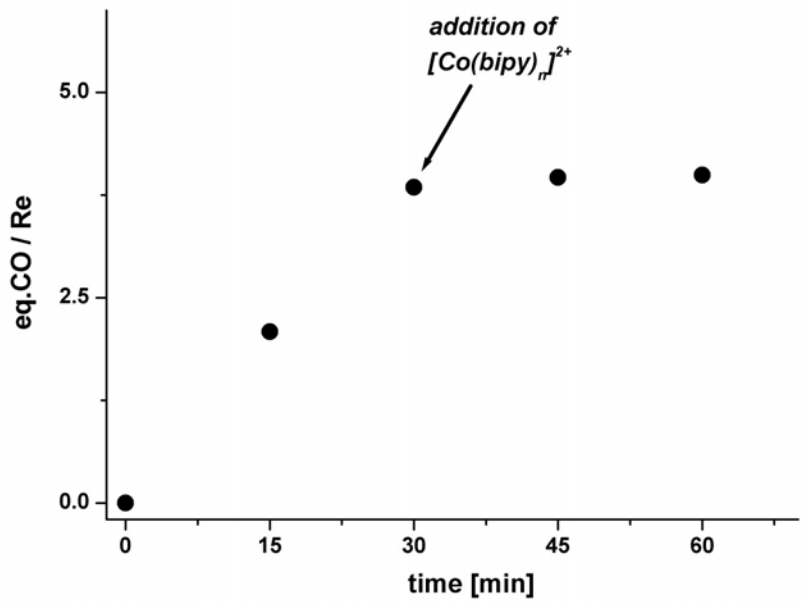

Figure 6.9 Formation of CO observed for a solution of **12** (1mM) and TEOA (1M) in DMF/H_2O (4:1) under a CO_2 atmosphere exposed to visible light (λ>400nm). After 30min., $[Co^{II}(bipy)_n]^{2+}$ is added to the system (final concentrations: 3mM $Co(ac)_2$ and 9mM bipy).

Despite the fact that the experiments described in this part were just few preliminary trials, they prove nevertheless that the electron transfer concept of Scheme 6.3 can be realised and used to reduce water to H_2. Unfortunately, the rates of water reduction achieved by the system are very small and the only usable electron source for the reduction found until now are ternary amines like TEOA. So it is still a very long way to go with many problems to be solved until a rhenium based photosensitiser might be useful in a photocatalytic water splitting system according to Scheme 1.8.

References

[1] J. C. Luong, L. Nadjo, M. S. Wrighton, *J. Am. Chem. Soc.* **1978**, *100*, 5790.

[2] H. Henning, D. Rehorek, *Photochemische und photokatalytische Reaktionen von Koordinationsverbindungen*, **1988**.

[3] K. Kalyanasundaram, *J. Chem. Soc., Faraday Trans. 2* **1986**, *82*, 2401.

[4] A. I. Krasna, *Photochem. Photobiol.* **1979**, *29*, 267.

[5] J. Hawecker, J. M. Lehn, R. Ziessel, *J. Chem. Soc., Chem. Comm.* **1983**, 536.

[6] G. J. Stor, F. Hartl, J. W. M. van Outersterp, D. J. Stufkens, *Organometallics* **1995**, *14*, 1115.

[7] C. Pac, K. Ishii, S. Yanagida, *Chem. Lett.* **1989**, 765.

[8] U. Abram, R. Huebener, R. Alberto, R. Schibli, *Z. Anorg. Allg. Chem.* **1996**, *622*, 813.

[9] K. Koike, J. Tanabe, S. Toyama, H. Tsubaki, K. Sakamoto, J. R. Westwell, F. P. A. Johnson, H. Hori, H. Saitoh, O. Ishitani, *Inorg. Chem.* **2000**, *39*, 2777.

[10] J. D. Atwood, T. L. Brown, *J. Am. Chem. Soc.* **1976**, *98*, 3155.

[11] J. D. Atwood, T. L. Brown, *J. Am. Chem. Soc.* **1976**, *98*, 3160.

[12] A. F. Holleman, E. Wiberg, *Lehrbuch der Anorganischen Chemie*, 34th ed., **1995**.

[13] K. Kalyanasundaram, J. Kiwi, M. Graetzel, *Helv. Chim. Acta* **1978**, *61*, 2720.

[14] E. Amouyal, *Sol. Energy Mat. Sol. Cells* **1995**, *38*, 249.

[15] C. V. Krishnan, C. Creutz, D. Mahajan, H. A. Schwarz, N. Sutin, *Isr. J. Chem.* **1982**, *22*, 98.

[16] J. M. Lehn, R. Ziessel, *Proc. Natl. Acad. Sci. USA* **1982**, *79*, 701.

[17] H. A. Schwarz, C. Creutz, N. Sutin, *Inorg. Chem.* **1985**, *24*, 433.

7. FINAL REMARKS

7.1 Summary and conclusion

The original aim of this thesis was the development of a new cyano-complex of ^{99m}technetium(I) as γ-emitting unit for radiopharmaceutical applications. The synthesis of a small, stable Tc^{I} unit was pursued inspired by the versatile $[(Tc^{I},Re^{I})(CO)_3]^{+}$ fragment. This goal could not be achieved, as both promising precursor complexes studied, $[(Tc^{I},Re^{I})(CN)_6]^{5-}$ and $[(Tc^{I},Re^{I})(CN)_4(NO)]^{2-}$, do not possess advantageous properties for a use as radiopharmaceutical synthons. The pure cyano- complexes $[(Tc^{I},Re^{I})(CN)_6]^{5-}$ were found to be too air sensitive to be useful starting points. Additionally, substitution reactions of these compounds were ill defined, as cyanide coordination equilibria cause a mixture of cyano- species to be present in solution. The mixed complexes $[(Tc^{I},Re^{I})(CN)_4(NO)]^{2-}$ are air-stable, as they contain the strong π-accepting ligand NO^{+} together with CN^{-}, but this unit proved to be too inert to allow any substitution reactions by bidentate ligands, which are necessary for derivatisations.

As a consequence, the attention was shifted to the well-studied $[(Tc^{I},Re^{I})(CO)_3]^{+}$- moiety and its reaction with cyanide in order to obtain cyano- carbonyl complexes resulting from carbonyl substitution by cyanide. It was found that such substitutions do not occur. Instead, the *trans* arrangement of cyanide and carbonyl ligands on Tc^{I} or Re^{I} centres proved to be exceptionally stable. Therefore, the reaction of the $[(Tc^{I},Re^{I})(CO)_3]^{+}$-fragment with cyanide results in the formation of mixed cyano- carbonyl compounds but not in the substitution of carbonyl ligands. The complexes $[(Tc^{I},Re^{I})(CN)_3(CO)_3]^{2-}$ were prepared and allowed a detailed case study on structure and bonding in mixed cyano- carbonyl- complexes.[1] Based on this investigation a new [2+1] labelling method involving cyanide was developed for ^{99m}Tc, as $[^{99m}Tc(CN)(CO)_3L_2]$ complexes, containing the very stable *trans*-CO/CN unit, are readily accessible for different bidentate ligands L_2.[2]

From these results it can be concluded that small, water- and air-stable cyano- complexes of Tc^{I} and Re^{I} can be prepared if they contain one of the

two strong π-acceptor ligands NO^+ or CO in addition to CN- to stabilise the complex against oxidation. The fragments $[(Tc^I,Re^I)(CN)_4(NO)]^{2-}$ and $[(Tc^I,Re^I)(CN)(CO)_3]$ offer the possibility to coordinate one mono- or bidentate ligand, respectively, which is necessary if such fragments are to be used for the labelling of biomolecules.

Model compounds prepared for the development of the [2+1] labelling method included $[(^{99m}Tc,Re)(CN)(CO)_3bipy]$ and the cyano- bridge dinuclear complex $[(Re(CO)_3bipy)_2(\mu\text{-}CN)]^+$. Such rhenium tricarbonyl diimine complexes were known in literature for their very interesting photochemical properties in the context of solar energy conversion.[3] Thus, work in the field of radiopharmacy was stopped and a detailed study of photoactive complexes of the type "$[Re(CO)_3(diimine)X]$" started.

The ultimate aim of this part of the thesis was to make a contribution to the very difficult problem of photocatalytic water splitting based on photoactive rhenium complexes. If feasible as an efficient large scale process, photocatalytic water splitting could be the solution for the problem of providing the world's population with a sustainable enrgy source. It had been shown that $[Re(CO)_3(diimine)X]$ complexes are able to act both as photosensitisers and reduction catalysts for the two-electron reduction of CO_2 to CO.[4] In this reaction, the photoexcited complex is acting as strong oxidizing agent and picks up an electron at high potentials from an electron donor molecule. In multiple steps two electrons are transferred to the substrate CO_2, which is coordinated to the rhenium centre. The energy needed for this process is provided by the absorbed light to achieve a photoinduced electron transfer of two electrons.

Two electrons are also needed for the reduction of water to molecular hydrogen. Therefore, a change of the complexes' photoreaction pathway from CO_2 to water reduction was envisioned. For this goal, different series of rhenium(I) carbonyl complexes containing different sixth ligands X, various diimines and even bridging diimines linked to other metals could be synthesised and characterised. In this way, compounds with greatly differing

absorption, fluorescence, structural and redox properties were prepared. Studies of the photoreactivity of these compounds led to three main results:

- Many of the $[Re(CO)_3(diimine)X]$- compounds retain activity as photocatalysts in the established system for photochemical CO_2 reduction. One of the new compounds, $[Re(SCN)(CO)_3(bipy)]$, seems to be an even better catalyst than the ones so far studied for this system. In general, it was found that only $[Re(CO)_3(diimine)X]$- complexes showing room temperature fluorescence in solution are active photocatalysts for the reduction of CO_2. As all heterodinuclear complexes, with the rhenium centre linked to another metal by a small bridging diimine, lack emission from the excited state, they all show no photoreactivity at all.
- Electron transfer from the amine electron donors to the excited state of the complexes is very fast and can be detected for all fluorescing complexes. The STERN-VOLMER constants K_{SV} for these reactions indicate the efficiencies with which these electron transfers occur. There is no correlation between K_{SV} and properties of the complexes like absorption maxima, redox potential, nature of the ligands or geometry of the complex. This indicates that the electron transfer reaction is a nearly diffusion-controlled outer sphere process whose rate is influenced only by the excited state lifetime τ of the complex. Unfortunately, no alternative was found for the known use of amines as electron sources.
- While many of the rhenium complexes are able to catalyse the two-electron photoreduction of CO_2, none shows any reactivity for the much more important substrate H_2O. Thus, water reduction can only be achieved if electrons are transferred from rhenium to a water reduction catalyst. Such an electron transfer chain was realised by using $[Co(bipy)_n]^{2+}$ as relay and Adams' catalyst (PtO_2) as the site of water reduction. The reaction rates for hydrogen generation in this relay system are very low, but a proof-of-

principle is given that rhenium complexes can be used as sensitisers for photocatalytic water reduction.

These results show that numerous variations of rhenium tricarbonyl diimine complexes with a wide range of properties can be prepared. As long as room temperature fluorescence is retained, these compounds are photochemically active as carbon dioxide reduction catalysts. For the presented outline of a biomimetic water splitting system (part 1.4), $[Re(CO)_3(diimine)X]$- complexes might therefore be used for the "reduction part" (Figure 7.1) of the overall process. As the complexes do not react directly with water in their reduced form, co-catalysts are needed to make the two-electron reduction step of water reduction possible.

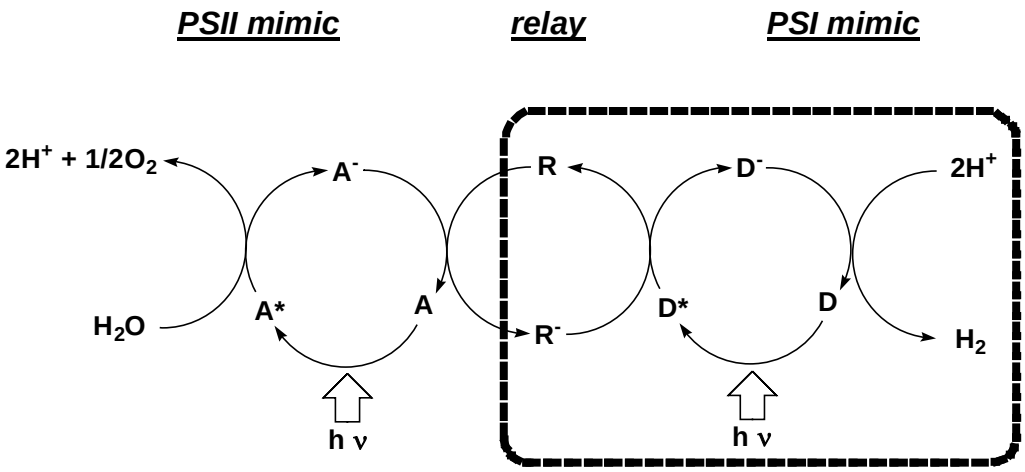

Scheme 7.1 Suggested system for photocatalytic water splitting. $[Re(CO)_3(diimine)X]$- complexes might act as photosensitisers D for the "reduction part" (dashed box).

7.2 Outlook

The fragment $[(Tc^{I},Re^{I})(CN)_4(NO)]^{2-}$ might deserve to be studied further. It is air stable and easily accessible in one reaction step directly from $[(Tc,Re)O_4]^-$ in water. But it remains a challenge to find a suitable way to bind a bioactive molecule to its vacant sixth position. As the fragment already carries a double negative charge, strongly binding, monodentate ligands like isonitriles might be interesting candidates. Another possibility might be the use of thiourea- derivatives, as thiourea was found to form stable complexes with $[(Tc^{I},Re^{I})(CN)_4(NO)]^{2-}$.[5]

Experiences from the [2+1] labelling approach for ^{99m}Tc involving cyanide proved to be useful for ongoing efforts to develop a similar scheme where isocyanides are used instead of CN- as strongly bound monodentate anchors for biomolecules.[6] Similarly, it was possible to construct cyano- bridges similar to the ones presented here between $[Re(CO)_3L_2]$- fragments and the central cobalt atom of vitamin B_{12}.[7]

The results from the second part of this thesis indicate that $[Re(CO)_3(diimine)X]$- compounds show very interesting and versatile properties as photoactive species. Their study therefore deserves more attention as they should be considered as promising alternative to the $[Ru(diimine)_3]^{2+}$- class of compounds which dominate the field of inorganic photosensitisers today. The excited states of the rhenium tricarbonyl diimines are stronger oxidising agents than the ruthenium species and therefore offer the possibility to use a wider range of electron sources. The key remaining problem is to find a suitable relay molecule (R in Scheme 7.1) to supply the rhenium water reduction component with electrons from a photo-oxidation process, ideally from a PSII mimic system where water is oxidised.

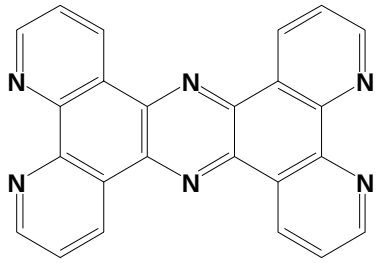

tpphz

Scheme 7.2 Structure of the large bridging diimine tpphz.

Two topics in particular are addressed in work currently in progress:

- Do systems with larger bridging diimines than the ones presented here offer the possibility to prepare dinuclear complexes that retain photoreactivity? The ligand to be studied as a first promising candidate here is tetrapyridophenazine (tpphz) (Fig 7.2).[8] The use of the extended diimine bridge might result in room temperature fluorescence, which proved to be the property critical for

photoreactivity of the complexes. As the extended bipy complex $[ReBr(CO)_3(dppz)]$ was found to be an active species, the tpphz-complex, formally just an extension of dppz, should show fluorescence and photoreactivity as well.

- A more detailed study will be carried out concerning the interesting relay system presented for photochemical water reduction. Are there alternatives to the cobalt(II) relay, e.g. vanadium or europium as suggested in the literature for similar systems?[9, 10] Can Adams' catalyst be replaced by much cheaper colloidal nickel?

So it is still a long way to go until a sustainable system to produce a "solar fuel" will be found. Whether rhenium complexes are good photosensitisers for such systems, only time can tell. Until then, we have to look at all the green, photosynthesising plants around us, ask "How do they do it?" - and admire nature.

References

[1] P. Kurz, B. Spingler, T. Fox, R. Alberto, *Inorganic Chemistry* **2004**, *43*, 3789.

[2] P. Kurz, B. Spingler, R. Alberto, in *Technetium, Rhenium and Other Metals in Chemistry and Nuclear Medicine 6* (Eds.: M. Nicolini, U. Mazzi), **2002**.

[3] D. J. Stufkens, *Comments Inorg. Chem.* **1992**, *13*, 359.

[4] J. Hawecker, J. M. Lehn, R. Ziessel, *Helv. Chim. Acta* **1986**, *69*, 1990.

[5] J. Smith, W. Purcell, G. J. Lamprecht, A. Roodt, *Polyhedron* **1996**, *15*, 1389.

[6] N. Agorastos, P. Haefliger, P. Kurz, R. Alberto, *Chimia* **2004**, *58*, 465.

[7] S. Kunze, F. Zobi, P. Kurz, B. Spingler, R. Alberto, *Angew. Chem., Int. Ed.* **2004**, *43*, 5025.

[8] B. Probst, Diploma thesis, University of Zurich **2005**.

[9] B. V. Koryakin, T. S. Dzhabiev, A. E. Shilov, *Dokl. Akad. Nauk SSSR* **1977**, *233*, 620.

[10] G. M. Brown, B. S. Brunschwig, C. Creutz, J. F. Endicott, N. Sutin, *J. Am. Chem. Soc.* **1979**, *101*, 1298.

8. EXPERIMENTAL PART

8.1 Analytical methods

HPLC analyses were performed on a Merck-Hitachi L-7000 system equipped with a EG&G Berthold LB 508 radiometric detector, using Macherey-Nagel C-18ec reversed-phase columns (5µm particle size, 100Å pore size, 250×3mm) for separation. HPLC solvents consisted of 0.1% trifluoroacetic acid in water (solvent A) and methanol (solvent B). HPLC gradient: 0–3 min 100% of solvent A; 3.1–9 min: 75% A and 25% B. At 9 min switch to 66% A and 34% B, followed by a linear gradient to 100% B from 9 to 20 min; 20–22 min: 100% B then switching back to 100% A. The flow rate was 0.5 ml min^{-1}.

UV-Vis spectra were measure using a Cary 50 spectrometer with solution samples in 1cm quartz cells. If necessary, cells with silicon septa lids were used to keep samples under an inert gas atmosphere during measurements.

Fluorescence measurements were performed on a Perkin Elmer LS50B fluorescence spectrometer with argon purged solution samples in 1cm cells.

IR spectra were recorded on a Bio-Rad FTS-45 spectrometer with samples in compressed KBr-pellets.

Electrospray ionisation mass spectra (ESI-MS) were recorded on a Merck Hitachi M-8000 spectrometer, reported are the values of the ^{187}Re isotope. In general, it proved to be impossible to measure mass spectra of any cyano-complexes. This observation was confirmed as even well-known commercial products such as $K_3[Fe(CN)_6]$ do not show any mass spectrometry signal.

^1H NMR spectra were recorded on Varian Mercury and Varian Gemini-2000 spectrometers (^1H at 199.97 MHz and 300.08 MHz, respectively). The chemical shifts are reported relative to residual solvent protons as a reference.

^{99}Tc NMR spectra were recorded on a Varian Gemini-2000 spectrometer (^{99}Tc resonance 67.40 MHz), referenced to $[^{99}TcO_4]^-$.

Elemental analyses were performed on a Leco CHNS-932 elemental analyser. It was found that cyano-compounds often show elemental analyses differing greatly from the expected calculated percentages. This analytical problem was observed for commercial, analytical grade chemicals like NaCN or $K_3[Fe(CN)_6]$ as well.

Scintillation counts were performed by a Packard 2200CA liquid scintillation analyser with samples dissolved in Packard Ultima Gold XR scintillation cocktail.

Electrochemical measurements were carried out in DMF, CH_2Cl_2 or MeCN containing 0.1M TBA PF_6 as conducting electrolyte. A Metrohm 757VA Computrace electrochemical analyser was used with a standard three-electrode setup of glassy carbon working and auxiliary electrodes and a Ag/AgCl reference electrode. All potentials are given vs. Ag/AgCl (NHE +221mV).

Gas chromatograms were recorded using a Varian CP-3800 gas chromatograph with helium as carrier gas. Cyclohexanone and cyclohexanol were separated on a 30m x 0.25mm Chrompack CP-Sil 8CB-MS capillary column and detected by a Varian Saturn 2000 mass spectrometer. Tests with solutions of known concentrations indicated that the ratios of the integrated total MS ion count curves showed an excellent correlation to the cyclohexanone / cyclohexanol ratio in solution.

The permanent gases CO, N_2, O_2 and H_2 were separated by a 3m x 2mm column packed with Varian molecular sieve 13X. The gases were detected using a thermal conductivity detector. Calibrations were performed by the injection of known quantities of pure gases.

For *X-ray diffraction studies*, suitable crystals were covered with Paratone N oil, mounted on top of a glass fibre and immediately transferred to a Stoe IPDS diffractometer. Data was collected at 183(2) K using graphite-monochromated Mo radiation (0.71073Å). Data was corrected for Lorentz and polarisation effects as well as for absorption. Structures were solved with direct methods using SHELXS-97[1] or SIR97[2] and were refined by full-matrix least-squares methods on F^2 with SHELXL-97[3]. The crystal data and

refinement parameters of the presented structures are summarized in the table of part 8.4.

8.2 Syntheses

Synthetic reactions were carried out under a nitrogen atmosphere using standard Schlenk techniques. All chemicals were of reagent grade and used without further purification. Water was doubly distilled before use. $Na^{99m}TcO_4$ was eluted from a $^{99}Mo/^{99m}Tc$ Mallinkrodt Ultra-TechneKow® generator in 0.9% saline.

The known complexes $[ReOCl_3(PPh_3)_2]$[4], $[Re(CO)_5Br]$[5] (**1**), $(NEt_4)_2[Re(CO)_3Br_3]$[6] (**2**), $(NEt_4)_2[Tc(CO)_3Cl_3]$[7] (**3**) and $[Pt(PPh_3)_4]$[8] as well as the ligands abpy[9], phd[10], dpq[11], dppz[12] were synthesized according to published procedures.

Caution! ^{99}Tc is a weak β-emitter with a half life of 2.12×10^5 years. Although radiation from low amounts of material is absorbed completely by the walls of the glassware, reactions should only be carried out in specially equipped laboratories and under well ventilated hoods to avoid contamination or ingestion.

$K_5[Re(CN)_6]$ (4). 420 mg (0.5 mmol) $[ReOCl_3(PPh_3)_2]$ and 1.63 g KCN (25 mmol) were suspended in a N_2-purged mixture of 10 ml of 0.5 M KOH and 10 ml of MeOH. 520 mg $Na_2S_2O_4$ were added in portions as solid. The mixture was heated to 90°C for 12h to yield a green solution and a green precipitate. After cooling, the green solid was filtered off, washed three times with 2 ml 0.5 M NaOH / MeOH (1:1), three times with 2 ml of THF and then dried in *vacuo*. Yield: 96 mg (35%). $\lambda_{max}(H_2O)$: 320nm (*sh*, ε=7000). IR(KBr): ν_{CN} = 2020 (m), 1934 (s). Raman: ν_{CN} = 2043 (m), 1966 (s). ESI-MS(H_2O/MeOH): *m/z* = 317 [M-CN^-], 307 [M-2CN^- + O], 291 [M-2CN^-]. Anal. Calcd. for $C_6K_5N_6Re_1$ (%): C, 13.40; N, 15.63. Found: C, 12.59; N, 13.91.

$K_2[Re(CN)_4(H_2O)(NO)]$ (5). A solution is prepared containing 101.3 mg (0.35 mmol) $KReO_4$, 91.1 mg KCN (4eq.) and 590 mg KOH (30eq.) in 5 ml H_2O. The solution is heated to 75°C and 365 mg $NH_2OH{\cdot}HCl$ in 2 ml H_2O are

added. The mixture is kept at 75°C for 1h before the solvent is removed in *vacuo*. The residue is extracted by 10 ml of MeOH and hexane is added to obtain the red product. Yield: 91 mg (65%). $\lambda_{max}(H_2O)$: 470nm (ε=2000). IR(KBr): ν_{CN} = 2076 (s), ν_{NO} = 1663 (s). ESI-MS(H_2O/MeOH): 321 ($M\text{-}H_2O^-$).

$(NEt_4)_2[(CO)_3(\mu\text{-}OH)Re(\mu\text{-}CN)Re(\mu\text{-}OH)(CO)_3]_2$ (6). 50 mg (6.5×10^{-5} mol) $(NEt_4)_2[Re(CO)_3Br_3]$ were dissolved in 3 ml of H_2O and 42 mg (6.5×10^{-4} mol) KCN in 3 ml of 1 mM KOH were added. The mixture was stirred for 1 h before the white precipitate was filtered off, washed several times with water and dried in *vacuo*. Yield: 14 mg (60%). IR(KBr): ν_{CN} = 2148 (w); ν_{CO} = 2016 (s), 1903 (s). Anal. Calcd. For $C_{30}H_{44}N_4O_{16}Re_4$ (%): C, 24.65; H, 3.03; N, 3.83. Found: C, 24.30; H, 2.95; N, 3.58. Recrystallisation from acetonitrile/ dichloromethane afforded crystals suitable for X-ray diffraction analysis.

$(AsPh_4)_2[^{99}Tc(CN)_3(CO)_3]$ (7). 15 mg (2.5×10^{-5} mol) $(NEt_4)_2[Tc(CO)_3Cl_3]$ were dissolved in 3 ml of MeOH and 16 mg (2.5×10^{-4} mol) KCN in 2 ml of MeOH were added. After stirring for 2 h at room temperature, the solvent was removed in *vacuo*. 3 ml of 0.1 M NaOH were added to the residue and the suspension was stirred for 2 h. After filtration, 55 mg (1.25×10^{-4} mol) $AsPh_4Cl \cdot H_2O$, dissolved in 2 ml of H_2O, were added to the solution. After 12 h, the white precipitate of **7** was filtered off, washed three times with 1 ml of H_2O and dried in *vacuo*. Yield: 23 mg (90%). IR(KBr): ν_{CN} = 2145 (w), 2106 (m); ν_{CO} = 2005 (s), 1896 (vs). ^{99}Tc NMR(MeOH-d_4): -2198.8(s). Crystals for X-ray diffraction analysis were obtained by layering a solution of **7** in EtOH with Et_2O.

$(AsPh_4)_2[^{99}Tc(^{13}CN)_3(CO)_3]$ (ca. 70% enriched) (7*). The same method as that for compound **7** was followed using 17 mg (2.8×10^{-5} mol) $(NEt_4)_2[Tc(CO)_3Cl_3]$, 18 mg (2.8×10^{-4} mol) $K^{13}CN$ (90% enriched) and 61 mg (1.4×10^{-4} mol) $AsPh_4Cl \cdot H_2O$. IR(KBr): ν_{CN} = 2106 (w), 2061 (m); ν_{CO} = 2001 (s), 1896 (vs). ^{99}Tc NMR(MeOH-d_4): -2198.7 (q); ^{13}C NMR (CD_3OD): 153.5 (decet).

$(AsPh_4)_2[Re(CN)_3(CO)_3]$ (8). The same method as that for compound **7** was followed using 50 mg (6.5×10^{-5} mol) $(NEt_4)_2[Re(CO)_3Br_3]$, 42 mg (6.5 x

10^{-4} mol) KCN and 80 mg (1.9 x 10^{-4} mol) $AsPh_4Cl \cdot H_2O$. Yield: 45 mg (55%) IR(MeOH): ν_{CN} = 2128 (w), 2107 (m); ν_{CO} = 2006 (s), 1921 (s). ESI-MS: *m/z* = 349 [M^-], 322 [M-CN^-]. Crystals for X-ray diffraction analysis were obtained by layering a solution of **8** in EtOH with Et_2O.

$(AsPh_4)_2[Re(^{13}CN)_3(CO)_3]$ (ca. 70% enriched) **(8*).** The same method as that for compound **7** was followed using 50 mg (6.5 x 10^{-5} mol) $(NEt_4)_2[Re(CO)_3Br_3]$, 43 mg (6.5 x 10^{-4} mol) $K^{13}CN$ (90% enriched) and 80 mg (1.9 x 10^{-4} mol) $AsPh_4Cl \cdot H_2O$. Yield: 40 mg (50%) IR(MeOH): ν_{CN} = 2115 (w), 2060 (m); ν_{CO} = 2001 (s), 1923 (s). ESI-MS: *m/z* = 352 [M^-], 324 [M-CN^-].

[^{99m}Tc(pico)$(CO)_3$(CN)] (9). A basic aqueous solution (1 ml, pH=9.5) of $[^{99m}Tc(CO)_3(H_2O)_3]^+$ was prepared in a N_2- purged, sealed vial according to the published procedure[13]. Now picolylamine was added to reach a ligand concentration of 1 mmol and the mixture was heated to 90°C for 30 min. Addition of a solution of KCN to reach a concentration of cyanide of 0.1 mmol, followed by heating to 90°C again for 30 min, yielded the product in a yield of >95% according to analysis by HPLC equipped with a γ- detector.

[^{99m}Tc(histam)$(CO)_3$(CN)] (10). The same procedure as for compound **9** was applied, with the difference that the histamine and cyanide concentrations were only 0.1 mmol and 0.05 mmol, respectively. This resulted in a lower yield of #10 of only 70% according to analysis by γ-detected HPLC.

[Re(pico)$(CO)_3$(CN)] (11). 100 mg (0.13 mmol) $(NEt_4)_2[Re(CO)_3Br_3]$ were dissolved in 5 ml of H_2O and 66.2 mg (3 eq.) $AgNO_3$ in 5 ml of H_2O added. The solution was stirred at room temperature for 30 min and the precipitate of AgBr was removed by filtration. 20µl of picolylamine (1.5eq.) were added and the solution was neutralised by the addition of K_2CO_3. After 12h at room temperature, KCN (25.4 mg, 3 eq.) was added as a solid. A white precipitate started to form after 5h, which was removed by filtration after 2d and dried in *vacuo*. Yield: 30 mg (55%). IR(KBr): ν_{NH2}= 3225(m), 3129(w); ν_{CN} = 2114 (w); ν_{CO} = 2020 (s), 1885 (s); ν_{pico} = 1613 (m), 1482 (w), 1439 (w), 1289(w),

773 (w). ESI-MS(MeOH): *m/z* = 405 [M^+], 379 [M-CN^-], 378 [M-CN^--H^+]. ^{1}H NMR(acetone-d_6): 8.85 (m, 1H), 8.06 (m, 1H), 7.73 (m, 1H), 7.48 (m, 1H), 2.83 (s,2H).

[Re(bipy)(CO)$_3$Br] (12). A procedure similar to the published method was applied[14]. 406 mg (1 mmol) of [$Re(CO)_5Br$] were suspended in 50 ml of petroleum benzene (bp. 100-130°C) together with 156 mg (1eq.) of bipy. The mixture was heated to 100°C for 3h and the yellow product was filtered off, washed with portions of petroleum benzene and ether and then dried in *vacuo*. Yield: 455 mg (90%). λ_{max}(DMF): 370nm (ε=3000). λ_{em}(DMF): 575nm. IR(KBr): ν_{CO} = 2019 (s), 1905 (s); ν_{bipy} = 1602 (m), 1471(m), 1443 (m), 772 (m). ESI-MS(acetone/MeOH): *m/z* = 529 [M+Na^+], 455 [M-Br^-+CO], 427 [M-Br^-]. ^{1}H NMR(acetone-d_6): 9.12 (d, 2H), 8.71 (d, 2H), 8.33 (m, 2H), 7.79 (m, 2H). Anal. Calcd. For $C_{13}H_8Br_1N_2O_3Re_1$ (%): C, 30.84; H, 1.59; N, 5.53. Found: C, 30.48; H, 1.54; N, 5.17.

[^{99}Tc(bipy)(CO)$_3$Cl] (13). $(NEt_4)_2[^{99}Tc(CO)_3Cl_3]$ (33 mg, 0.06 mmol) was stirred in 5 ml of H_2O for 2 h. Some insoluble impurity, most probably TcO_2, was removed by filtration and the amount of Tc in the colourless solution was found by a scintillation count to be slightly higher than expected (0.07 mmol). Now bipy (15.5 mg, 0.1 mmol) was added, dissolved in a mixture of EtOH (1 ml) and H_2O (2 ml). After 30 min a yellow precipitate started to form, which was filtered off after a reaction time of 12 h, washed with ether and dried in *vacuo*. Yield: 18 mg (80%).

[Re(bipy)(CO)$_3$(H$_2$O)](OTf) (14). Compound **12** (150 mg, 0.3 mmol) was dissolved in 15 ml of acetone and 76.1 mg AgOTf (1 eq.) in 5ml of acetone were added. The mixture was heated to 70°C for 2 h, before the white precipitate of AgBr was filtered off and the solvent was removed in *vacuo*. The yellow residue was suspended in 20ml of water and stirred at room temperature for 3 h. Insoluble parts were filtered off and the yellow solution was lyophilized to obtain the yellow, slightly hydroscopic product. Yield: 105 mg (60%). λ_{max}(DMF): 350 nm (*sh*, ε=4000), 553 nm (ε=1500). IR(KBr): ν_{CO} = 2036 (s), 1918 (s); ν_{bipy} = 1604 (m), 1475(m), 1447 (m), 771

(m); ν_{OTf} = 1291 (m), 1230 (m), 1179 (m). ESI-MS(acetone/MeOH): *m/z* = 427 [M-H_2O]. ^{1}H NMR(MeOH-d_4): 9.17 (m, 2H), 8.70 (m, 2H), 8.39 (m, 2H), 7.82 (m, 2H).

[Re(bipy)(CO)$_3$(CN)] (15). 100 mg (0.13 mmol) $(NEt_4)_2[Re(CO)_3Br_3]$ were dissolved in 5 ml of H_2O and 66.2 mg (3 eq.) $AgNO_3$ in 3 ml of H_2O added. The solution was stirred at room temperature for 30 min and the precipitate of AgBr was removed by filtration. Now bipy (20.3 mg, 1 eq.), dissolved in 2 ml of EtOH was added. After 12 h at room temperature, HPLC analysis confirmed the nearly quantitative formation of $[Re(bipy)(CO)_3(H_2O)]^+$. The addition of KCN (25.4 mg, 3 eq.), followed by 20 h of stirring the mixture at 100°C, resulted in the quantitative conversion of this species to **15,** as detected by HPLC. The solvent was removed in *vacuo* and the product obtained by extraction of the residue with three 5 ml portions of THF. Yield: 45 mg (75%). λ_{max}(DMF): 354nm. (ε=2300). λ_{em}(DMF): 540nm. IR(KBr): ν_{CN} = 2117 (w); ν_{CO} = 2006 (s), 1878 (s); ν_{bipy} = 1603 (m), 1473 (m), 1445 (m), 775 (m). ^{1}H NMR(acetone-d_6): 9.07 (d, 2H), 8.21 (d, 2H), 8.07 (m, 2H), 7.54 (m, 2H).

[(Re(bipy)(CO)$_3$)$_2$(μ-CN)](ClO$_4$) (16). 100 mg (0.13 mmol) $(NEt_4)_2[Re(CO)_3Br_3]$ were dissolved in 10 ml of H_2O and 80.8 mg (3 eq.) $AgClO_4$ in 3 ml of H_2O added. The solution was stirred at room temperature for 30 min and the precipitate of AgBr was removed by filtration. Now bipy (20.3 mg, 1 eq.), dissolved in 5 ml of EtOH was added. After 20 h at room temperature, HPLC analysis confirmed the nearly quantitative formation of $[Re(bipy)(CO)_3(H_2O)]^+$. To this solution 4.2 mg KCN (0.5 eq.) dissolved in 2 ml of H_2O were added. After 2 h at 100°C, a yellow precipitate started to form from the mixture, which was filtered off after 20 h, washed with H_2O and ether and dried in *vacuo*. Yield: 28 mg (45%). λ_{max}(DMF): 363nm. (ε=2000). λ_{em}(DMF): 535nm. IR(KBr): ν_{CN} = 2151 (w); ν_{CO} = 2025 (s), 1910 (s), 1896 (s); ν_{bipy} = 1605 (m), 1473 (m), 1446 (m), 771 (m); ν_{ClO4} = 1121 (m). ^{1}H NMR(acetone-d_6): 8.83 (br, 4H), 8.00 (br, 4H), 7.60 (br, 4H), 7.41 (br, 4H).

[Re(bipy)(CO)$_3$(SCN)] (17). Compound **12** (50.6 mg, 0.1 mmol) was dissolved in 5 ml of acetone and 17.1 mg AgOTf (1 eq.) in 2ml of acetone were added. The mixture was heated to 70 °C for 2 h, after which the precipitate of AgBr was filtered off and the solvent was removed in *vacuo*. The residue was stirred in 10 ml of MeOH for 1 h and a small insoluble part was removed by filtration. Now KSCN (20 mg, 2 eq.), dissolved in 2 ml of H_2O, was added to the solution and the mixture was heated to 70 °C for 4 h to obtain a clear yellow solution, from which the product precipitated after 1 d in the refrigerator at 4 °C. The yellow compound was filtered off, washed with cold H_2O, cold MeOH and ether and dried in *vacuo*. Yield: 30 mg (60%). λ_{max}(DMF): 376 nm (ε=2500). λ_{em}(DMF): 580nm. IR(KBr): ν_{SCN} = 2093 (s); ν_{CO} = 2020 (s), 1928 (s), 1914 (s); ν_{bipy} = 1602 (m), 1471(m), 1444 (m), 765 (m). ESI-MS(acetone/MeOH): *m/z* = 485 [M^+]. ^{1}H NMR(acetone-d_6): 9.15 (m, 2H), 8.77 (m, 2H), 8.42 (m, 2H), 7.86 (m, 2H).

[Re(phen)(CO)$_3$Br] (18). As for compound **12**, a procedure similar to the published method was applied. A suspension was prepared consisting of [Re(CO)$_5$Br] (100 mg, 0.24 mmol) and phen (47.6 mg, 1 eq.) in 10 ml of petroleum benzene (bp. 100-130°C). The suspension was heated to 100 °C for 2 h to obtain the product as a yellow precipitate. The powder was filtered off, washed with portions of petroleum benzene and ether and then dried in *vacuo*. Yield: 120 mg (95%). λ_{max}(DMF): 372 nm (ε=3500). λ_{em}(DMF): 570nm. IR(KBr): ν_{CO} = 2018 (s), 1933 (s), 1900 (s); ν_{phen} = 1425 (m), 852 (m), 723(m), 668 (m). ESI-MS(MeOH): *m/z* = 478 [M-Br+CO]$^+$, 450 [M-Br]$^+$. ^{1}H NMR(MeOH-d_4): 9.43 (m, 2H), 8.58 (m, 2H), 8.05 (s, 2H), 7.90 (m, 2H). Anal. Calcd. For $C_{15}H_8Br_1N_2O_3Re_1$ (%): C, 33.97; H, 1.52; N, 5.28. Found: C, 34.18; H, 1.53; N, 5.17.

[Re(dpq)(CO)$_3$Br] (19). The same procedure as for compound **18** was applied, using [Re(CO)$_5$Br] (50 mg, 0.12 mmol) and dpq (28.5 mg, 1 eq.), to obtain **19** as a yellow powder. Yield: 70 mg (quantitative). λ(DMF): 400 nm (*sh*, ε=2500). λ_{em}(DMF): 585nm. IR(KBr): ν_{CO} = 2025 (s), 1948 (s), 1902 (s); ν_{dpq} = 1402 (m), 1384 (m), 820 (w), 729(w), 631 (w). ESI-MS(MeOH): *m/z* =

531 $[M\text{-}Br+CO]^+$, 503 $[M\text{-}Br]^+$. ^1H NMR(acetone-d_6): 9.96 (m, 2H), 9.82 (m, 2H), 9.38 (s, 2H), 8.45 (m, 2H).

[Re(dppz)(CO)$_3$Br] (20). The same procedure as for compound **18** was applied, using $[Re(CO)_5Br]$ (50 mg, 0.12 mmol) and dppz (33.8 mg, 1 eq.), to obtain **20** as an orange powder. Yield: 50 mg (65%). λ(DMF): 400 nm (*sh*, ε=5000). λ_{em}(DMF): 520nm. IR(KBr): ν_{CO} = 2018 (s), 1918 (s), 1890 (s); ν_{dppz} = 1493 (m), 1418 (m), 1384 (m), 1360 (m), 822 (w), 773 (w), 729 (w). ESI-MS(MeOH): *m/z* = 581 $[M\text{-}Br+CO]^+$, 553 $[M\text{-}Br]^+$. ^1H NMR($CDCl_3$): 10.04 (m, 2H), 9.88 (m, 2H), 8.47 (m, 2H), 8.08 (m, 2H), 7.26 (m, 2H). Anal. Calcd. For $C_{21}H_{10}Br_1N_4O_3Re_1$ (%): C, 39.88; H, 1.59; N, 8.86. Found: C, 39.53; H, 1.77; N, 8.58.

[Re(biq)(CO)$_3$Br] (21). A suspension of $[Re(CO)_5Br]$ (100 mg, 0.24 mmol) and biq (70.5 mg, 1 eq.) in 10 ml of a 1:1- mixture of toluene and petroleum benzene (bp. 100-130°C) was heated to 120 °C for 30 min. Upon cooling, **21** precipitated from solution as a orange-red powder, which was washed with portions of toluene and ether and dried in *vacuo*. Yield: 140 mg (95%). λ_{max}(DMF): 433 nm (ε=2000). IR(KBr): ν_{CO} = 2014 (s), 1895 (s); ν_{biq} = 1615 (w), 1595 (m), 1510 (m), 1430 (m), 1375 (m), 1145 (m), 820 (m), 783 (w). ESI-MS(acetone/MeOH): *m/z* = 527 $[M\text{-}Br]^+$. ^1H NMR($CDCl_3$): 9.01 (d, 2H), 8.58 (d, 2H), 8.40 (d, 2H), 8.01 (m, 4H), 7.79 (m, 2H). Anal. Calcd. For $C_{21}H_{12}Br_1N_2O_3Re_1$ (%): C, 41.59; H, 1.99; N, 4.62. Found: C, 41.62; H, 1.90; N, 4.54.

(NEt$_4$)[Re(CO)$_3$(Hdcbipy)Br] (22). $(NEt_4)_2[Re(CO)_3Br_3]$ (154 mg, 0.2 mmol) was dissolved in 15 ml of H_2O and H_2dcbipy (53.7 mg, 1.1 eq.) was added as a solid. The pH of the solution was raised to pH~6-7 by the careful addition of 10 mM NaOH. The mixture was stirred for 2 d at room temperature and some yellow precipitate formed, which was filtered off. The filtrate was lyophilized, triturated three times with 5 ml of CH_2Cl_2 to remove NEt_4Br and then dried in *vacuo*. Yield: 75 mg (50%). IR(KBr): ν_{CO} = 2024 (s), 1896 (s); ν_{dcbipy} = 1719 (w), 1619 (m), 1551 (w), 1366 (m), 1289 (m), 1071 (w), 766

(m), 682 (m). ESI-MS(MeOH): *m/z* = 569 $[M\text{-}COOH\text{-}H]^-$. ^1H NMR(D_2O/Na_2CO_3): 9.05 (m, 2H), 8.67 (m, 2H), 7.82 (m, 2H).

$[Re(CO)_3(bpm)Br]$ (23). $(NEt_4)_2[Re(CO)_3Br_3]$ (385 mg, 0.5 mmol) was dissolved in 20 ml of H_2O and bpm (87 mg, 1.1 eq.), dissolved in 2 ml of EtOH was added. The mixture was stirred for 20 h at room temperature, after which a fine orange precipitate had formed. The solid was filtered off, washed with H_2O, cold EtOH and ether, and dried in *vacuo*. Yield: 210 mg (80%). λ_{max}(DMF): 383 nm (ε=2500). IR(KBr): ν_{CO} = 2030 (s), 1931 (s), 1906 (s); ν_{bpm} = 1575 (m), 1547 (w), 1407 (s), 834 (w), 755 (w). ESI-MS(acetone/MeOH): *m/z* = 508 $[M]^+$. ^1H NMR(acetone-d_6): 9.41 (dd, 2H), 9.36 (dd, 2H), 7.98 (dd, 2H).

$[Re(CO)_3(bpm)(NO_3)]$ (24). $(NEt_4)_2[Re(CO)_3Br_3]$ (500 mg, 0.65 mmol) was dissolved in 20 ml of H_2O. A solution of $AgNO_3$ (332 mg, 3eq.) was added and after 30 min. stirring at room temperature, the precipitate of AgBr was removed by filtration. Now bpm (155 mg, 1.5 eq.), dissolved in 3 ml of EtOH, was added, and the mixture was heated to 90 °C for 15 h to obtain an orange solution, which was taken to dryness under reduced pressure. The residue was extracted two times with 5 ml portions of $CHCl_3$ to remove NEt_4NO_3 and then two times with 30 ml portions of THF to obtain the orange product. The extracts were combined and dried in *vacuo*. Yield: 126 mg (40%). λ_{max}(H_2O, NaOH, pH=9): 310 nm (ε=2000), 400 nm (*sh*, ε=1000). IR(KBr): ν_{CO} = 2034 (s), 1926 (s), 1907 (s); ν_{bpm} = 1577 (m), 1550 (w), 1488 (m), 1407 (s), 825 (w), 755 (w), ν_{NO3} = 1384 (s), 1286 (s). ^1H NMR(D_2O): 9.32 (dd, 2H), 9.19 (dd, 2H), 7.84 (dd, 2H).

$[Re(CO)_3(bpm)(CN)]$ (25). Compound **23** (50 mg, 0.1 mmol) was dissolved in 10ml of acetone and solid AgOTf (25mg, 1eq.) was added. The solution was heated to 60 °C for 1h, after which the precipitated AgBr was removed by filtration. Now solid KCN (30 mg, 5 eq.) was added and the suspension was heated to reflux for 3 h. The excess KCN was filtered off, the solvent was removed and the residue extracted with 10 ml of H_2O. The extract was lyophilized to obtain the product as a orange powder. Yield: 25 mg (50%).

λ_{max}(DMF): 365 nm (ε=1250). IR(KBr): ν_{CN} = 2106 (w); ν_{CO} = 2011 (s), 1917 (s); ν_{bpm} = 1587 (m), 1560 (m), 1407 (s), 1179 (m), 1035 (m), 818 (w), 768 (w), 643 (m). ^{1}H NMR(acetone-d_6): 9.44 (dd, 2H), 9.38 (dd, 2H), 8.01 (dd, 2H).

[(Re(bpm)(CO)$_3$)$_2$(μ-CN)](NO$_3$) (26). Compound **24** (96mg, 0.2 mmol) was dissolved in 10 ml of H_2O. An aqueous solution of KCN (6.5 mg, 0.5 eq.) was added and the mixture was stirred at 50 °C for 7 d. After this time conversion of >90% of the used **24** into a new species was confirmed by HPLC analysis. The solution was taken to dryness under reduced pressure and the residue was extracted two times with 10 ml portions of CH_2Cl_2 to obtain the orange product. Yield:70 mg (75%). IR(KBr): ν_{CN} = 2145 (w); ν_{CO} = 2030 (s), 1925 (s); ν_{bpm} = 1578 (m), 1549 (m), 1408 (s), 1020 (w), 821 (w), 753 (m), 641 (w); ν_{NO3} = 1384 (s). ESI-MS(MeOH): *m/z* = 884 $[M]^+$. ^{1}H NMR(D_2O): 9.14 (m, 4H), 9.04 (dd, 2H), 8.98 (dd, 2H), 7.69 (m, 4H). Anal. Calcd. for $C_{23}H_{12}N_{10}O_9Re_2$(%): C, 29.24; N, 14.82; H, 1.28; Found: C, 30.23; N, 15.08; H, 2.01.

[Re(CO)$_3$(abpy)Br] (27). $(NEt_4)_2[Re(CO)_3Br_3]$ (76 mg, 0.1 mmol) was dissolved in 5 ml of H_2O and abpy (27 mg, 1.5 eq.), dissolved in 2 ml of H_2O was added. The mixture was stirred for 2 d at room temperature. During this time a violet-blue precipitate formed, which was filtered off, washed with H_2O, cold EtOH and ether, and dried in *vacuo*. Yield: 50 mg (95%). λ_{max}(DMF): 361 nm (ε=5000), 553 nm (ε=1500). IR(KBr): ν_{CO} = 2020 (s), 1924 (s), 1900 (s); ν_{abpy} = 1465 (w), 1433 (m), 1370 (w), 797 (m). ESI-MS(acetone/MeOH): *m/z* = 533 $[M-H]^+$, 454 $[M-H-Br]^+$. ^{1}H NMR(acetone-d_6): 9.33 (m, 1H), 8.96 (m, 1H), 8.87 (m, 1H), 8.57 (td, 1H), 8.20 (br, 2H), 8.00 (br, 1H), 7.85 (br, 1H). Anal. Calcd. For $C_{13}H_8Br_1N_4O_3Re_1$ (%): C, 29.22; H, 1.51; N, 10.49. Found: C, 29.61; H, 1.43; N, 10.56.

[Re(CO)$_3$(abpy)(CN)] (28). A suspension of compound **27** (30 mg, 0.05 mmol) and AgOTf (14mg, 1 eq.) in 5ml of MeOH was stirred at room temperature for 2 h. The precipitate of AgBr was removed by filtration and NaCN (8.3 mg, 3eq.) was added as a solid. The mixture was stirred at room temperature for 2 d, when HPLC analysis indicated a >95% conversion of **27**

into **28**. The solvent was removed under reduced pressure and the product was obtained by extraction of the residue into two 5 ml portions of CH_2Cl_2. Yield: 20 mg (75%). λ_{max}(DMF): 485 nm (ε=2500), 553 nm (ε=1500). IR(KBr): ν_{CN} = 2119 (m); ν_{CO} = 2016 (s), 1909 (s); ν_{abpy} = 1460 (s), 1260 (s), 1173 (s), 1037 (s), 795 (m), 645 (m).

[Re(CO)$_3$(phd)Br] (29). $(NEt_4)_2[Re(CO)_3Br_3]$ (500 mg, 0.65 mmol) was dissolved in 20 ml of H_2O and phd (163 mg, 1.2 eq.), suspended in 2 ml of EtOH was added. The mixture was stirred for 1 d at room temperature. During this time an orange precipitate formed, which was filtered off, washed with H_2O, cold EtOH and ether, and dried in *vacuo*. Yield: 350 mg (95%). λ(DMF): 375 nm (*sh*, ε=3000). IR(KBr): ν_{CO} = 2033 (s), 1943 (s), 1885 (s); ν_{phd} = 1703 (m), 1573 (w), 1427 (m), 1298 (w), 1026 (w), 828 (w), 727 (w). ESI-MS(MeOH): *m/z* = 512 $[M\text{-}Br+MeO]^+$, 480 $[M\text{-}H\text{-}Br]^+$. ^{1}H NMR(acetone-d_6): 9.34 (dd, 2H), 8.81 (dd, 2H), 8.05 (dd, 2H). Anal. Calcd. For $C_{15}H_6Br_1N_2O_5Re_1$ (%): C, 32.15; H, 1.08; N, 5.00. Found: C, 32.37; H, 1.12; N, 5.08.

[(CO)$_3$BrRe(μ-bpm)Cu(PPh$_3$)$_2$](BF$_4$) (30). The compound was synthesized in a manner similar to the published procedure[15]. A suspension was prepared containing compound **23** (152 mg, 0.3 mmol), $Cu(BF_4)_2{\cdot}6H_2O$ (55 mg, 0.5 eq.), Cu powder (10 mg, 0.5 eq.) and PPh3 (175 mg, 2 eq.) in 15 ml of CH_2Cl_2 and 5 ml of MeOH. The mixture was stirred at room temperature for 12 h to form a red suspension. Some precipitate was filtered off and 15 ml of hexane was added to the filtrate to obtain a slightly turbid solution, which was kept at –20 °C for 1 d to precipitate the product as a red powder. The product was removed by filtration, washed with hexane and dried in *vacuo*. Yield: 100 mg (30%). λ_{max}(DMF): 382 nm (ε=5000). IR(KBr): ν_{CO} = 2031 (s), 1934 (s), 1887 (s); ν_{bpm} = 1479 (w), 1409 (m), 744 (w); ν_{BF4} = 1121 (m), 1083 (s); ν_{PPh3} = 2925 (m), 2851 (w), 1435 (m), 694 (m). ^{1}H NMR($CDCl_3$): 9.24 (d), 9.17 (br), 7.81-7.24 (m,br). Anal. Calcd. For $C_{47}H_{36}B_1Br_1Cu_1F_4N_4O_3P_2Re_1$ (%): C, 47.71; H, 3.07; N, 4.74. Found: C, 47.32; H, 2.98; N, 4.65.

$[(CO)_3(H_2O)Re(\mu\text{-bpm})Ir(H_2O)Cp^*](OTf)_3$ (31). Two aqueous solutions were prepared seperately: in a first vial, compound **23** (51 mg, 0.1 mmol) and AgOTf (26 mg, 1 eq.) were suspended in 5 ml of H_2O and stirred for 1 d at room temperature, after which the precipitated AgBr was removed by filtration. In a second vial, the same procedure was applied to a mixture of $[Cp^*IrCl_2]_2$ (40 mg, 0.5 eq.) and AgOTf (52 mg, 2 eq.) in 5 ml of H_2O. The two filtrates were combined and after 12 h at room temperature, the solution was filtered and lyophilized to obtain the red product. Yield: 100 mg (80%). λ_{max}(DMF): 425 nm (*sh*, ε=2500), 553 nm (ε=1500). IR(KBr): ν_{CO} = 2046 (s), 1936 (s); ν_{bpm} = 1583 (w), 1414 (m), 1384 (w), 517 (w); ν_{OTf} = 1259 (s), 1169 (m), 1031 (s), 640 (m). ESI-MS(MeOH): *m/z* = 864 $[M\text{-}H_2O\text{+}3MeOH]^+$. ^{1}H NMR(MeOH-$d_4$): 9.69 (m, 2H), 9.59 (m, 2H), 8.30 (m, 2H), 1.66/1.63 (two s, combined 15H).

$[(CO)_3(H_2O)Re(\mu\text{-abpy})Ir(H_2O)Cp^*](OTf)_3$ (32). The same procedure as for compound **31** was applied, using **27** (30 mg, 0.056 mmol), $[Cp^*IrCl_2]_2$ (22 mg, 0.5 eq.) and the appropriate amounts of AgOTf. Yield: 50 mg (60%). λ_{max}(DMF): 449 nm (ε=6500), 508 nm (ε=6250), 700 (*sh*, ε=2500). IR(KBr): ν_{CO} = 2028 (s), 1917 (s); ν_{abpy} = 1452 (m), 1384 (w), 764 (w); ν_{OTf} = 1262 (s), 1172 (s), 1033 (s), 643 (s). ESI-MS(MeOH): *m/z* = 781 $[M\text{-}2H_2O]^+$, 895 $[M\text{-}H_2O\text{+}3MeOH]^+$.

$[(CO)_3BrRe(\mu\text{-phd})Pt(PPh_3)_2]$ (33). Compound **29** (15 mg, 0.027 mmol) was dissolved in 5 ml of CH_2Cl_2 and the solution was heated to 40 °C. A solution of $[Pt(PPh_3)_4]$ (37 mg, 1.1 eq.) in 2 ml of CH_2Cl_2 was added and the mixture kept at 40 °C for 30 min. A dark red solution was obtained to which 8 ml of hexane was added. The mixture was cooled to –20 °C for 12 h to obtain **33** as a red precipitate, which was filtered off, washed with hexane and ether and dried in *vacuo*. Yield: 27 mg (80%). λ_{max}(DMF): 430 (*sh*, ε=3500), 550 (ε=700). IR(KBr): ν_{CO} = 2017 (s), 1910 (s), 1889 (s); ν_{phd} = 1608 (m), 1410 (m), 1372 (m), 1072 (m), 745 (w), 554 (m); ν_{PPh3} = 1436 (m), 1097 (m), 804 (w), 692 (m). ^{1}H NMR($CDCl_3$): 9.29 (dd, 2H), 8.73 (dd, 2H), 7.83 (dd, 2H), 7.54- 7.14 (m, 30H).

8.3 Catalysis experiments

Cyclohexanone reductions catalysed by [Cp*Ir(H_2O)(diimine)]- complexes (Scheme 5.9) were carried out in 25ml Schlenk flasks with septum caps under nitrogen. 10ml of an aqueous solution containing 0.5mM catalyst, 0.1M cyclohexanone and 1M formic acid were heated to 70°C. In some experiments the solvent was 0.5M acidic phosphate buffer (pH=2). 100µl solution samples were taken by syringe and extracted with 100µl of Et_2O. The ether extract was injected into the GC-MS for a determination of the cyclohexanone/cyclohexanol ratio.

Photochemical carbon dioxide reductions catalysed by [$Re(CO)_3$(diimine)X]- complexes (Scheme 6.1) were tested in 50ml septum capped Schlenk tubes. Exact volumes were determined gravimetrically. 10ml of a solution containing TEOA (1M) and the catalyst (1mM) in DMF (or one of the other solvent systems mentioned in part 6.2) were prepared, wrapped in black foil and degassed using a CO_2-purged Schlenk-line. The mixture was equilibrated under 1.5bar CO_2-pressure for 15min. and then transferred to a dark room for illumination. The light source was a Leica Pradovit S AF slide projector equipped with a 250W Osram Xenophot HLX lamp. The light was filtered by a 400nm cut-off filter (Schott GG 400) before reaching the sample at 40cm distance from the projector. Light intensities illuminating the sample were determined by a TES 1332A luxmeter to be 46000lux. 100µl gas samples were drawn from the headspace above the solution and injected into the GC-TCD gas analyser.

8.4 Crystallographic tables

Compound No.		**6**·2MeCN	**7**
Figure No.	*2.2*	*2.3*	*2.5*
Formula	$C_{50}H_{93.50}K_2N_8O_{17.50}Re$	$C_{38}H_{56}N_8O_{16}Re_4$	$C_{54}H_{40}As_2N_3O_3Tc$
M_r	1351.23	1625.71	1026.73
T/K	183(2)	183(2)	183(2)
Crystal system	triclinic	monoclinic	monoclinic
Space group	P-1	C2/c	Cc
a/Å	11.4720(5)	15.7422(12)	19.6520(9)
b/Å	12.7447(6)	18.2865(9)	16.8995(7)
c/Å	23.1105(11)	18.0539(12)	16.1837(7)
α/°	74.605(5)		
β/°	89.243(6)	93.103(9)	100.971(5)
γ/°	85.002(6)		
V/Å^3	3245.1(3)	5189.6(6)	5276.5(4)
Z	2	4	4
D_c/g cm^{-3}	1.383	2.081	1.292
μ(Mo-Kα)/mm^{-1}	2.068	9.369	1.559
F(000)	1405	3072	2072
Crystal size/mm	0.33x0.22x0.20	0.38x0.25x0.17	0.43x0.33x0.29
Crystal description	colourless block	colourless needle	colourless block
θ range/°	2.54 - 28.02°.	2.50 - 28.10°.	2.73 - 30.46
Total no. of data	44056	36092	34538
No. of unique data	14527	6152	15851
Observed data [a]	12991	4957	10437
Max./min. transmission	0.7233 / 0.5020	0.2520 / 0.0825	0.6796 / 0.5273
Data/restraints/parameters	14527 / 2 / 708	6152 / 0 / 304	15851 / 2 / 568
Goodness-of-fit on F^2	1.019	0.940	0.946
R^{ab}	0.0301	0.0406	0.0583
wR_2^{ac}	0.0846	0.0975	0.1653
Max., min. peaks/e·Å^{-3}	1.587, -0.535	2.139, -2.638	1.128, -0.399

[a] Observation criterion: $I > 2\sigma(I)$. [b] $R = \Sigma||F_o| - |F_c||/\Sigma|F_o|$. [c] $wR_2 = \{\Sigma[w(F_o^2 - F_c^2)^2]/\Sigma[w(F_o^2)^2]\}^{1/2}$

Compound No.	**11**	**13**	**16**
Figure No.	*2.8*	*3.4*	*2.9*
Formula	$C_{10}H_8N_3O_3Re$	$C_{26}H_{16}Cl_2N_4O_6Tc_2$	$C_{27}H_{16}ClN_5O_{10}Re_2$
M_r	404.39	747.33	978.30
T/K	183(2)	183(2)	183(2)
Crystal system	monoclinic	triclinic	monoclinic
Space group	P21/n	P-1	P21/m
a/Å	6.8350(5)	10.9879(8)	11.4814(6)
b/Å	11.2556(7)	11.5003(9)	11.9749(9)
c/Å	15.9683(11)	11.1203(9)	14.7125(10)
α/°		93.703(10)	
β/°	92.144(8)	103.282(9)	108.041(7)
γ/°		86.214(9)	
V/Å^3	1227.61(15)	1362.87(18)	1923.3(2)
Z	4	2	2
D_c/g cm^{-3}	2.188	1.821	1.689
μ(Mo-Kα)/mm^{-1}	9.898	1.259	6.408
F(000)	752	736	920
Crystal size/mm	0.18x0.17x0.10	0.27x0.21x0.08	0.15x0.14x0.12
Crystal description	colourless block	yellow plate	yellow block
θ range/°	3.20 - 30.39	2.83 - 30.48	2.52 - 28.17
Total no. of data	14361	24830	27077
No. of unique data	3549	7607	4569
Observed data [a]	2624	4769	2868
Max./min. transmission	0.4733 / 0.2527	0.8983 / 0.7214	0.5439 / 0.4387
Data/restraints/parameters	3549 / 0 / 154	7607 / 0 / 361	4569 / 0 / 226
Goodness-of-fit on F^2	0.903	0.867	0.837
R^{ab}	0.0388	0.0426	0.0314
wR_2^{ac}	0.0882	0.0990	0.0740
Max., min. peaks/e·Å^{-3}	1.630, -2.418	0.661, -0.970	1.080, -0.522

[a] Observation criterion: $I > 2\sigma(I)$. [b] $R = \Sigma||F_o| - |F_c||/\Sigma|F_o|$. [c] $wR_2 = \{\Sigma[w(F_o^2 - F_c^2)^2]/\Sigma[w(F_o^2)^2]\}^{1/2}$

Compound No.	**19**	**21**	**26**$^{+}$OTf·H_2O
Figure No.	*4.1*	*4.2*	*4.10*
Formula	$C_{21}H_{10}BrN_4O_3Re$	$C_{21}H_{12}BrN_2O_3Re$	$C_{24}H_{12}F_3N_9O_{10}Re_2S$
M_r	632.44	606.44	1047.89
T/K	183(2)	183(2)	183(2) K
Crystal system	triclinic	triclinic	orthorhombic
Space group	P-1	P-1	Pbca
a/Å	6.9955(7)	7.5081(10)	12.2404(5)
b/Å	12.9547(11)	9.7573(10)	20.0119(7)
c/Å	13.2653(12)	12.9934(18)	26.2631(14)
α/°	111.200(10)	94.697(15)	
β/°	98.272(11)	94.288(16)	
γ/°	95.110(11)	106.434(14)	
V/Å^3	1096.10(17)	905.1(2)	6433.2(5)
Z	2	2	8
D_c/g cm^{-3}	1.916	2.225	2.164
μ(Mo-Kα)/mm^{-1}	7.394	8.946	7.669
F(000)	596	572	3936
Crystal size/mm	0.11x0.07x0.03	0.16x0.08x0.04	0.24x0.07x0.07
Crystal description	orange plate	red prism	yellow needle
θ range/°	2.81 - 26.37	3.04 - 26.37	3.04 - 29.50
Total no. of data	8562	7516	40699
No. of unique data	4193	3460	8949
Observed data [a]	2978	2660	4519
Max./min. transmission	0.8078 / 0.4619		0.6410 / 0.3247
Data/restraints/parameters	4193 / 0 / 279	3460 / 1 / 249	8949 / 0 / 442
Goodness-of-fit on F^2	0.926	1.042	0.803
R^{ab}	0.0593	0.0749	0.0539
wR_2^{ac}	0.1685	0.1893	0.1203
Max., min. peaks/e·Å^{-3}	3.063, -1.710	2.066, -2.314	2.097, -1.599

[a] Observation criterion: $I > 2\sigma(I)$. [b] $R = \Sigma||F_o| - |F_c||/\Sigma|F_o|$. [c] $wR_2 = \{\Sigma[w(F_o^2 - F_c^2)^2]/\Sigma[w(F_o^2)^2]\}^{1/2}$

Compound No.	**28**	**29**	**30**·CH_2Cl_2
Figure No.	*4.9*	*4.5*	*5.1*
Formula	$C_{14}H_8N_5O_3Re$	$C_{15}H_6BrN_2O_5Re$	$C_{48}H_{38}BBrCl_2CuF_4N_4O_3P_2Re$
M_r	480.45	560.33	1268.12
T/K	183(2) K	183(2)	183(2) K
Crystal system	triclinic	orthorhombic	orthorhombic
Space group	P-1	Pnma	Pbca
a/Å	7.0390(6)	7.2858(5)	11.6069(4)
b/Å	9.0268(7)	12.7348(6)	20.4962(6)
c/Å	12.2472(10)	16.7641(9)	41.4899(12)
α/°	88.694(10)		
β/°	78.761(10)		
γ/°	73.919(10)		
V/Å^3	732.99(10)	1555.43(15)	9870.3(5)
Z	2	4	8
D_c/g cm^{-3}	2.177	2.393	1.707
μ(Mo-Kα)/mm^{-1}	8.312	10.409	3.925
F(000)	452	1040	4976
Crystal size/mm	0.40x0.15x0.07	0.07x0.03x0.01	0.34x0.23x0.02
Crystal description	black plate	brown plate	red plate
θ range/°	3.20 - 30.47	3.05 - 29.50	2.63 - 30.47
Total no. of data	10938	20700	115877
No. of unique data	4024	2256	14983
Observed data [a]	3370	1604	9040
Max./min. transmission	0.4977 / 0.1699	0.8167 / 0.2772	0.9067 / 0.3118
Data/restraints/parameters	4024 / 0 / 208	2256 / 96 / 135	14983 / 0 / 604
Goodness-of-fit on F^2	1.031	1.047	0.877
R^{ab}	0.0458	0.0701	0.0542
wR_2^{ac}	0.1149	0.1835	0.1358
Max., min. peaks/e·Å^{-3}	3.401, -4.181	2.002, -1.804	2.357, -1.041

[a] Observation criterion: $I > 2\sigma(I)$. [b] $R = \Sigma||F_o| - |F_c||/\Sigma|F_o|$. [c] $wR_2 = \{\Sigma[w(F_o^2 - F_c^2)^2]/\Sigma[w(F_o^2)^2]\}^{1/2}$

Compound No.	**32**·H_2O	**33**·CH_2Cl_2
Figure No.	*5.4*	*5.2*
Formula	$C_{26}H_{14}F_9IrN_4O_{15}ReS_3$	$C_{52}H_{38}BrCl_2N_2O_5P_2PtRe$
M_r	1267.99	1364.88
T/K	183(2) K	183(2) K
Crystal system	monoclinic	triclinic
Space group	P21/n	P-1
a/Å	8.4372(4)	12.9126(9)
b/Å	38.2745(18)	14.6315(10)
c/Å	12.0048(5)	15.4384(10)
α/°		68.116(7)
β/°	97.829(5)	75.521(7)
γ/°		67.830(7)
V/Å^3	3840.6(3)	2486.1(3)
Z	4	2
D_c/g cm^{-3}	2.193	1.823
μ(Mo-Kα)/mm^{-1}	6.888	6.267
F(000)	2396	1312
Crystal size/mm	0.33x0.06x0.02	0.13x0.11x0.04
Crystal description	black needle	red plate
θ range/°	2.34 - 25.00	2.80 - 30.52
Total no. of data	16896	53947
No. of unique data	6714	13718
Observed data [a]	3320	7930
Max./min. transmission	0.8701 / 0.2620	0.7691 / 0.3730
Data/restraints/parameters	6714 / 0 / 247	13718 / 18 / 595
Goodness-of-fit on F^2	0.882	0.834
R^{ab}	0.0893	0.0454
wR_2^{ac}	0.2099	0.0981
Max., min. peaks/e·Å^{-3}	2.172, -1.680	1.775, -1.728

[a] Observation criterion: $I > 2\sigma(I)$. [b] $R = \Sigma||F_o| - |F_c||/\Sigma|F_o|$. [c] $wR_2 = \{\Sigma[w(F_o^2 - F_c^2)^2]/\Sigma[w(F_o^2)^2]\}^{1/2}$

References

[1] G. M. Sheldrick, *Acta Crystallogr., Sect. A: Fundam. Crystallogr.* **1990**, *46*, 467.

[2] A. Altomare, M. C. Burla, M. Camalli, G. L. Cascarano, C. Giacovazzo, A. Guagliardi, A. G. G. Moliterni, G. Polidori, R. Spagna, *J. Appl. Crystallogr.* **1999**, *32*, 115.

[3] G. M. Sheldrick, University Göttingen, **1997**.

[4] G. W. Parshall, *Inorg. Synth.* **1977**, *17*, 110.

[5] S. P. Schmidt, W. C. Trogler, F. Basolo, *Inorg. Synth.* **1990**, *28*, 160.

[6] R. Alberto, A. Egli, U. Abram, K. Hegetschweiler, V. Gramlich, P. A. Schubiger, *J. Chem. Soc., Dalton Trans.* **1994**, 2815.

[7] R. Alberto, R. Schibli, P. A. Schubiger, U. Abram, T. A. Kaden, *Polyhedron* **1996**, *15*, 1079.

[8] R. Ugo, F. Cariati, G. La Monica, *Inorg. Synth.* **1968**, *11*, 105.

[9] A. Kirpal, E. Reiter, *Chem. Ber.* **1927**, *60*, 664.

[10] C. Hiort, P. Lincoln, B. Norden, *J. Am. Chem. Soc.* **1993**, *115*, 3448.

[11] R. van Belzen, R. A. Klein, W. J. J. Smeets, A. L. Spek, R. Benedix, C. J. Elsevier, *Recl. Trav. Chim. Pays Bas* **1996**, *115*, 275.

[12] J. E. Dickeson, L. A. Summers, *Austr. J. Chem.* **1970**, *23*, 1023.

[13] R. Alberto, K. Ortner, N. Wheatley, R. Schibli, A. P. Schubiger, *J. Am. Chem. Soc.* **2001**, *123*, 3135.

[14] A. Juris, S. Campagna, I. Bidd, J. M. Lehn, R. Ziessel, *Inorg. Chem.* **1988**, *27*, 4007.

[15] W. Matheis, W. Kaim, *Z. Anorg. Allg. Chem.* **1991**, *593*, 147.

ZUSAMMENFASSUNG

Ursprüngliches Ziel dieser Arbeit war die Entwicklung eines neuen Cyano-Komplexes von ^{99m}Technetium(I), der als Quelle von γ-Strahlen für die Radiopharmazie nutzbar sein könnte. Es wurde versucht, eine kleine, stabile Tc^{I}- Einheit zu synthetisieren, wobei sich die Versuche an den Resultaten der Untersuchungen des vielsitig einsetzbaren Fragments $[(Tc^{I},Re^{I})(CO)_3]^{+}$ orientierten. Dieses ursprüngliche Ziel konnte jedoch nicht erreicht werden, da die vielversprechenden Ausgangsverbindungen $[(Tc^{I},Re^{I})(CN)_6]^{5-}$ und $[(Tc^{I},Re^{I})(CN)_4(NO)]^{2-}$ unvorteilhafte Eigenschaften für radiopharmazeutische Anwendungen zeigten. Der reine Cyano- Komplex $[(Tc^{I},Re^{I})(CN)_6]^{5-}$ ist als äußerst luftempfindliche Verbindung als Ausgangsmaterial ungeeignet. Zusätzlich stellen sich für diese Substanz in Lösung Gleichgewichte zwischen verschiedenen Cyano- Species ein, die die Umsetzung zu einheitlichen Substitutionsprodukten erschweren. Der gemischte Komplex $[(Tc^{I},Re^{I})(CN)_4(NO)]^{2-}$, der neben Cyanid auch den starken π-Akzeptorliganden NO^{+} enthält, ist stabil an der Luft. Die Cyanide dieses Fragments sind aber so stark gebunden, daß sie keine Substitution durch bidentate Liganden zulassen, wie sie zur Derivatisierung nötig wäre.

In Konsequenz wurden Reaktionen der bekannten $[(Tc^{I},Re^{I})(CO)_3]^{+}$- Einheit mit Cyanid untersucht. Man erwartete, durch Substitution von Carbonyl durch Cyanid gemischte Cyano- Carbonyl- Komplexe zu erhalten. Solche Substitutionen finden aber nicht statt, da ein *trans* zu einem Carbonyl koordiniertes Cyanid dieses außergewöhnlich stark stabilisiert und so eine Substitution verhindert. Daher bilden sich als Produkte einer Reaktion des $[(Tc^{I},Re^{I})(CO)_3]^{+}$- Fragments mit Cyanid zwar Cyano- Carbonyl- Komplexe, eine Carbonylsubstitution findet aber nicht statt. Die Komplexe $[(Tc^{I},Re^{I})(CN)_3(CO)_3]^{2-}$ konnten auf diesem Weg dargestellt werden, deren Untersuchung eine detaillierte Studie zu Struktur- und Bindungsverhältnissen für gemischte Cyano- Carbonyl- Komplexe ermöglichte.[1] Auf der Basis dieser Experimente wurde eine neue [2+1] Markierungsmethode unter Verwendung von Cyanid entwickelt, da sich Komplexe des Typs

[^{99m}Tc(CN)(CO)$_3$L$_2$], die die sehr stabile *trans*-CO/CN Einhalt enthalten, als einfach zugänglich erwiesen.[2]

Diese Ergebnisse zeigen, daß kleine, wasser- und luftstabile Cyanokomplexe von Tc^{I} and Re^{I} synthetisiert werden können. Sie müssen aber auch noch starke π-Akzeptorliganden wie NO^{+} or CO enthalten, um die Komplexe gegenüber Oxidation zu stabilisieren. Die Fragmente [(Tc^{I},Re^{I})(CN)$_4$(NO)]$^{2-}$ und [(Tc^{I},Re^{I})(CN)(CO)$_3$] bieten die Möglichkeit, einen weiteren mono- bzw. Bidentaten Liganden einzuführen, wie es für das Markieren von Biomolekülen nötig ist.

Für die Entwicklung der erwähnten [2+1] Markierungsmethode wurden Modellverbindungen hergestellt, unter diesen die Komplexe [(^{99m}Tc,Re)(CN)(CO)$_3$bipy] und die cyanoverbrückte dinukleare Species [(Re(CO)$_3$bipy)$_2$(μ-CN)]$^{+}$. Solche Tricarbonyldiimine- Verbindungen von Rhenium(I) sind aus der Literatur wegen ihrer sehr interessanten photochemischen Eigenschaften bekannt, die im Kontext der Sonnenenergiewandlung diskutiert wurden.[3] Infolgedessen wurden die Arbeiten auf dem Gebiet der Radiopharmazie beendet zugunsten einer detaillierten Untersuchung photoaktiver Komplexe des Typs "[Re(CO)$_3$(Diimin)X]".

Das Ziel der Arbeiten dieses Teils der Dissertation war es, mit einer Untersuchung photoaktiver Rheniumverbindungen zum komplexen Problem der photokatalytischen Wasserspaltung beizutragen. Ließe sich eine effiziente photokatalytischen Wasserspaltung großtechnisch realisieren, könnte sich so das Problem einer nachhaltigen globalen Energieversorgung lösen lassen. In früheren Untersuchungen hatte sich gezeigt, daß [Re(CO)$_3$(Diimin)X]- Komplexe in der Lage sind, bei der Zwei-Elektronen-Reduktion von CO_2 zu CO sowohl als Lichtabsorber als auch als Reduktionskatalysatoren zu wirken.[4] In solchen Reaktionen oxidiert der photoangeregte Zustand des Komplexes schwer oxidierbare Elektronendonormoleküle. In mehreren sich anschließenden Schritten werden zwei Elektronen auf das am Rhenium koordinierte Substrat CO_2

übertragen. Die Energie, die für diesen Prozeß benötigt wird, liefern absorbierte Photonen, so daß der Gesamtvorgang eine photoinduzierte Zweielektronenübertragung darstellt.

Für die Reduktion von Wasser zu molekularem Wasserstoff werden ebenfalls zwei Elektronen benötigt. Es schien daher interessant, nach Möglichkeiten zu suchen, die Photoreaktivität der $[Re(CO)_3(Diimin)X]$-Komplexe so zu ändern, daß eine Reduktion von Wasser statt CO_2 möglich werden könnte. Zu diesem Zweck wurden mehrere Reihen verschiedener Rhenium(I)carbonylkomplexe, $[Re(CO)_3(Diimin)X]$, synthetisiert und charakterisiert, die verschiedene sechste Liganden X, verschiedene Diimine und sogar verbrückende Diimine gebunden an weitere Metallzentren enthielten. Auf diese Weise standen Verbindungen von unterschiedlicher Lichtabsorption, Fluoreszenz, Geometrie und Redoxverhalten zur Verfügung, deren Photoreaktivität untersucht wurde. Dabei konnten drei wichtige Beobachtungen gemacht werden:

- Auch viele der modifizierten $[Re(CO)_3(Diimin)X]$- Verbindungen sind aktive Photokatalysatoren im bekannten System für die photochemische CO_2- Reduktion. Eine der neuen Substanzen, $[Re(SCN)(CO)_3(bipy)]$, scheint sogar ein besserer Katalysator als die bisher bekannten Komplexe zu sein. Generell zeigen nur $[Re(CO)_3(Diimin)X]$- Komplexe Aktivität als Photokatalysatoren, für die sich Fluoreszenz bei Raumtemperatur in Lösung messen läßt. Für heterodinuklearen Komplexe konnte weder eine Fluoreszenz des angeregten Zusatnds noch Photoreaktivität beobachtet werden.
- Die Elektronenübertragung von den als Elektronenquelle dienenden Aminen zum angeregten Zustand der Komplexe ist sehr schnell und findet bei allen fluoreszierenden Komplexen statt. Für solche Vorgänge ist die STERN-VOLMER-Konstante K_{SV} ein Maß für die Effizienz der Elektronenübertragung. Es scheint keine Korrelation zu bestehen zwischen K_{SV} und Absorptionsmaxima, Redoxpotentialen, Art des Diiminliganden oder der Geometrie der

Komplexe. Dies deutet darauf hin, daß es sich bei den Elektronenübertragungen um nahezu diffusionskontrollierte outer-sphere-Prozesse handelt, deren Rate einzig von der Lebensdauer τ der einzelnen Komplexe abhängt. Es gelang leider nicht, andere Elektronenquellen als die bekannten Amine zu finden.

- Obwohl mehrere der Rheniumverbindungen aktive Photokatalystoren für die Zweielektronenreduktion von CO_2 sind, ist keiner von ihnen in der Lage, Wasser zu H_2 zu reduzieren. Die Reduktion von Wasser scheint nur in Anwesenheit eines weiteren Katalysators möglich. So ließ sich ein System zur Übertragung von Reduktionsäquivalenten realisieren, bei dem die Elektronen vom photoreduzierten Rheniumkomplex über $[Co(bipy)_n]^{2+}$ als Vermittler auf den bekannten Adams-Katalysator transferiert werden. Die Bildung von Wasserstoff in diesem System geschieht nur außerordentlich langsam, es beweist jedoch, daß Rheniumkomplexe prinzipiell als Photoabsorber für die photokatalytische Wasserreduktion geeignet sind.

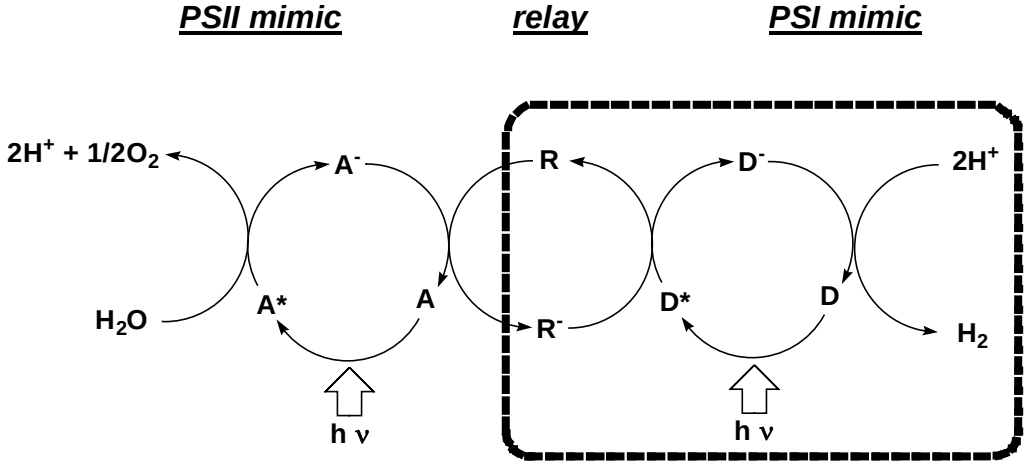

Abbildung 7.1 Schema eines möglichen Systems zur photokatalytischen Wasserspaltung. $[Re(CO)_3(diimine)X]$- Komplexe könnten als Photoabsorber D im „Reduktionsteil“ (gestrichelter Kasten) eingesetzt werden.

Diese Ergebnisse zeigen die Möglichkeit, zahlreiche Variationen des $[Re(CO)_3(Diimin)X]$- Systems mit einer großen Bandbreite an physikochemischen Eigenschaften darzustellen. Alle fluoreszierenden Verbindungen dieses Typs sind auch in der Lage, photochemisch

Kohlendioxid zu reduzieren. In einem möglichen Gesamtkonzept zur photochemischen Wasserspaltung (Abbildung 7.1) könnten diese Verbindungen den „Reduktionsteil“ übernehmen. Da die Verbindungen nicht direkt mit Wasser reagieren können, sind für diesen Vorgang allerdings Cokatalysatoren nötig.

Literatur

[1] P. Kurz, B. Spingler, T. Fox, R. Alberto, *Inorganic Chemistry* **2004**, *43*, 3789.
[2] P. Kurz, B. Spingler, R. Alberto, in *Technetium, Rhenium and Other Metals in Chemistry and Nuclear Medicine 6* (Eds.: M. Nicolini, U. Mazzi), **2002**.
[3] D. J. Stufkens, *Comments Inorg. Chem.* **1992**, *13*, 359.
[4] J. Hawecker, J. M. Lehn, R. Ziessel, *Helv. Chim. Acta* **1986**, *69*, 1990.

Acknowledgements

I think that every single member of the Institute of Inorganic Chemistry helped me in some way or the other during my four years at the University of Zurich. So it is impossible to create a complete list of thanks and I would therefore like to firstly thank the Institute as a whole for all everyone did for me. Nevertheless, I would like to acknowledge a number of people in particular for their extraordinary support:

Prof. Roger Alberto, who was the mastermind behind many of the strategies presented in this thesis. For me, it was great to be in a position where I could learn so much from him about inorganic chemistry in general. In particular, his enthusiasm to always look for new topics, new routes, new fields to address, was very inspiring throughout the years.

Dr. Bernhard Spingler, with whom I had the pleasure of spending countless hours - in particular enjoying to have an excellent crystallography teacher, but of many other topics, too: synthesis, analysis – and IT!

Dr. Jae Kyoung Pak, to whom I turned with many questions – especially those stemming from my very limited knowledge of organic synthesis.

Dr. Susanne Kunze and *Dr. Stefan Mundwiler* who introduced me to HPLC analysis.

The mass spectrometry team of *Dr. Jae Kyoung Pak*, *Dr. Chiara da Pieve*, *Dr. Fabio Zobi*, *Nikos Agorastos* and *Lukas Kromer*.

Dr. Thomas Fox for the measurements of NMR spectra, especially of ^{99}Tc.

Heinz and *Barbara Spring* for elemental analyses and technical support.

Hanspeter Stalder for many repairs and constructions done in the Institute's mechanical workshop.

Prof. Richard Fish (Lawrence Berkeley Nat. Lab., USA) for his help with the iridium chemistry.

The *group of Prof. Jon Dilworth* (Oxford University, UK), where I had the possibility to carry out the first preliminary CO_2 reduction experiments using their excellent equipment.

And, last but not least, *Prof. Heinz Berke* and *Prof. Jay Siegel* from the University of Zurich for reading and correcting this thesis as members of my Ph.D. committee.

Big thanks to you all!

Curriculum vitae

KURZ

Philipp Günther Elfried

born January 9th 1976

German citizen

EDUCATION

1986- 1995	Ratsgymnasium Bielefeld, Germany. Abitur 1995.
1996- 1998	Undergraduate studies in chemistry at the University of Leipzig, Germany. Vordiplom 1998.
1998- 2000	Undergraduate studies in chemistry at ETH Zurich, Switzerland. Diplom 2000.
2000	Diploma thesis in geochemistry under the supervision of Prof. B. Wehrli at the Swiss Federal Institute of Environmental Science and Technology (EAWAG), Kastanienbaum, Switzerland. Title: *$CaCO_3$ Biomineralization in Freshwater Picoplankton*.
2001- present	Ph.D. thesis in the field of synthetic inorganic chemistry and photochemistry in the research group of Prof. R. Alberto, Inorganic Chemistry Institute, University of Zurich, Switzerland.